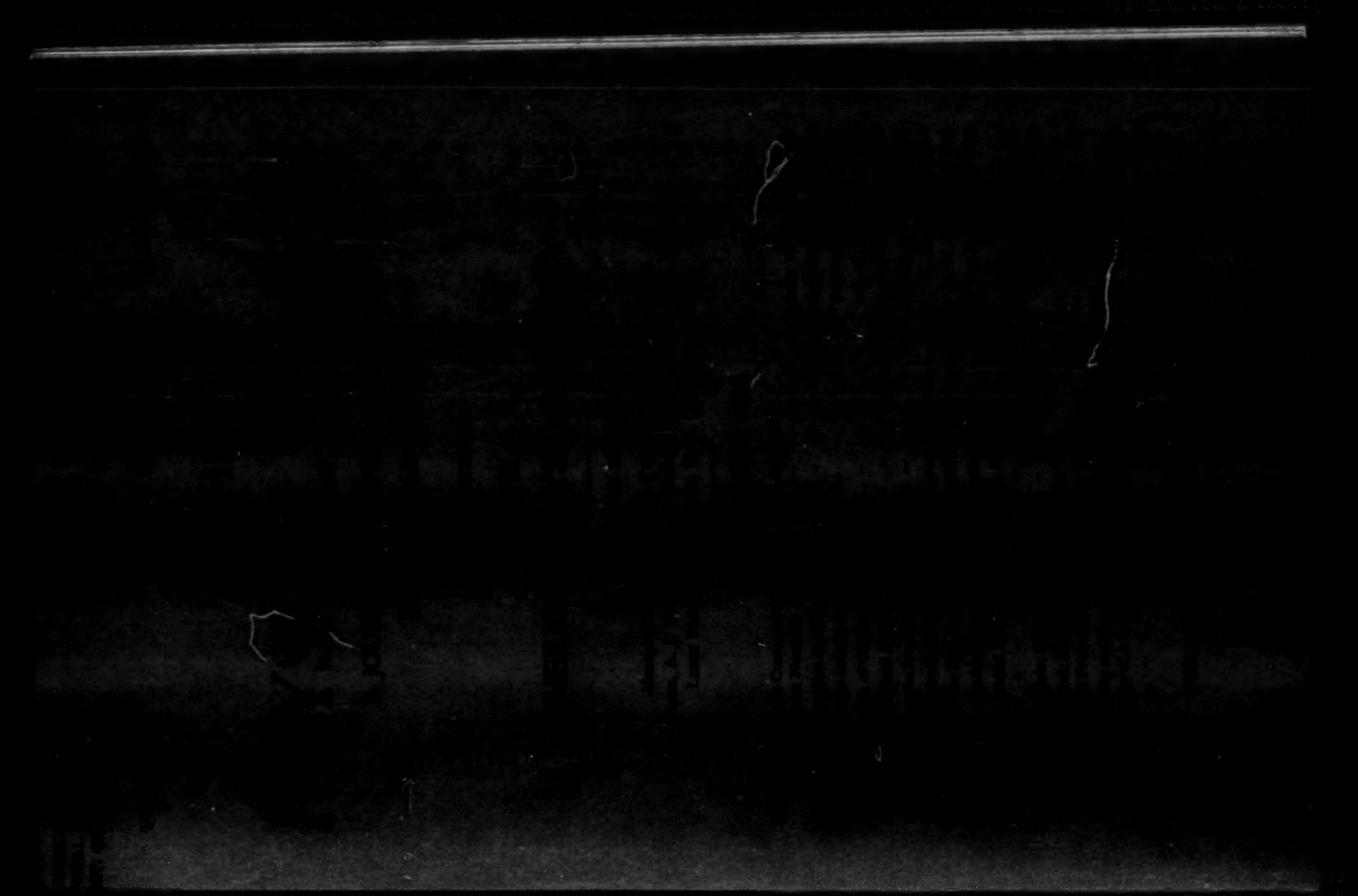

THE AMERICAN PHYSICAL SOCIETY

OFFICERS OF THE SOCIETY

President:	C. R. MENDENHALL	Univ. of Wisconsin, Madison, Wis.
Vice-President:	D. C. MILLER	Case School of Applied Science, Cleveland, Ohio
Secretary:	E. W. WEBB	Columbia University, New York City
Treasurer:	G. B. PEGRAM	Columbia University, New York City
Editor:	G. S. FULCHER	Corning, N. Y.
Local Secretary for the Pacific Coast:	D. L. WEBSTER	Stanford University, Calif.

THE PHYSICAL REVIEW

Published monthly. Two volumes annually

First series. From July 1, 1893 to January 1, 1913, the REVIEW was conducted by Edward L. Nichols, Ernest Merritt and Frederick Bedell, with the financial support of Cornell University. The first four volumes were issued annually; subsequent volumes, semi-annually; thirty-five volumes, in all.

Second series. On January 1, 1913, the REVIEW was transferred to the American Physical Society as announced on the first page of the new series which was then begun. Since then it has been conducted by a Board of Editors elected by the Society. Semi-annual volumes begin in January and July.

Communications are referred to page 2 of the advertisements for further information.

Annual Subscription, throughout the Postal Union, $7.00 in advance.

Single Copies, $.75.

Canadian English, 1893–1920, $6.00, in advance.

Back Volumes, $6.50 per volume; Back Numbers, $.75 per copy. Postage is free if remittance accompanies order; otherwise postage is extra. No bound volumes can be supplied. The REVIEW offers to purchase a limited number of First Series, Vol. 1, No. 1 (at $1.50 each); Second Series, Vol. 7, No. 1, January 1916; Vol. 7, March 1916 and Vol. 9, No. 2, February 1917 (at $1.50 each); Vol. 15, No. 1, January 1922 (at $.75 each).

Advertisements. Rates will be supplied by the Editor on request. Copy for each number must be received at Corning before the 15th of the preceding month; old copy is used until new copy is received. Send electrotypes direct to the printers, George Banta Publishing Co., Menasha, Wisconsin.

Discount of ten per cent is allowed subscription agencies and members of the American Physical Society.

Complaints of failure to receive the REVIEW, in the case of members of the Physical Society, should be addressed to the Treasurer; otherwise, to the REVIEW, Corning, N. Y.

Correspondence should be addressed to the Physical Review, Corning, N. Y.

Entered at the postoffice at Menasha, Wis., as second class matter.
Acceptance for mailing at special rate of postage provided for in section 1103, Act of October 3, 1917
authorized September 4, 1918

Second Series *November, 1924* *Vol. 24, No. 5*

THE

PHYSICAL REVIEW

AN EXTENSION OF BOHR'S CORRESPONDENCE PRINCIPLE TO APPLY TO SMALL QUANTUM NUMBERS

By Pierce W. Ketchum

Abstract

Generalized correspondence principle for the Bohr atom.—It is shown that when an electron spirals in from an orbit of quantum number n_2 to an orbit of quantum number n_1, the frequency of the radiation emitted is equal to an integer (n_2-n_1) times the mean frequency of rotation in its orbit during the spiraling, assuming that the number of rotations made for a change of quantum level dn is proportional to dn. That is, the mean is defined as the ratio to (n_2-n_1) of the integral from n_1 to n_2 of $\nu_c\,dn$ where ν_c is the classical frequency of rotation corresponding to any value of n. No explanation is offered as to why radiation begins and stops at integral values of n, nor why the radiation emitted in the manner assumed is monochromatic.

ACCORDING to classical theory an electron rotating about the positive nucleus of an atom would radiate energy with a frequency equal to its frequency of rotation. In the Bohr atom on the basis of the quantum theory this is generally not true. The Bohr theory postulates radiation by an electron only on dropping from one orbit to another. The frequency of the radiation is obtained from the energy change. The mechanism by which radiation is produced when the electron passes between the orbits is an open question. Many prefer to consider the electron as jumping instantaneously from one orbit to another.

Consider an atom with a centralized positive charge of Z units, with one electron of mass m and charge e, in rotation about it in a circular orbit, with velocity v, at distance a from the nucleus. Bohr has assumed (I) that the force of attraction is inversely proportional to the square of the distance, so that

$$Ze^2/a^2 = mv^2/a, \tag{1}$$

and (II) that

$$mav = nh/2\pi \tag{2}$$

where h is Planck's quantum of action and n is a positive integer; and (III) that the frequency of radiation is equal to the difference in energy between any two orbits (i.e. any two values of n) divided by h.

From these three assumptions Bohr arrived at the following expression for radiation frequency, which agrees well with experiments

$$\nu = \frac{2\pi^2 mZ^2e^4}{h^3}\left[\frac{1}{n_1^2} - \frac{1}{n_2^2}\right]; \quad n_2 > n_1 . \tag{3}$$

Assumptions (1) and (II) are also valid from the classical viewpoint provided the rotation of the electron is not restricted to any particular orbits. From classical mechanics using Eqs. (1) and (2), the frequency of rotation or the classical radiation frequency would be

$$\nu_c = 4\pi^2 mZ^2e^4/n^3h^3 , \tag{4}$$

where n may now vary continuously.

Bohr in his principle of correspondence[1] has already shown that (3) and (4) become identical for changes of n by one integer at large values of n.

The Generalized Correspondence Principle

Up to the present time no simple exact correspondence has been obtained between classical and quantum frequencies which holds for small quantum numbers as well as large. Such a relation, however, can be obtained by integrating the classical frequency with respect to n between limits which are positive integers, thus from (4)

$$\int_{n_1}^{n_2} \frac{4\pi^2 mZ^2e^4}{n^3h^3}dn = \frac{2\pi^2 mZ^2e^4}{h^3}\left[\frac{1}{n_1^2} - \frac{1}{n_2^2}\right]. \tag{5}$$

The right hand member of (5) is identical with the radiation frequency as obtained from quantum theory so that the generalized correspondence principle may be written

$$\nu = \int_{n_1}^{n_2} \nu_c dn \tag{6}$$

which gives an exact relation between the rotational frequency of the electron and the radiation frequency for any value of n and any change in n.

Bohr's correspondence principle is a special case of the generalized principle, since the right hand member of (6) becomes equal to ν_c when n is very large and $n_2 - n_1 = 1$.

[1] Sommerfeldt, Atomic Structure and Spectral Lines, 3rd Ed., English trans., p. 577

Physical Significance of the Generalized Correspondence Principle

Eq. (6) acquires an additional significance if we consider that according to classical theory a radiating electron would lose energy continuously and would fall in toward the nucleus spirally. At each instant the electron would have a frequency as expressed in (4). On dropping from orbit n_2 to n_1 the mean of these frequencies with respect to n would be

$$\bar{\nu}_c = \int_{n_2}^{n_1} \nu_c dn \Big/ \int_{n_2}^{n_1} dn = \int_{n_2}^{n_1} \nu_c dn \Big/ (n_2 - n_1). \tag{7}$$

From (6) and (7) it follows that

$$\nu = \bar{\nu}_c (n_2 - n_1). \tag{8}$$

Therefore if an electron drops one orbit it radiates with a frequency equal to the mean frequency of rotation. If it drops by more than one quantum orbit it radiates an overtone of the mean vibration frequency.

It is believed that the above is a step toward reconciling the Bohr theory with classical mechanics, but it still remains unexplained as to why the electron begins and ceases to radiate only when n has integral values. It would also seem that from the classical standpoint the atom would radiate with a continuously varying wave-length rather than with a single frequency.

In conclusion the writer wishes to thank Dr. W. H. Rodebush of the Department of Chemistry, University of Illinois, for his valuable suggestions and criticisms.

University of Illinois,
June 30, 1924.

SERIES LIMIT ABSORPTION IN SODIUM VAPOR

By George R. Harrison[1]

Abstract

Transmission curves of sodium vapor for wave-lengths near the principal series limit, 2550 to 2150A.—*Reliable ultraviolet photometric measurements* were secured by using a steady rotating disk cadmium spark as source and by taking on a single plate, in addition to three absorption spectra, exposures for eight different intensities varied in steps from 2 to 100 by means of oscillating screens, each exposure being for the same time. (The exposure time was reduced to 16 sec. by using an absorption furnace with a column of vapor only 10 cm long.) Measurements of a single plate thus gave the characteristic curves for that plate which were needed to determine from the absorption spectra the actual transmission as a function of wave-length. As the wave-length decreases, the transmission rises to a maximum at 2465A, then decreases regularly to a sharp minimum at the series limit 2414A, then rises to a value at 2200 about equal to that at 2465. The series limit absorption thus decreases rapidly with decreasing wave-length. The eighteen curves obtained for different vapor densities are very similar, all being convex upward. The maximum discontinuity observed is from 34 per cent transmission at 2465A to 20 per cent at 2414A, for vapor of medium density; for greater or less densities of saturated vapor the discontinuity is smaller. Due to the presence of band absorption even beyond the limit, the precise variation of atomic absorption with wave-length cannot as yet be determined from these results.

Densitometer curves for sodium principal series absorption and for hydrogen diffuse series absorption in stars show great similarity near the limits.

Introduction

A STRIKING correlation made by the Bohr theory between spectroscopic phenomena and atomic behavior is the explanation of the continuous region of absorption or emission frequently found beginning at a series limit and extending towards shorter wave-lengths. The absorption is important because it corresponds to the photo-electric effect in the absorbing vapor, while the emission is due to the fall of free electrons of varying velocities into ionized atoms. Bohr[2] explains the two cases as being due to jumps between a quantized state and a free state incapable of quantization. Taking the principal series of sodium in absorption, for example, we have a large number of lines due to electron jumps from the 1σ level to the various π levels, and finally a continuous region of absorption where electrons have been raised clear of the atom. Thus the original

[1] National Research Fellow.

[2] Bohr, Phil. Mag. **26**, 16 (1913)

energy $h\nu$ of the light of frequency ν, if more than enough to free the electron completely, is divided into two parts, W, that required to lift the electron above the highest virtual orbit, and a remainder $\frac{1}{2}mv^2$ going into kinetic energy of the freed electron.

In the x-ray region, similarly, we have continuous absorption below the K, L, and M limits. Most investigators find that this absorption decreases as the cube of the wave-length, though the exponent varies for different observers between 2.5 and 3. Kramers[3] has theoretically derived an expression of similar form to that found experimentally, and his work suggests that a λ^3 law might be expected to hold in the optical region as well, although his assumptions apply strictly only to the inner shells of the atom. Milne,[4] attacking the problem from a different angle, expects a λ^2 law to hold in the optical region. The importance of finding the true law connecting series limit absorption with wave-length has been emphasized, but the experimental data are very meager.

In the laboratory the continuous optical absorption has apparently been noted at limits of principal series only, having been found by Wood[5] in sodium, and by Holtsmark in sodium and potassium.[6] It is visible also in the spectra published by Bevan[7] for rubidium and caesium, although not mentioned by him. In hydrogen stars continuous absorption is frequently found at the limit of the Balmer series, but this seems to be the only case so far observed where a subordinate series has been strongly enough absorbed to show the effect.

The ions produced when the vapor absorbs frequencies higher than the convergence frequency of its principal series have been detected by Kunz and Williams[8] and by Williamson.[9] Apparently no measurements have yet been made on the relative efficacy of various wave-lengths shorter than the series limit in producing photo-electrons. This information is desirable as it would afford a second method of attack on the problem considered in the present paper.

The discontinuities occurring at the series limits of sodium and potassium have been roughly measured by Holtsmark[6] and by the writer.[10] In the latter paper it was stated that the continuous absorption in Na and K, beginning near the series limits, does not extend undiminished into the

[3] Kramers, Phil. Mag. **46,** 836 (1923)
[4] Milne, Phil. Mag. **47,** 209 (1924)
[5] Wood, Astrophys. Jour. **29,** 97 (1909)
[6] Holtsmark, Phys. Zeit. **20,** 88 (1919)
[7] Bevan, Proc. Roy. Soc. **83,** 421 (1910); **85,** 54 (1912)
[8] Kunz and Williams, Phys. Rev. **15,** 550 (1920); **22,** 456 (1923)
[9] Williamson, Proc. Nat. Acad. Sci. **8,** 255 (1922); Phys. Rev. **21,** 107 (1923)
[10] Harrison, Proc. Nat. Acad. Sci. **8,** 260 (1922)

extreme ultraviolet as might be supposed from a casual inspection of the photographs obtained, but decreases quite rapidly with increasing frequency. Rough curves were published showing in a general way the transmission of these vapors to light of wave-length between 2100 and 5000 A.

Purpose of the Investigation

The objects of the present work were to develop a satisfactory method of photographic photometry which could reasonably be assumed correct, to find the curve connecting transmission with wave-length for sodium vapor between 2600 and 2100 A, to measure the magnitude of the discontinuity occurring at the series limit and to study the cause of any variations that might appear.

Since the convergence limits of the principal series of all elements other than the alkali metals lie below 2100 A, we are limited at once in the choice of vapors to be studied. In order to make accurate measurements a fairly large quantity of the vapor must be used, which has so far prevented the study of Rb, Cs, and Li. All samples of potassium studied showed so much sodium as an impurity that the band around line 2853 masked the true form of the potassium absorption curve beginning at 2867. It is hoped that results for other metals than sodium may be obtained shortly, since the interpretation of the results of the present work depends to some extent on the behavior of other elements.

Experimental Arrangements

After studying various methods, a general system of photographic photometry was developed which has been briefly described elsewhere,[11] and which has since been somewhat improved in certain details. In Fig. 1 is shown the general arrangement of the sensitometer used. The requirements as to light source were that it should be relatively free from lines over stretches of 20 A between 2100 and 2600 A, or else that it should contain a large number of lines of approximately equal photographic intensity in this region, regularly distributed. It should also be steady as regards total intensity to within one per cent for a period of ten minutes, and its energy distribution should not vary appreciably during that time. The cadmium spark in air was chosen for work between 2100 and 2600 A. It was found that the greatest steadiness could be obtained when the spark was between two disks rotating edge to edge, an arrangement recently described by Bovie.[12] Both disks were driven by rubber bands

[11] Harrison and Hesthal, J. Opt. Soc. Am. and R. S. I. **8**, 471 (1924)
[12] Bovie, J. Opt. Soc. Am. and R. S. I. **7**, 1026 (1923)

running from a common shaft driving an air blower. This blower was necessary to prevent coating of the lenses by cadmium oxide, which accumulated rapidly. The spark housing was made fairly airtight, and a number of holes were cut in each lens holder. Air was drawn through these by the blower, and the resulting current carried the cadmium oxide and ozone out of the room through a flexible tube.

In order to be able to regulate the spark length readily, the two shafts containing the disks were mounted on vertical ways, and their heights could be separately adjusted by turning screws with insulated handles on top of the housing. In this way the spark length could be varied while running, which was desirable, since this was the finest adjustment for

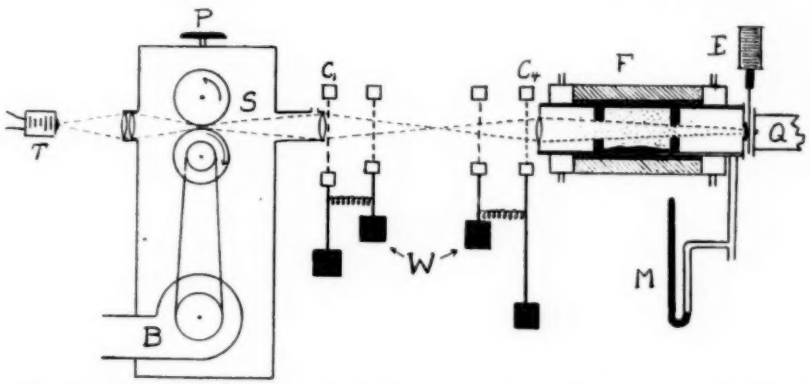

Fig. 1. Detail of part of the sensitometer used. *T*, thermopile; *S*, spark; *C*, screens; *W*, pendulums rocking the screens; *F*, furnace; *E*, magnetic shutter; *Q*, quartz spectrograph slit.

obtaining a "purring" spark, the condition of greatest steadiness. This condition, which existed when a regular number of discharges took place each half-cycle, occurred when the spark voltage, spark length, and capacity in parallel with the spark had the proper values.

A bismuth-silver thermocouple measured the total radiation from the spark. No provision was made for measuring the energy distribution in the spectrum, conditions being held constant to prevent its variation. Changes in line voltage, which were rare, were quickly compensated by a variable impedance in the primary of the 30 kv, 2 kw transformer feeding the spark.

In order to vary the intensity of each wave-length by the same amount, the screen method was adopted, with several improvements. It was found possible to calibrate the screens and keep them constant in transmission to 0.2 per cent over long periods if certain simple precautions were observed. The screens must not be of too fine or too coarse mesh,

they should be carefully oxidized so as to avoid further surface changes, and must be kept in motion laterally while being used or measured, being always put in a beam of fairly large cross-section. Five standard screens were used, which let 51.4, 48.0, 35.1, 35.7, and 31.2 per cent of the light through, respectively. By using combinations of these, from one to four at a time, it was possible to vary the intensity of the light falling on the slit of the quartz spectrograph from 100 to 1.87 by fairly even steps. Each screen was mounted on a pendulum support, and was kept in side to side motion of amplitude covering at least ten small apertures. All four pendulums were kept in irregular oscillation by a heavy master pendulum. Thus errors due to the finite distance between apertures were reduced to a minimum. The screens were also kept in motion while being measured in the thermoelectric densitometer.

The absorption furnace as finally used was a steel tube 30 cm long and 4 cm in diameter, closed with a thin quartz lens at one end, and a quartz plate at the other, both cemented on with sealing wax. Water coolers were placed about 3 cm from each end. A thin layer of mica was wrapped around the central portion of the tube, and on this 20 turns of No. 10 nichrome wire were wound. This was finally covered with asbestos paste, and the whole enclosed in a brass jacket. A 3 kw transformer provided heating current at 40 volts, only about 900 watts being found necessary to keep the furnace at 800°C.

The column of hot sodium vapor was only 10 cm long. Diaphragms were placed in the tube limiting the column to the centermost portion, having apertures just equal to the cross-section of the beam. These were found absolutely necessary for such a short furnace. In Wood's work, and in most of the preceding work on sodium vapor done by the writer, tubes from one to three meters long were used. With these, however, exposures of 20 min. to half an hour were necessary, so the furnaces used were gradually shortened until an exposure of 16 sec. was ample. It was found possible to use such a short column provided the pump was never run while the vapor was hot, and hydrogen at a pressure of several cm was always left in the tube to prevent too rapid distillation. One charge was sufficient to run the tube for an hour at 800°C and at the end of that time the tube could be opened and the sodium which had distilled over into the cold ends could be scraped up and replaced in the center of the furnace.

When fresh sodium was introduced the windows became coated with oxide and hydroxide fairly rapidly. After several heatings, however, the cleaned windows remained clear for some time.

A Hilger quartz spectrograph was used for photographing the spectra. In most cases a wide slit was used to facilitate setting in the center of a line on the densitometer. The plate holder carried two plates; eleven spectra were photographed on each, and they were then fastened back to back with rubber bands and developed and fixed together. Six spectra were absorption pictures, and the remaining 16 were used in two sets of eight each for plotting characteristic curves. The set for the first characteristic curve was taken first, then three absorption pictures; three absorption pictures were then taken on the second plate, and finally the eight points for the second characteristic curve. Thus any coating of the windows occurred after the first curve and before the second, and was corrected for. The time of exposure was controlled by a standard clock operating a magnetic shutter.

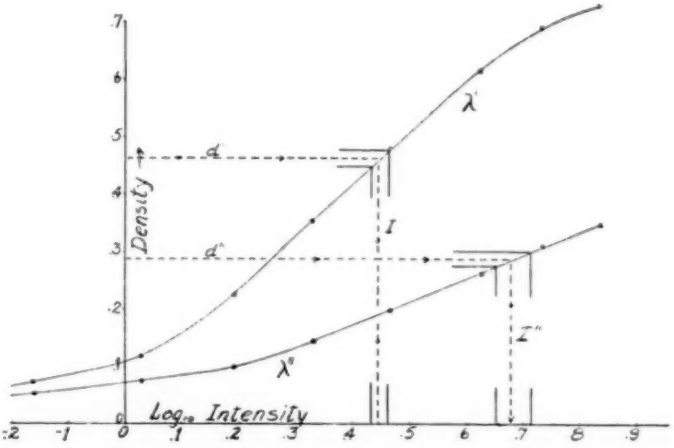

Fig. 2. Typical characteristic curves for two different wave-lengths, as used for determining the intensity which caused a deposit of given density in the negative.

In all of the present work the image densities compared were in each case developed, washed, and fixed at the same time. Since comparatively little is known of the characteristics of photographic emulsions when exposed to ultraviolet light, five standard brands of plate were used.

The densitometer was of the familiar thermo-electric type, improved so that its readings can be trusted to 0.2 per cent. A systematic hunt for the causes of all irregularities, generally less than 1 per cent, has been made, resulting in several simplifications and improvements. Where measurements were to be made at a given wave-length, easily found, the "spotting" densitometer was used, but this would not do for setting on narrow lines or regions in the spectrum where density was changing rapidly with wave-length. For such regions the "running" densitometer

was used. A particular wave-length was chosen, and the density of the negative at this wave-length was measured for each spectrum. Each density obtained was then plotted against the logarithm of the transmission of the screen used to produce it. Two typical characteristic curves, for different wave-lengths, are shown in Fig. 2. From such curves the transmissions corresponding to the densities of the absorption pictures were readily obtained. In this way two characteristic curves were plotted for each measured wave-length for each pair of plates, and on each characteristic curve the transmission of the sodium vapor for three separate conditions could be measured. About forty plates were taken in this way, but many being discarded for various reasons, eighteen curves were finally chosen as best representing the data obtained.

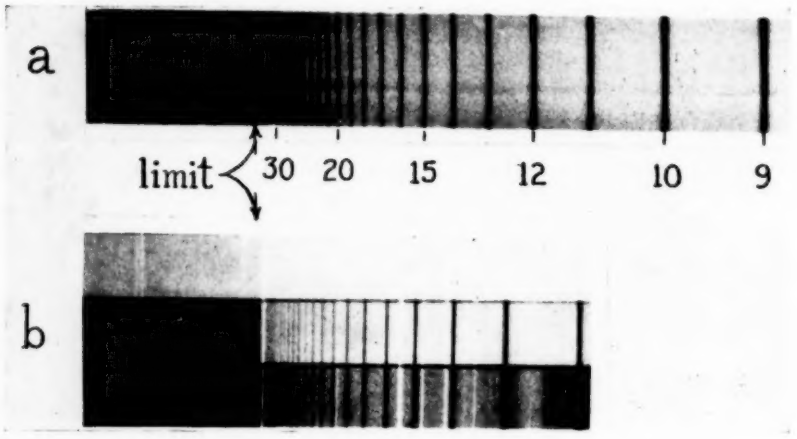

Plate I.

(a) The limit of the Na principal series in absorption, with Al under-water spark background, showing the apparent absence of discontinuity.

(b) The series limit with Cd spark background, showing how the continuous absorption varies with vapor density.

In Fig. 3 is shown an isochronat, connecting wave-length, density, and in a third dimension intensity. The network of points measured on one of the above-mentioned plates forms such a surface. Comparison of the absorption curve with this set of curves gives the true transmission for each wave-length.

Results Obtained

In Fig. 4 are shown three curves plotted by the running densitometer. (a) shows the density distribution in a spectrogram of the region near the limit 1σ in sodium vapor, taken with an aluminum under-water spark as a background. This was run from a negative. (b) shows the same

region as measured on a positive (this being reproduced in (a) of Plate I). A comparison of (a) and (b) indicates that practically all of the density range lies on the straight-line portions of the various characteristic curves. (c) is a similar tracing made from a negative of the Balmer limit in Vega, very kindly loaned the writer by Professor Wright of Lick

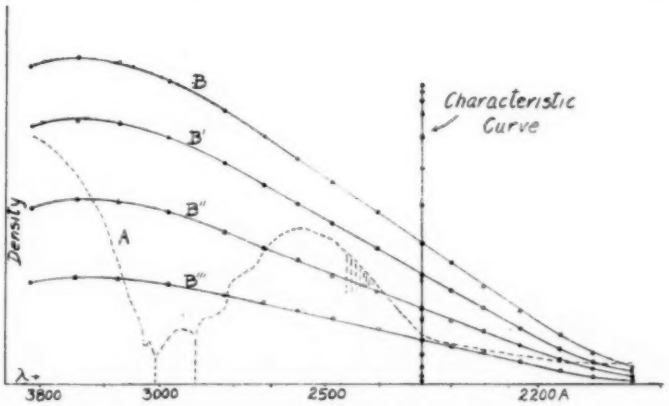

Fig. 3. An isochronat, or surface containing points of equal exposure time. The curves *B*, *B'*, etc. are curves of equal relative intensity, being for points all taken with the same screen covering the light source. Each vertical set of points marks part of a characteristic curve seen edge on. The dotted curve shows the density of the absorption spectrum for various wave-lengths, the relation of dotted to solid curves giving the true transmission for the absorbing medium for each wave-length.

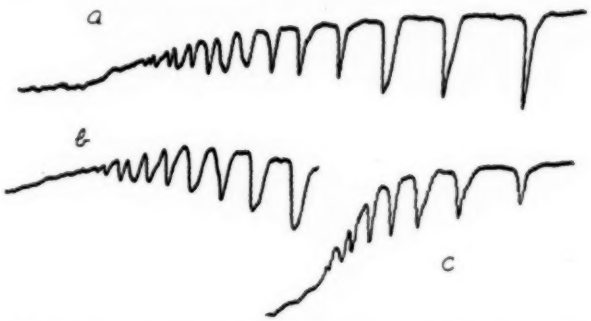

Fig. 4. (a) Densitometer tracing of the principal series limit in sodium vapor, from a negative. (b) Same, from a positive. (c) The Balmer series limit in Vega, showing great similarity to sodium (a) and (b).

Observatory. Most of the differences between the two kinds of curve can be traced to differences in the backgrounds and in the characteristics of the emulsions used for the different spectral regions.

In what follows it should be borne in mind that all curves are true transmission curves and not merely density curves as are those in Fig. 4.

In Fig. 5 are given seven typical transmission curves for sodium vapor at various densities. The scale is the same for each, but they have been displaced somewhat along the vertical axis in order to keep the various sets of points apart. The true position of each curve can be found by use of the decimal marked under it, this giving the transmission for the vapor at the series limit, perfect transmission being taken as unity.

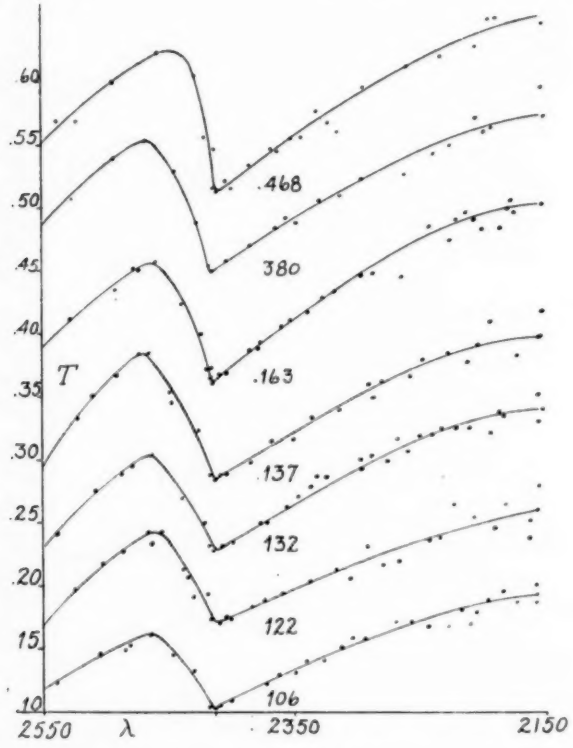

Fig. 5. Transmission wave-length curves for sodium vapor near the principal series limit. The curves for various vapor densities are on the same scale, but are displaced vertically. The decimals under each curve give the true transmission just below the series limit.

A, the angle between the horizontal and the line drawn from T at the series limit to maximum T above the series limit.

B, the angle between the horizontal and the tangent to the lower part of the curve at the series limit.

C, the angle between the horizontal and the line joining T at the limit to T at the lower end of the curve, 2144A.

L, the value of T at the series limit, 2414A.

M, the maximum value of T between series lines below 2600A.

N, the maximum value of T below the limit, always at 2144A.

H_1, the difference $M-L$, or amount of discontinuity at limit.

H_2, the difference $N-L$, or increase in transmission between 2414 and 2144A.

To find how the various shapes varied with conditions, each curve had the following quantities measured, shown graphically in Fig. 6.

The values of these quantities are listed in Table I, arranged in the order of increasing vapor density.

Inspection of this table shows the following facts:

(1) Every plate measured gives B greater than C; that is, the transmission curves are always convex upwards.

(2) In every curve H_1 and H_2 are approximately the same, H_2 being generally slightly the greater. That is, the discontinuity at the limit is offset in a space of 270 A below the limit. On an average, H_2 is 5 per cent greater than H_1.

(3) The value of H_1 rises slowly as the vapor density increases, then falls. That is, a certain vapor density gives the maximum discontinuity at the limit. For the conditions of the present work, the maximum discon-

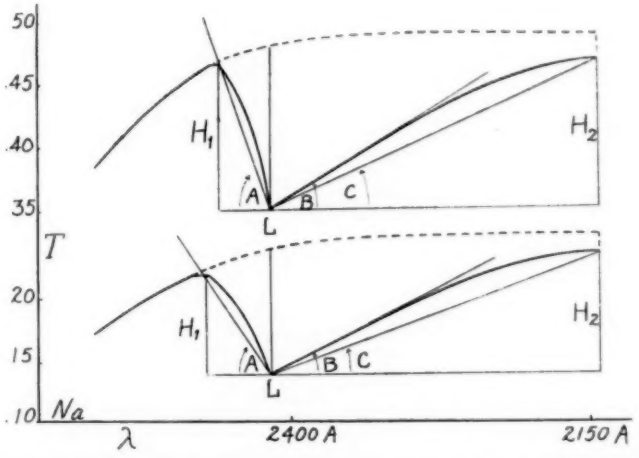

Fig. 6. Two typical average curves drawn from those in Fig. 5 and Table I, showing the shape factors which were measured.

tinuity obtained was about 14 per cent of the light entering the tube; that is, 34 per cent of the original light was transmitted between the lines near the limit, and only 20 per cent just below the limit.

(4) The value of H_2 also slowly rises as the vapor density increases, until a certain density is reached, when it begins to fall.

(5) As the vapor density increases, L, M, and N all decrease.

It is evident that the absorption here measured is due to several causes, and we may expect these to be: (1) The true atomic absorption producing photo-electrons; (2) the band absorption by the molecule Na_2 or NaH, or whatever molecule it may be which produces the well known secondary

absorption in Na vapor; and (3) scattering by droplets, molecules, and free electrons.

No photographs show bands in the region below the limit. At the vapor densities used in this work, all light for some distance around the D-lines has been wiped out, as well as around the 3303 doublet. Around the third member bands are still strongly visible, and to some extent near the

TABLE I

Shape factors for sodium series limit absorption curves

The data are arranged in order of increasing vapor density. Decimals denote fraction of light passing through vapor, perfect transmission being 1.00

Plate	*A*	*B*	*C*	*L*	*M*	*N*	H_1	H_2
18a1	73	37	28	.468	.578	.610	.110	.142
18a2	73	32	21	.437	.546	.546	.109	.109
18a3	74	30	20	.398	.520	.502	.122	.104
18b4	67	29	20	.380	.480	.477	.100	.097
18b5	64	30	21	.354	.450	.456	.096	.102
18b6	58	34	25	.350	.455	.475	.105	.125
19a1	70	38	33	.285	.417	.458	.132	.173
19a2	70	40	31	.230	.370	.390	.140	.160
19a3	71	40	31	.205	.350	.370	.145	.165
15a1	53	23	18	.181	.237	.259	.056	.078
15b4	64	38	28	.163	.262	.305	.099	.142
15a3	60	31	20	.147	.224	.245	.077	.098
15a2	60	27	16	.142	.206	.224	.064	.082
16b4	59	26	18	.137	.230	.230	.093	.093
15b5	54	33	23	.132	.208	.245	.076	.113
16b6	61	34	18	.126	.220	.215	.094	.089
16b5	56	24	19	.122	.200	.214	.078	.092
15b6	49	27	20	.106	.163	.197	.057	.091

fourth. Beyond these the bands are very faint, but densitometer measurements indicate that they still exist, since the decrease in transmission on the long wave side of the limit in the curves of Fig. 5 is due to them. By raising the furnace temperature 100° above the temperatures commonly used, it is possible to wipe out completely all light except in the very transparent region between the lower D bands and the 3303 bands, and in the short wave-length region around 2200. It is evident, then, that a semi-continuous but variable band absorption must be considered even below the series limit. We can roughly extrapolate the curve beyond the series limit, assuming the atomic absorption to be absent, but this will not give a definite form for the absorption function of which we can be certain. It will not serve, for instance, to differentiate between Kramers' λ^3 law and Milne's λ^2 law.

For this reason it does not seem possible in the present paper to determine rigorously the exact relation between atomic absorption and wave-

length. Where other elements are used, as potassium, this function should be similar, whereas the band absorption will probably be found different. Therefore a detailed discussion of this relation will be reserved until results for one or more other metals have been obtained. A determination of the relative intensities of the absorption series lines in sodium is now in progress, this being independent of bands.

The writer wishes to express his gratitude to Professor D. L. Webster for his interest and advice in the early part of the work, which was done at Stanford University, and to Professors Theodore Lyman and F. A. Saunders for similar favors during its completion.

JEFFERSON PHYSICAL LABORATORY,
HARVARD UNIVERSITY.
June 15, 1924.

SOFT X-RAYS AND SECONDARY ELECTRONS

By Joseph A. Becker*

Abstract

Velocity distribution of photo-electrons excited by soft x-rays.—The apparatus was similar to that used in the magnetic analysis of β rays. Soft x-rays excited by primary electrons with 150 to 1500 volts energy, fall on a radiator of W, Pt, Al, etc. The photo-electrons emitted in a plane approximately normal to the uniform magnetic field acting, each travel in a circle with a radius proportional to the speed; those of a given speed which pass through two fixed slits strike a photographic plate, after describing a semi-circle, along a line depending on their speed, thus giving a spectrum. The plates each show a sharp line with a considerable amount of energy right at the $h\nu$ limit corresponding to the energy of the primary electrons. A band due to electrons which had lost from 4 to 11 volts in coming out of the radiator, was also observed. These lines and bands indicate that free or loosely bound electrons are more readily ejected than internal electrons by soft x-rays. However, other lines were obtained due to electrons from various levels of the radiator atoms, with energies diminished by amounts corresponding to the critical potentials.

Critical potentials obtained by magnetic analysis of photo-electrons.—For *aluminum* radiator: L_2L_3, 70 volts; L_1, 80 volts. For *silver*: N_1, 134 volts; M_6, 365-370 volts. When the target for the primary electrons got covered with tungsten oxide, x-rays corresponding to jumps between N and O levels produced photo-electrons of corresponding energy. In this way the following *characteristic lines in the* N *spectrum of tunsgten were observed:* N_3O_5,410; N_2O_4, 482; N_1O_3, 560; N_5O_2, 305; and N_4O_2, 312, all in volts. N_4O_6 is missing, indicating that the O_6 level is not occupied. All the values agree well with the Bohr theory predictions and with other results.

RUTHERFORD,[1] De Broglie,[2] Ellis,[3] and Robinson[4] have shown that beautiful, clearcut, and precise results can be obtained from a magnetic analysis of the velocity distribution in a beam of photo-electrons produced by γ and x-rays, and that this method can be used to measure the absolute frequencies of x-rays with a precision comparing favorably with that which can be obtained by the use of crystals. The following article describes the application of this method to radiation in the soft x-ray region produced by 200 to 1000 volt electrons. This radiation can give important evidence on atomic structure. Incidentally it appeared that the apparatus was also well suited for the study of secondary electrons.

*National Research Fellow.

[1] Rutherford and Robinson, Phil. Mag. **26**, 717 (1923); **28**, 277 (1914).

[2] DeBroglie, Jour. de Phys. et Rad., Sept. 1921, p. 265.

[3] Ellis, Proc. Roy. Soc. **A99**, 261 (1921); **A101**, 1 (1923).

[4] Robinson, Proc. Roy. Soc. **A104**, 455 (1923).

Fig. 1 shows the essential parts of the apparatus. The housing consists of a brass cylinder with an inside diameter of 20 cm and a height of 5.0 cm which is screwed onto a base and made airtight by means of a rubber gasket and 36 screws. T is a target screwed into the top of the cylinder. The electrons are supplied by a hot spiral filament which is about 1 cm above the target. The grid G consists of a cylinder completely surrounding the target and filament. On the side towards R this cylinder has an opening covered over with a thin wire screen of about 1 mm mesh. Thus radiation and, if the potentials are suitable, also secondary electrons from T can strike the radiator R. Any photo-electrons and tertiary electrons coming from R in the proper direction are bent into circular paths by a

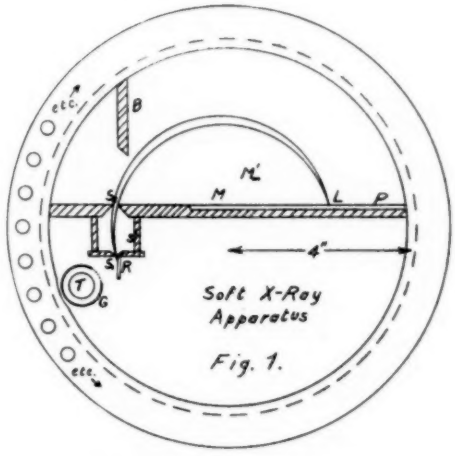

Fig. 1. Sketch of apparatus.

magnetic field perpendicular to the plane of the figure, pass through a narrow slit S_1 and a broader slit S_2, and then strike a Schumann photographic plate P. The magnetic field is produced by a large cylindrical solenoid which can be lowered over the whole apparatus. Its length is 127.2 cm; its mean radius 13.8 cm; its constant 13.05 gauss per ampere. All the electrons from R which have the same velocity and have the proper direction so they can pass through S_1 and S_2 will produce a single line L on P whose width is only slightly greater than S_1, which was usually 0.1 to 0.4 mm, while S_2 was 2.0 mm wide. The relation between this velocity v, the radius of the path ρ, and the magnetic field strength H is given by

$$\rho H = mv/e. \tag{1}$$

ρ can readily be computed from the distances S_1S_2, S_2M, and ML where M is a sharp-edged or sharp-pointed piece of brass placed immediately

above P so as to cast a shadow on P. Hence v can be determined and from it the equivalent voltage or the equivalent frequency ν given by

$$Ve = \tfrac{1}{2}mv^2 = h\nu. \quad (2)$$

M' is another marker used to test the sharpness of the shadow cast by the electrons. B is a baffle plate.

The chamber is evacuated by means of a two stage mercury vapor pump backed by a Cenco oil pump. With the filament cold, the pressure as indicated on a MacLeod gauge was less than 10^{-6} mm. With a hot filament the pressure rose to 1 or 2×10^{-4} mm, depending on the type of filament. Ordinary Coolidge tube tungsten filaments were first used but later it was found more advantageous to use oxide coated platinum. Unfortunately the apparatus could not be baked out because of its size and the use of rubber gaskets. This had the result that the target would almost invariably become contaminated. Consequently most of the runs were made with a brass target and only the radiator was changed. It would undoubtedly be advantageous to have everything enclosed in glass and use modern high vacuum technique. Presumably this would necessitate the use of an electrostatic detector since the photographic plate could not stand the baking. The currents involved are not so extremely small as to make this a difficulty.

In the earlier experiments the filament was connected to the negative end of a generator whose voltage could be varied from 300 to 1400 volts. It was found, however, that the voltage varied during each revolution, and besides that there were considerable fluctuations of the r.m.s. value. Later, storage batteries were used almost exclusively for the accelerating voltage, which was varied from 150 to 250 volts.

In all about 150 plates have been exposed. About half of these have been worth saving. In describing the work the results will not be presented in the order in which they were obtained but rather in an order which will bring out the facts most clearly.

Plate R1, shown in Fig. 2, was taken under the following circumstances: Target of brass; radiator of aluminum; filament at -192 volts; target, cylinder, and radiator at zero potential; grid at -203 volts or 11 volts more negative than the filament; filament drop 2.2 volts; field strength 7.46 gauss; current of 10 m-amp. filament to target for $1\frac{1}{2}$ hours. The 192 volt electrons which strike the target produce either soft x-rays or secondary electrons. Of these only the rays can get through the grid to the radiator since the field which opposes the electrons which travel from the target toward the grid is 11 volts greater than the field which has accelerated them. The radiation which strikes the radiator can either eject electrons which are free or only loosely bound to atoms, or electrons

which are located at an atomic energy level whose critical voltage V_c is less than the equivalent voltage of the radiation V_r. In the first case the equivalent voltage of the line which appears on the plate V_l will be equal to V_r. In the second case

$$V_l = V_r - V_c . \tag{3}$$

If the atom from which the photo-electron is expelled is beneath the surface, the electron may lose more or less energy in getting out of the radiator and consequently will register with a slower speed than those which come from surface atoms. We should therefore expect a band with a sharp intense edge on the high velocity or right side and which gradually becomes weaker towards the left. The most conspicuous feature of plate R1 is the narrow line A. Its high velocity edge corresponds to 192 ± 2

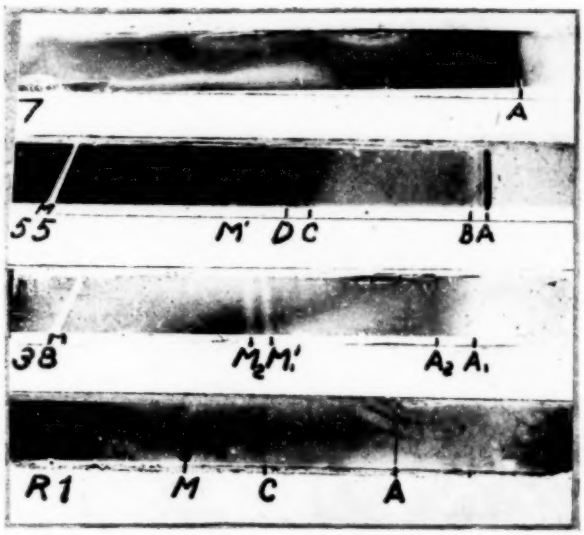

Fig. 2. Plates 7, 55, 38, R 1.

volts; its width corresponds to 2 volts. The only way we can explain this line is by assuming (1) that 192 volt electrons which strike the target produce x-rays whose energy distribution curve has a narrow sharp peak right at the $h\nu$ limit, and (2) that when this monochromatic radiation strikes the radiator it ejects electrons which are free or loosely bound more readily than others. The width of the line corresponds to the velocity distribution of the primary electrons due to the filament voltage drop.

The head of the band at C can also be explained as due to the same incident x-rays which have produced A. In this case, however, the

electrons are apparently ejected from the energy level next beneath the valence shell. If we number the energy levels in order from the nucleus outward this is the L_3 level of aluminum. The voltage of the edge of C is 122 volts. The critical voltage of the L_3 level computed from (3) is then 70 volts. Bohr and Coster[5] assign 70 volts to the L_3 and L_2 levels.

On the original negative a third faint band can be seen to the left of C. Treating it in the same way as C we conclude that it is due to electrons which have come from the L_1 level of aluminum and have lost 80 volts in getting out of the atom. This value agrees well with Millikan and Bowen's[6] value of 83 volts.

These assumptions concerning the energy bunching at the $h\nu$ edge and the ejection of free electrons received further support from the following experiments: Plate 38 (Fig. 2) was exposed without any radiator for 11.5 m-amp.-hr. with an accelerating field of 525 volts from the generator. That the voltage from the generator fluctuated during each revolution is shown by this and numerous other plates such as plate 7 (Fig. 2) in which the band corresponding to A was broadened out. For plate 38 (Fig. 2) an additional marker M' was placed 2 cm from the plate as shown in Fig. 1. This new marker actually cast two sharp and distinct shadows M_1' and M_2' on the plate. By using one of these shadows, together with M' and S_2 as three points on a circle, it was clearly shown that S_1 was acting as one source of electrons and that another source was located at S_1' the intersection of the line TS_1 and the side of the tube supporting S_1 and S_2. Furthermore there were two distinct A bands in the right places to support this conclusion. It would be impossible for secondary electrons from T to produce these effects. To clinch the argument a thin collodion window weighing 0.8 mg/cm² was placed over S_1 and the experiment performed. This also gave two A bands in the same positions as before but much weaker, while radiation for the lower voltages was almost entirely absorbed. These bands must therefore be due to x-radiation and cannot be caused by secondary electrons from T. Of course in future plates double sources were avoided by obvious methods.

The second assumption made above, namely that in this region of voltages, 150 to 500 and perhaps higher, the electrons most easily ejected are the free or most loosely bound electrons, receives further support from three plates which are not reproduced here. Plate 9 was the result of an accident. Early in the exposure a stopcock was accidentally turned

[5] Bohr and Coster, Zeits. f. Phys. **12**, 342 (1923)

[6] Millikan and Bowen, Phys. Rev. **23**, 1 (1924)

so as to admit air into the chamber. This oxidized the tungsten filament which was being used and as a result tungsten oxide was deposited over the radiator and target. The accelerating voltage in this case was 1350 to 1430 volts, but the field strength was such that any high velocity electrons would be stopped by the baffle plate *B*. The plate showed two unmistakable bands and three or four others which might be classed as doubtful but quite probable. The strongest ones had equivalent voltages of 410 and 475. If we use Bohr's values and apply the selection principle to predict what lines should occur in the N spectrum of tungsten, we find that the two strongest ones correspond to jumps N_3-O_5, and N_2-O_4 with 410 and 482 equivalent volts. Other jumps that are predicted are N_1-O_3, N_5-O_3, and N_4-O_2 with 551, 305, and 314 volts. The other faint lines on the plate correspond to 560, 305, and 312 volts. This agreement is possible only if we assume that the photo-electrons were essentially free in the atom. The fact that no line appeared for the N_4-O_6 jump which should be a strong line according to the rule, indicates that the O_6 level has not yet been filled in tungsten.

Similar evidence although less complete was obtained from plates 29 and 31, in which the targets consisted of thin sheets of zinc which were supported so as to be heated and vaporized by the bombarding current. In this case the bands corresponded to the L spectrum of zinc. It is significant that these two cases are the only ones in which we have been able to obtain radiations characteristic of the target material. Usually our targets were cool while here they were probably vapors. This would agree with the experience of Foote and Mohler and others, that the efficiency of transformation of electronic to radiant energy is much greater for vapors than solids.

Plate 55 (Fig. 2) shows several interesting features. This plate was taken with a copper target and brass radiator. There is the customary band *A* corresponding to the $h\nu$ radiation ejecting detached electrons, and the band *C* which is produced by the same $h\nu$ radiation ejecting *M* electrons out of zinc and copper in the radiator, thus causing the band to be blurred. At *D* we have a clear case of a reversed band, i.e. increase in blackening towards lower velocities and then a sudden break. We believe that this phenomenon can only be the result of an absorption edge in the photographic plate. We think this band at 134 volts is due to the N_1 or innermost absorption edge of silver. Electrons having more than this energy can excite the silver atom more readily than electrons with a smaller energy. On a number of plates we have found such reversed

bands for the M_6 level of silver at 365 to 370 volts, and for the M_3 level of bromine at 160 volts.

For this plate and all the plates yet to be described, the grid was always at the same potential as the target. Consequently any secondary electrons from the target could strike the radiator and produce tertiary electrons which could then reach the photographic plate. On plate 55 (Fig. 2) to the left of band *A* there is a region of about 2 mm with practically no more blackening than that due to fogging and scattering; then band *B* begins. This new band does not have an intense head and changes its intensity gradually, usually decreasing and then increasing toward the left until at the low velocities it is the most intense feature on the plate. Since on the original plates the background is usually much more pronounced when the grid is at zero potential than when it is more negative than the filament, and since in the latter case there is no head to indicate the presence of band *B*, we think that this band is due to secondary electrons. The distances between *A* and *B* varies from 4 to 11 volts, depending on the radiator. Part of *A* may also be due to secondary electrons. If our analysis is correct we can conclude that when an electron enters a solid and comes out again it has lost either no energy or at least 4 to 11 volts.

Plates obtained with platinum, brass and aluminum as radiators showed that the intensity of *A* decreases as the atomic number of the radiator increases, and as the resistance increases. It would be interesting to decide which if either of these two is the controlling factor.

These plates illustrate a few of the results that one can hope to obtain by studying soft x-rays and secondary electrons with a magnetic analysis method. The conclusions these experiments seem to force on us are startling indeed, but no other explanation is satisfactory. In ordinary x-rays there is no bunching of energy at the $h\nu$ limit. Holweck,[7] however, who has made a lengthy study of soft x-rays, also came to the conclusion that in the soft x-ray region most of the energy is near the short wave-length limit. The conclusion that for soft x-rays there is a considerable amount of bunching right at the $h\nu$ limit should be a useful tool in the future study of these rays. It ought to be instructive to see whether there is any bunching near the $h\nu$ limit for rays in the neighborhood of 10 A which could be studied by crystal methods in a vacuum spectrograph.

The conclusion that the free or loosely bound electrons are most strongly affected by soft x-rays is not so surprising. For penetrating x-rays the most tightly bound electrons are most readily affected, but

[7] Holweck, Ann. der Phys. **17**, 5 (1922).

as the rays get softer this rule must be modified as both Ellis[3] and Robinson[4] have shown.

In conclusion, the author wishes to express his thanks to Professor R. A. Millikan for his continued interest and stimulation in the work. He is also indebted to Mr. E. L. Rose, who is continuing the work, for his assistance in conducting some of the later experiments.

NORMAN BRIDGE LABORATORY OF PHYSICS,
PASADENA, CALIFORNIA.
June 10, 1924.

INDEX OF REFRACTION OF CALCITE FOR X-RAYS

By C. C. Hatley

Abstract

Index of refraction of calcite for MoKα_1 rays.—Previous work has indicated that in the case of first order reflection from calcite the bending due to refraction is only 3″. As suggested by Bergen Davis, however, the effect can be greatly increased by using a wedge shaped crystal with a surface ground and polished so as to make an angle φ with the cleavage planes slightly less than the angle of reflection. The first crystal was ground with φ equal to 5°48.3′ so that rays which entered at an angle of 12.5° with the surface, after first order reflection left making an angle of 54′ with the surface. The refraction bending was 29″. A second crystal was ground with $\varphi = 6°21.5'$ so that the glancing angle was only 21′ and the refraction bending was 64″. The lack of symmetry due to the refraction bending at one surface was determined either by rotating the crystal about a horizontal axis perpendicular to the crystal planes or by using two halves of a split crystal, one ground and the other with natural cleavage, placed one over the other so as to get reflection from each in turn. The mean result is $\mu = 1-(2.03\pm.1)\times10^{-6}$. This agrees well with the value given by the Lorentz dispersion formula, $1-1.91\times10^{-6}$.

Wave-length of MoKα_1 corrected for refraction.—The correction is .017 per cent for first order reflection by calcite. Special measurements gave the corrected wave-length as .70772A (assuming $d = 3.028\times10^{-8}$), in good agreement with Duane's value.

SINCE the discovery of x-rays the question of their refraction has been of considerable interest to the physicist. Roentgen and others were satisfied that x-rays passed through matter without being refracted. This was explained on the assumption that the atoms contained no electrons whose natural frequencies were near those of x-rays a view in harmony with the earlier pulse theory of x-radiation. The above assumption is now known to be untenable.

Chapman[1] made the first effort to measure with any degree of precision the index of refraction of a substance for x-rays. He used a prism of ethyl bromide and concluded that the index differed from unity by less than 3×10^{-4}. Later Barkla[2] used two prisms of potassium bromide and showed that the index differed from unity by less than 5×10^{-6}. Webster and Clark[3] concluded from theoretical considerations that the maximum refractive effect of a resonance frequency was limited to a narrow band of the spectrum. Their results, using a rhodium prism, showed that the

[1] Chapman, Proc. Camb. Phil. Soc. (1912) p. 574
[2] C. G. Barkla, Phil. Mag. **31**, 257 (1916)
[3] D. L. Webster and H. Clark, Phys. Rev. **8**, 528 (1916)

index must differ from unity by less than 2×10^{-4} over quite a range of the spectrum.

Stenstrom[4] first noticed deviations from Bragg's relation, $n\lambda = 2\,d \sin\theta$, and attributed them to the refractive effect. His method of measurement involved the determination of the relative displacement of the different orders of a characteristic radiation when reflected from the crystal to be tested. He gives values for the index of refraction of sugar crystals and of calcium sulphate for wave-lengths near 3 A. In the case of calcite, the displacements were very small when compared with the magnitude of the possible errors, so no actual value was obtained for the index. Darwin[5] seems to have been the first to point out that Bragg's relation cannot be strictly true and to give the relation between θ, the observed glancing angle, and θ_1 the glancing angle given by Bragg's relation as

$$\theta - \theta_1 = \delta \operatorname{cosec}\theta \sec\theta$$

where $1-\delta$ is the index of refraction of the crystal for the x-rays. Duane and Patterson[6] and Siegbahn[7] have found that wave-lengths determined by Bragg's law differ slightly for different orders.

If a substance has a refractive index less than unity it is possible to determine its value by means of total reflection. A. H. Compton[8] has in this way obtained values for glass, silver and lacquer which show a remarkably close agreement with those predicted by the Lorentz equation. Davis and Terrill[9] determined the index of calcite both by Stenstrom's method and the total reflection method. By the first method they obtain a value of 3×10^{-6} for δ but the error limits were such as to make this result very uncertain. The value found by total reflection is $1.7 \pm .5\times10^{-6}$.

The purpose of the present work was to determine the index of some calcite crystals with a much higher degree of precision than has been obtained heretofore, using two independent methods.

Spectrometer

The spectrometer used in this investigation was the one used by Davis and Terrill in their measurements,[10] with the added advantage that an optical lever was used to check all calibrations. To calibrate the worm

[4] Strenstrom, dissertation, Lund (1919)
[5] C. G. Darwin, Phil. Mag. **27,** 318 (1914)
[6] Duane and Patterson, Phys. Rev. **16,** 532 (1920)
[7] M. Siegbahn, Comptes Rendus (1920) p. 1350; idem (1922), p. 745.
[8] A. H. Compton, Bull, Nat. Research Coun. No. 20, p. 48 (1922); Phil. Mag. **45,** 1121 (1923)
[9] Bergen Davis and H. M. Terrill, Nat. Acad. Sci. **8,** 357 (1922)
[10] H. M. Terrill, J. Opt. Soc. Amer. (May 1922)

gear by which the crystal table was slowly rotated, a millimeter scale was reflected from a plane mirror on the crystal table back over a path of about 110 feet into a three inch telescope. A deviation of one second in three hundred, the scope of a single calibration, could be detected. The least count on the worm gear read to 3 seconds and could be estimated to half seconds. The complete calibration showed that the worm gear was slightly eccentric. Although a complete revolution of the worm introduced an error of less than one part in 7000, equal fractions of a revolution of the worm, taken at different angular positions, revolved the crystal through slightly different angles. Tables II and III have been corrected for this eccentricity. The error due to this, however, turned out to be only a small part of the total possible error due to the screw, since in most of the work it so happened that either the worm was turned for each setting through a whole number of revolutions or else the error was cancelled by turning the worm first in one direction and then in the opposite direction.

I. Wedge Method

If we assume that x-rays are propagated as electromagnetic waves and that the Lorentz equation holds approximately, we are to expect refraction to cause a displacement of the Mo $K\alpha_1$ first order line when reflected from calcite, of only about three seconds of arc when the glancing angle is about $6^\circ\ 42'\ 43''$. The effect may be considerably increased, however, by adopting a method suggested by Prof. Bergen Davis. A clear calcite crystal was ground and polished to an optical surface on the (100) face, so as to make an angle φ of $5^\circ\ 48'\ 20'' \pm 20''$ with the cleavage planes of the crystal, thus presenting a wedge-like appearance. The crystal was mounted on the spectrometer table and also on the end of a horizontal axle which enabled it to be rotated 180° about a horizontal axis so that either the thin edge AD of the crystal or the thick edge BC could be placed nearest the source of x-rays (Fig. 1). In the first position, called the obtuse position, the radiation from the direction P_1T makes an angle $(\theta_1+\varphi)$ with the polished surface AB (where θ_1 is the Bragg angle for the Mo$K\alpha_1$ radiation used and φ is the angle BAO of the polished face with the crystal planes), and is reflected in the direction OSQ_1', making an angle $r=\theta_1-\varphi$ with the polished surface. Since the angle r in this case is less than one degree, the refraction at the surface is not negligible as is the case at T where the angle of incidence is over 12°, so the emerging ray SQ_1 makes an angle i with AB which is greater than r. We shall call the difference γ so that $i=r+\gamma$.

Now suppose the crystal rotated 180° about an axis XX' which is exactly perpendicular to the crystal planes. This is equivalent to supposing the rays come from the right instead of the left. Evidently the rays must strike the surface AB in the direction Q_1S in order to be reflected. But this direction makes an angle $\theta_1+\gamma$ with the cleavage planes whereas the incident rays actually make the angle θ_1, the same as in the first position. Hence the crystal must be turned about a vertical axis so as to increase the angle of incidence by γ. By measuring this angle of turning, we measure γ.

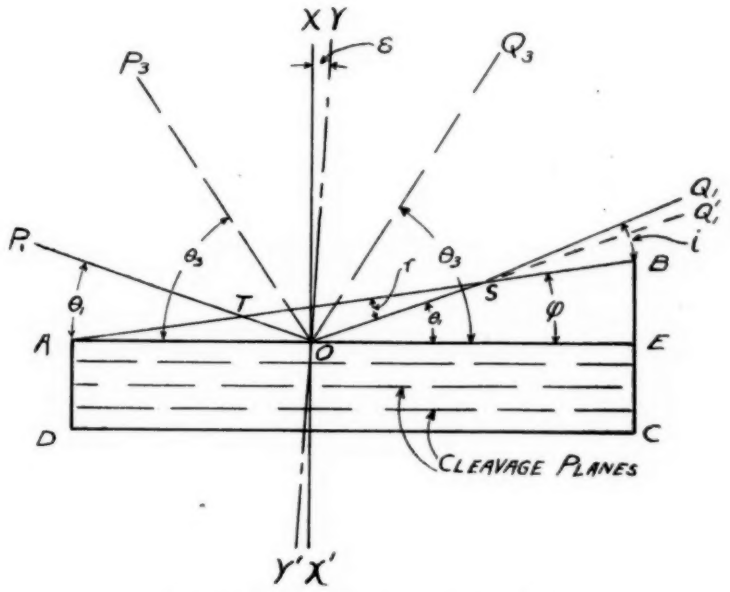

Fig. 1. Paths of rays in wedge method.

Now suppose the horizontal axis is not exactly perpendicular to the crystal planes but has a direction YY' making a horizontal angle ϵ with the perpendicular to the planes XX'. After a rotation of exactly 180° about this axis the angle between the incident x-rays and the crystal planes is not θ_1 but $\theta_1-2\epsilon$, and to get reflection the crystal must be turned so as to increase the angle of incidence by $2\epsilon+\gamma$. The value of 2ϵ may be determined however by use of the third order reflection P_3OQ_3. Here the angles are so large that the refraction is negligible; therefore after rotation through 180° the angle which the crystal must be turned through to give reflection is equal to 2ϵ.

The actual procedure was to mount the crystal as shown in Fig. 1 for obtuse reflection and so orient it as to reflect the third order of Ka_1. The

angular reading was called B_3'. Then the crystal was turned so as to reflect the first order $K\alpha_1$, the reading being called B_1'. After rotation through 180° about the horizontal axis, corresponding readings B_1 and B_3 were taken. Evidently $B_3-B_3'=2\epsilon$ and $B_1-B_1'=2\epsilon+\gamma$. Hence

$$\gamma=(B_1-B_1')-(B_3-B_3')=i-r. \tag{1}$$

The index of refraction is given by

$$\mu=\frac{\cos i}{\cos r}=\frac{\cos(r+\gamma)}{\cos r}=1-\delta \tag{2}$$

where $r=\theta_1-\varphi$. Since $\cos(r+\gamma)=\cos i\cos\epsilon-\sin r\sin\epsilon=\cos r-\epsilon\sin r$, evidently

$$\delta=\gamma\tan r=[(B_1'-B_1)-(B_3'-B_3)]\tan(\theta_1-\varphi), \tag{3}$$

and it is unnecessary to determine r with greater precision than γ can be measured.

We have assumed that refraction for angles 12° and greater is negligible. After the index has been approximately determined, however, the various readings can be corrected for the refraction and still more accurate values obtained. In Table I are given the refractive effects for the various orders computed by using the mean values of δ obtained from the results of both methods given below.

TABLE I

Refractive effect computed for various orders of reflection.

Order	Angle of incidence	Refractive effect $\gamma=(i-r)$
1st acute	54′ 51″	28.0″
2nd "	7° 42′ 47″	3.0″
3rd "	14° 43′ 15″	1.6″
1st obtuse	12° 31′ 03″	1.9″
2nd "	19° 19′ 27″	1.2″
3rd "	26° 19′ 55″	.8″

PROCEDURE

The x-rays were rendered practically parallel by means of two narrow slits 28 cm apart between lead blocks adjustable by micrometer screws. By using slits only .02 mm wide at the first order, a beam parallel within 30″ was obtained. The tube carried about 1.5 kw so that the peaks of the curves from which the line positions were determined with reference to the direction of the incident x-rays were very sharp; at half maximum the width of the curves from which $K\alpha_1$ first order was located were less than 1.5′ of arc. The crystal was mounted on the spectrometer table and so oriented as to reflect the third order of $K\alpha_1$ in the position of obtuse

incidence; then having determined the angular direction B_3' of this line (OQ_3 Fig. 1), the crystal was turned by means of the worm gear into position to reflect first order $K\alpha_1$ and the angular direction B_1' of this line SQ_1 determined. The crystal was next rotated through 180° about the horizontal axis YY', then rotated around the vertical axis a few minutes of arc γ until first order of $K\alpha_1$ in the position of acute incidence was reflected, and reading B_1 taken. Finally the crystal was rotated so as to reflect $K\alpha_1$ third order acute incidence and reading B_3 made. The first four columns of Table II give the result of a number of determinations. Similar readings made for the second order are denoted by B_2 and B_2'.

TABLE II

Readings made with wedge of 5° 48′ 20″.

B_1	B_1'	$(B_3'-B_3)$	γ_3	$(B_2'-B_2)$	γ_2
114° 58′ 46″	115° 08′ 31.1″	10′ 10.8″	25.7″	10′ 05.8″	20.7″
114° 58′ 41″	115° 08′ 30.1″	10′ 12.8″	23.7″	10′ 15.8″	26.7″
114° 58′ 38″	115° 08′ 28.1″	10′ 19.8″	29.7″	10′ 17.8″	27.7″
114° 58′ 41″	115° 08′ 19.1″	10′ 07.8″	29.7″	10′ 12.8″	34.7″
114° 58′ 28″	115° 08′ 08.1″	10′ 13.8″	33.7″	10′ 06.8″	26.7″
114° 57′ 39″	115° 07′ 13.1″	10′ 04.8″	30.7″	10′ 05.8″	31.7″
114° 57′ 29″	115° 07′ 14.1″	10′ 15.8″	30.7″	10′ 14.8″	29.7″
		Averages	29.1″		28.3″

Final average 28.7″

All readings in the above table have been corrected for eccentricity of the worm gear and all except B_1 have been corrected for refraction in accordance with Table I. From equation (1) γ is known and μ is determined from equation (2). The fifth column of Table II gives a value for γ exactly analogous to column three, using the corrected readings for the second order reflections. Since the B's in columns three and five have all been corrected for refractive effects it is clear that we should have

$$(B_3'-B_3)=(B_2'-B_2)=2\epsilon.$$

The differences between columns 3 and 5 are not much greater than the errors of experimentation. This is likewise true of columns 4 and 6. The average of γ_3 and γ_2 was used in the final determination of the mean index by this method which gave

$$\delta=(2.21\pm.16)\times10^{-6}.$$

II. Differential Wedge Method

In this method the crystal is rotated through only a small angle and less than a complete revolution of the worm gear (10′ of arc) is used. The ionization chamber is not moved and the collimating slits are not

changed during a determination. This was accomplished by having only the upper half of the crystal ground and polished to the desired angle, leaving the lower half a natural crystal.

In Fig. 2, let the lower half of the compound crystal $A'B'CD$ present cleavage faces only while the upper half $ABCD$ has one ground and polished face AB making an angle $6°21'30''\pm20''$ with the cleavage planes. In order to do this polishing the crystal must be split in half, but we will suppose the two halves are cemented together again so that cleavage planes of each are accurately parallel. Then readings taken by reflecting first from the lower half and then from the upper half should differ by the angle between SQ and SQ' which as in Fig. 1 is equal to $i-r=\gamma$, and from this and $(\theta_1-\varphi)$, μ and δ can be immediately determined. If, however, the crystal planes of $A'B'C'D'$ make an angle ψ with those of $ABCD$ the difference in readings will be $\psi+\gamma$ and ψ must be determined either by use of second and third order or by reflection from the back surfaces CD and $C'D'$, assuming these are parallel to the respective front cleavage planes.

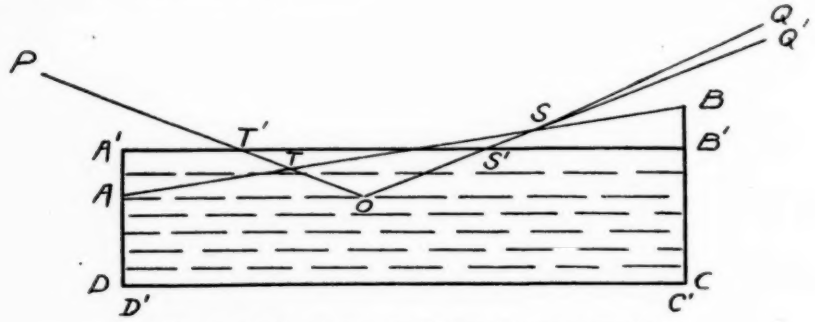

Fig. 2. Paths of rays in differential wedge method.

Procedure

The compound crystal was mounted on the table so as to reflect from either of the two cleavage surfaces CD or $C'D'$. The positions of $K\alpha_1$ third order for the upper and the lower half respectively were determined. This difference B_3-B_3' determines the angle ψ, the lack of parallelism between the (100) planes of the upper and lower halves. The crystal is now moved across the table a distance equal to its thickness. Reflection may now take place from either half face AB or $A'B'$ (Fig. 2). The angular position B_1' of the crystal when reflecting $K\alpha_1$ first order from the split half $A'B'$, the upper half being covered, is determined. The crystal is rotated a few minutes of arc and its position B_1 when reflecting the same line first order from the ground-polished face AB, is

determined. Table III gives the five separate sets of readings. All the readings have been corrected for the eccentricity of the worm gear and B_1' has been corrected for refraction. Since φ in this case is larger than in the first case, the glancing angle i is less and the value of γ is greater.

TABLE III

Readings made with differential wedge of 6° 21′ 30″.

B_1	B_1'	(B_3-B_3')	γ
66° 02′ 06.5″	65° 53′ 34.5″	7′ 32″	1′ 00″
66° 02′ 07.5″	65° 53′ 28.5″	7′ 34″	1′ 05″
66° 02′ 24.0″	65° 53′ 44.0″	7′ 34″	1′ 06″
66° 02′ 01.0″	65° 53′ 21.0″	7′ 33″	1′ 07″
66° 02′ 02.5″	65° 53′ 30.5″	7′ 32″	1′ 00″
		Average	1′ 03.6″

The method of computation of μ and δ is the same as for the first method.

The average deviations in Table III are of the same order as those in Table II.

Since the angle of incidence is smaller with this wedge than with the wedge used in Method I, the peaks of the curves are broader and consequently the determination of the position is less accurate in II than in I. In the second method the line reflected from the polished face could not be located by a single trial closer than 4 or 5 seconds. This broadening of the peak of the line accounts for the deviations in table III. From the curves the lines with wedge I could be located to within 2 or 3 seconds since the peaks of the curves were sharp. The deviations in Table II are chiefly due to the fact that the crystal had to be rotated over larger angles and many other adjustments made that were avoided in method II. Since the average absolute deviations are about the same for the two methods and since the refractive effect is over twice as great in II as in I the results from method II are weighed twice as much as those from method I.

The average deviation in each method is near 3″. The number of determinations is too small to warrant the use of the probability law to establish the precision. Instead a value of 2″ is chosen as best representing the precision of the final results.

The final value is expressed in terms of δ instead of μ.

From method I, $\delta = (2.21 \pm .16) \times 10^{-6}$;

From method II, $\delta = (1.94 \pm .06) \times 10^{-6}$.

Final mean, $\delta = (2.03 \pm .09) \times 10^{-6}$.

This value for δ agrees very well with that given by the Lorentz equation for refraction which in the simplified form required by this case may be written

$$\delta = Ne^2/2\pi m\nu^2 = 1.91\times 10^{-6}\,.$$

The critical frequencies of the calcite are too far removed from the frequency of the incident radiation to show any of the effects of resonance involved in the development of the Lorentz dispersion formula.

Correction of Wave-Length for Refraction

The value of θ, the angle made by the external incident beam and the surface, was determined for Mo $K\alpha_1$ reflected from a split crystal. First the radiation was reflected to the right and the angular position of the crystal was recorded. Then the crystal was rotated around the vertical axis of the spectrometer through $(180°-2\theta)$ so that the energy was reflected to the left. The angle $(180°-2\theta)$ was determined by means of the optical lever and the worm gear described above. The average of the two positions gives the zero of the crystal and the value of θ. From this value and the value of δ given above, the magnitude of θ_1, the true angle between the internal incident beam and the planes, was computed by the equation

$$\sin\theta_1 = \sin\theta - \delta\tan\theta\cos\theta.$$

Using the first orders of $K\alpha_1$, the value of θ comes out $6°\ 42'\ 44''$. When all three orders are properly weighted, the average value is $6°\ 42'\ 43.3''$. This value of θ when substituted in above equation gives $\theta_1 = 6°\ 42'\ 39.8''\pm .5''$. If we assume a value for d of 3.0280×10^{-8} cm for calcite and compute γ from Bragg's relation we get for Mo $K\alpha_1$

$$\gamma\ (\text{in calcite}) = .707718\pm 15\ \text{A.}$$

Due to refraction, the value in air will be slightly less and is given by

$$\gamma\ (\text{in air}) = \gamma\ (\text{in calcite})\times(1-\delta) = .707717\pm 15\ \text{A.}$$

If we allow for refraction this agrees very well with Duane's value $.70783\pm 8$ A.

The writer wishes to express his indebtedness to Professor Bergen Davis who suggested the problem and gave many valuable suggestions during the experimental work, and to other members of the Physics Department of Columbia University for their interest and assistance throughout the investigation.

Columbia University,
May 22, 1924.

COLORATION OF THE ALKALI HALIDES BY X-RAYS

By P. L. Bayley

Abstract

Coloration of alkali halides and other salts by x-rays.—(1) *Hues produced.* CsF, RbF, CaF_2, CsCl, RbCl, KCl, NaCl, LiCl, AgCl, BaCl, BeCl, $CaCl_2$, CsBr, RbBr, KBr, KI, NaI, CdI, HgI and K_2SiO_3 were colored, whereas KF, NaF, LiF, NaBr, RbI, ZnCl, NH_4Cl and about 20 other salts showed no coloration with 5 hours exposure to intense radiation. (2) *Spectral absorption of colored halite and sylvite.* Halite (NaCl), colored amber, has a broad absorption band from 0.3μ to 1.3μ with a maximum at 0.46μ. Sylvite (KCl), colored purple, has a similar absorption band with a maximum at 0.55μ. (3) *Spectral fading of colored alkali chlorides.* The colors fade logarithmically when exposed to daylight, the time varying from a few seconds to days. When exposed to the spectrum of a 500 watt Mazda C lamp, colored NaCl, KCl, RbCl and CsCl fade most rapidly at wave-lengths 0.51μ, 0.61μ, 0.68μ and 0.62μ respectively. When correction is made for the energy distribution, halite and sylvite are found to fade most rapidly at wave-lengths where their absorption increase due to their coloration is a maximum.

HOLZKNECT[1] was the first to discover that x-rays produce in certain chemicals colors similar to those due to cathode ray bombardment and to exposure to radiation from radium compounds. Colors produced by any such type of radiation usually fade under the action of light. Holzknect found it necessary to cover many materials with black paper in order that the x-rays might produce coloration in them. For such substances, the rate of fading due to light in the room exceeded the rate of production of the color by the radiation. Attention was directed, in this laboratory, to these phenomena when Perrine,[2] studying the ultra-violet fluorescence produced by x-rays in such materials, noticed that in nearly every case the materials that gave off fluorescent light were colored at the end of the required long exposure. The author, after observing the hues[3] of the colors in many compounds, has studied the physical properties of the colors chiefly in halite (natural sodium chloride) and sylvite (natural potassium chloride).

A Coolidge x-ray tube of 30 m-amp. capacity was used and was operated at 50 kv and 3 m-amp. The samples were placed in a thin light-tight paper box within two inches of the tube and not more than

[1] Holzknect, Verh. Deutsch. Phys. Ges. **4**, 25 (1902)

[2] Perrine, Phys. Rev. **22**, 48 (1923)

[3] Throughout this paper, colors will be described by the words *brilliance*, *hue*, and *saturation*, as defined in the Report of Committee on Colorimetry, J. Opt. Soc. Amer. R. S. I. **6**, 534 (1922)

five inches from the target. In all cases reported, where no color developed, the exposure was of five hours duration. The radiation was sufficiently strong to produce noticeable coloration in CsCl and KCl within five minutes. A fan was kept running to keep air circulating around the x-ray tube so that the samples would not get warm from the heat from the tube, since heating as well as exposing to light fades these colors.

Study of Hues

The hue of the color produced depends upon the preparation of the sample. The coloration due to an impurity may mask that of the chemical under study,[4] and moisture of the sample may prevent coloration.[5] The more highly divided the particles of the material, the more unsaturated[6] are the colors. This is due to the large amount of white light reflected from the innumerable faces of the crystals of the powder. Although meaningless in general, the saturation of a few colors is given below in order to show a markedly higher saturation for those materials than for others of the same crystal size. In all the following work concerning the hues, the material was prepared in a fused mass or in as large crystals as possible so that coloration could be most surely detected if it existed.

In the table below are shown the hues observed for a group of halides. The results of a few other experimenters are included in order to show the variation in the colors obtained. The small letters after the hue indicate the speed of fading of the sample exposed to the daylight of an ordinarily light room; the capital letter refers to the experimenter, when other than the author and the final small letters to the methods of preparation of the samples, all as shown in the key following the table.

Since there seems to be no correlation between the color and the position of the element in the chemical table, no attempt has been made to state the exact hues. The word "bright" refers to the brilliance[3] and "deep" means highly saturated.

The chlorides of caesium, rubidium, and potassium were of such exceptional purity that the highly saturated colors produced in them if due to impurities must be due to extremely minute traces. Furthermore since the same hues are obtained in materials prepared by widely different methods, the coloration must be caused by the same impurities left in the compounds by several of the usual methods of purification.

[4] Goldstein, Nature, **94**, 494 (1914)

[5] Goldstein, Ann. der Phys. **54**, 371 (1895)

[6] Doelter: (a) Das Radium und die Farben, Dresden (1910), contains references to all important papers of the subject up to the date of publication; (b) Sitz. d. K. Akad. Wiss. Wein. (I) **121**, 891 (1912); (c) Idem, (II) **119**, 1091 (1910)

The following materials also were found to be colored by x-rays: AgCl, permanent bluish gray; $BaCl_2+2H_2O$ and BaCl, pale yellow; BeCl, trace of yellowish brown; $CaCl_2$, pale yellow; CaF_2 natural crystal, purplish gray; CdI, permanent brown; HgCl, permanent brown; and K_2SiO_3 fused in flame, grayish blue.

TABLE I

Coloration of alkali halides by x-rays

For comparison coloration due to cathode rays is given in round brackets, and coloration by radium rays in square brackets

	Fluoride	Chloride	Bromide	Iodide
Cs	greenish blue, *bce*	deep blue, *f*, *abd* (no color—G) [greenish—D]	blue, *vf*, *ab*	
Rb	purple, *h*, *bce*	deep sky blue, *m*, *ad* (no color—G)	greenish blue, *vf*, *be*	no color, *be* (yellowish—G)
K	no color, *bce*	deep purple, *f*, *abd* violet, *f*—H (blue, *f*—N) (violet—G)	blue, *m*, *b* blue green, *m*—H) [sea green, *f*—N] (deep blue—G)	green, *m*, *b* [brown—N] (bright green—G)
Na	no color, *ac* (rose—G)	amber, *d*, *ab* chamois yellow, *m*—H [trace yellow—D] ([brown—N]) (amber, *m*—G)	no color, *a* (rose lilac—G)	brownish yellow, *d*, *b* (heliotrope, *m*—G)
Li	no color, *bce*	faint yellow, *h*, *b* straw, *d*, *c* (purple—G)	(dark gray—G)	(brown yellow—G)

Preparation of materials (When not otherwise stated, the material was only c.p. grade)

a: Open to atmospheric moisture.

b: Heated to about 200°C in a Pyrex tube; at that temperature the tube was sealed off with a flame some distance from the end of the tube so that moisture from the flame could not reach the sample.

c: Fused as a bead on a platinum wire in a bunsen flame; bead placed in a Pyrex tube and treated as in *b*.

d: Prepared by Dr. J. Papish of the Chemistry department, exceptionally pure; contained only spectroscopic traces of sodium, calcium, magnesium, iron, and silicon.

e: Prepared in Physics department by D. T. Wilber; made in paraffined paper dishes from c. p. halogen acid and alkali carbonate which was especially free from other alkalis.

Time of fading:

vf: Very fast, 1 minute or less.
f: 1 to 5 minutes.
m: 5 to 30 minutes.
h: 30 minutes to several hours.
d: one or more days.

Experimenter

D: Doelter[6]
G: Goldstein[7]
H: Holzknect[1]
N: Newberry and Lupton[8]

The following showed no coloration with 5 hours exposure: $AgNO_3$, $AgSO_4$, $CsCl_2I$, CsClBrI, $CsAl(SO_4)_2+12H_2O$, $Cs(NH_4)Cl$, $Ca(CH_3CO_2)_2$,

[7] Loc. cit.[4,6a] and also many other references.

[8] Newberry and Lupton, Manchester Mem. **62**, (1918)

KCH_3CO_2, $KHCO_3$, KNO_3, KSO_4, K_2SiO_3 powdered, $LiCO_3$, $NaCO_3$, $NaNO_2$, Na_2MoO_4, $NaAlF_4$ (cryolite), $NaSO_4$, NH_4Cl, $(NH_4)_2SO_4$, ZnCl.

Spectral Absorption of Halite and Sylvite Colored By X-rays

The sample of halite, which was quite clear, was a gift from the International Salt Co. of New York, Ithaca, N. Y., and came from the Detroit Rock Salt Co. A thin slab about 1 cm thick was cut out along natural cleavage planes. It was then ground down on very fine sandpaper until the thickness was uniform as tested by a micrometer caliper. The surfaces were polished by rubbing on chamois skin one half of which was barely moistened with water. While the sample was being rubbed back and forth on the moist portion, it was gradually drawn toward the dry portion, the rubbing being stopped just as the surface became dry. This process gave fairly polished surfaces.

The transmission was measured in the visible spectrum with a Schmidt and Hensch spectrophotometer. The transmission in the ultraviolet out to .200μ was measured by Miss S. A. McNulty with a Hilger sector disk spectrophotometer as modified by Howe,[9] and in the infra-red to 2.5μ by Prof. J. R. Collins.[10] The original sample showed a transmission of .87 at 2.5μ which decreased rather uniformly to .20 at 0.200μ. After coloration the sample showed absorption above that of the uncolored sample in the region between .3μ and 1.3μ. The curve plotted with ordinates equal to the ordinates of the transmission curve of the uncolored material minus those of the colored material will be referred to as the *color transmission* curve of the material. In the same terminology, then, the color absorption of halite begins at .3μ, has its maximum at .46μ, and ends at 1.3μ. The color absorption band is fairly pronounced, the ordinates of half the maximum occurring at .4μ and .5μ. The sample was left exposed to daylight during all of the following week and its transmission measured every day. The yellow color grew more faint but at every test the maximum absorption was found at .46μ.

Many samples of rocksalt from Detroit and Louisiana were colored and then heated quickly over a bunsen flame. The color faded rapidly but in no case did a blue color develop as has been reported for the case of coloration by cathode ray bombardment.[11] In a few samples a very pale pink color seemed to remain after the yellow vanished, but in every

[9] H. E. Howe, Phys. Rev. **8**, 674 (1916)
[10] J. R. Collins, Phys. Rev. **20**, 486 (1922)
[11] Goldstein, Sitz. d. K. Akad. Wiss. Berlin 1894, p. 937.

case all color disappeared when the heating was continued to the point of the explosion of the crystal.

The sample of sylvite from Stassfurt was obtained from the Ward Natural Science Establishment. A plate about 2 mm thick was prepared in the same manner as that of halite. The sample faded so rapidly as a result of the light passing through it when its transmission was being measured, that in ten minutes all color had disappeared. The transmission was determined at intervals of .04μ from .47μ to .67μ. Settings of the Schmidt and Hensch instrument were made as rapidly and at as regular intervals as possible back and forth throughout the range. Thus a non-repeating set of curves was obtained showing less and less absorption, but each curve showed a maximum absorption at .55μ with half values at about .48μ and .63μ.

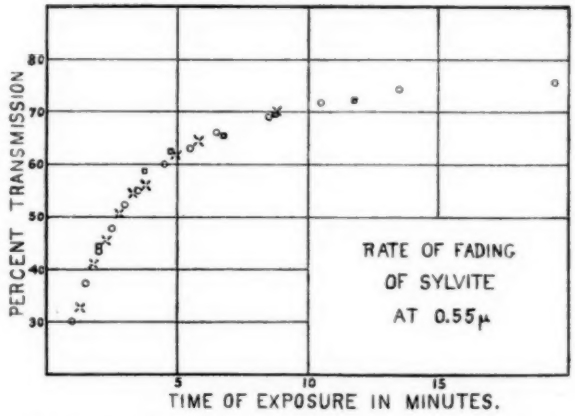

Fig. 1. Rate of fading of sylvite on exposure to daylight after coloration by x-rays.

Rate of Fading of Colors

The blue produced in caesium bromide by x-rays fades in less than 10 seconds exposure to daylight and is the shortest lived of any color observed by the author. The amber color of rocksalt is the longest lived. Sylvite fades rapidly enough to enable its rate of fading to be quickly determined. The same sample of sylvite used above was colored to .44 transmission. The spectrophotometer was set at .55μ, the position of maximum absorption. The adjustable slit was adjusted continuously to keep the fields matched in intensity and at regular intervals of time the slit width was recorded. The sample was again colored to .30 transmission, as it happened, and its rate of fading observed. A third test from .33 transmission was made. The data are shown in Figure 1. The curves have been shifted along the time axis to make the initial

values of each curve coincide. It is seen that alternate coloration and fading do not change the optical transmission of the material. The curves vary slightly but not consistently. The rate of fading is approximately proportional to the existing saturation of the color, which suggests that the recombination involved is an ordinary photochemical reaction.

Spectral Fading of NaCl, KCl, RbCl, and CsCl

These four chlorides show highly saturated colors. They were each ground to a fine powder in a glass mortar and pressed in a very thin uniform layer on a glass plate. They were then moistened with a saturated solution of their respective salts and left to dry. Lithium chloride is too hygroscopic to be studied by this method. The materials formed a smooth surface sticking tightly to the plate, practically a thin sheet of very tightly packed crystals which had a minimum amount of reflected white light and so showed decided colors after exposure to x-rays. A plate of one of the colored salts was put in a plate holder and placed in a spectrograph. The image of a type C 500 watt mazda lamp with filaments in a plane was formed on the slit of the spectroscope. After a short exposure the plate holder was removed and the sample examined in a very dim light. The edges of the region of the material that was faded white were marked with a fine pencil and the material given a further exposure and the whole process repeated. Except for NaCl the edges of the faded region could be determined within 1 mm or .01μ. The total exposures were approximately 10 sec., 30 sec., 1 min., 5 min., and 10 min., but for NaCl the exposures made with wide slits were several hours and the edges of the faded regions were very indefinite. The results are shown in Fig. 2. The scales of the time ordinates have been changed for each curve to make them fit into the same space. After about 50 times the exposure necessary to produce the first noticeable fading, further exposures produced only extremely slow widening of the faded region.

The points of tangency of the curves with the wave-length axis gives the wave-length of most rapid fading. The maxima for NaCl and KCl are shifted toward the long wave-length side of the maximum absorption of halite and sylvite respectively. To show that the shift was caused by the larger amount of energy in the red end of the spectrum from the mazda lamp, the energy distribution from the lamp operated at 2850°C was calculated from Planck's radiation formula and corrections made for the absorption of the crown glass prism. A curve was plotted with the ordinates given by the product of the energy incident upon the sample and the percent color absorption of the sample. Those ordinates then

represented the relative amounts of energy actually absorbed by the material and it was found that for halite and sylvite such curves had maxima respectively at 0.50μ and 0.595μ which are close to the wavelengths of most rapid fading. The positions of the regions of most rapid fading are not all in the order of the atomic number of the alkali metals. That may be due to a peculiarity in the color absorption of RbCl and CsCl. Since large enough crystals of the latter two chlorides can not be obtained to make their color transmission determinable, it is hoped that

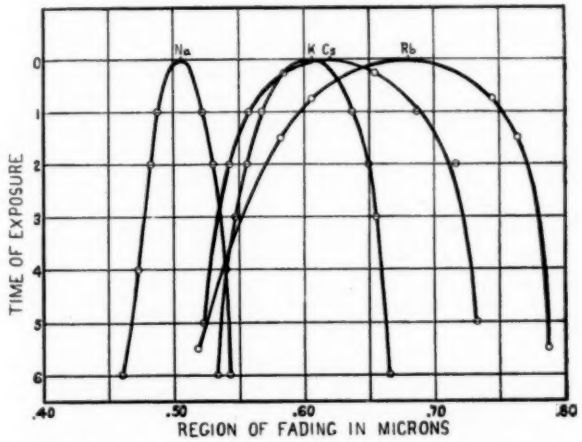

Fig. 2. Limits of faded region as a function of time of exposure in the spectrograph in arbitrary units.

their absorption can later be measured by the light which they reflect, although their rapid fading will make the work difficult. From the two cases completely studied it seems quite probable that the fading of materials colored by x-rays is primarily due to the energy gained by their color absorption alone.

The author is indebted to Prof. Ernest Merritt and Prof. R. C. Gibbs for many suggestions during the progress of this work.

CORNELL UNIVERSITY.

May 6, 1924.

ON THE NATURE OF THE IONS IN AIR AND IN CARBON DIOXIDE

By Henry A. Erikson

Abstract

Mobilities of ions of air and CO_2 in initial and final stages.—It has previously been shown that in air the positive ions have an initial mobility equal to that of negative ions, 1.87 cm/sec./volt/cm, which decreases in about 1/50 sec. on the average to 1.36 cm/sec./volt/cm. Using improved apparatus with an air speed of 20 m/sec. and fields of over 1000 volts/cm., curves were obtained showing clearly the presence of both initial and final ions. These are the same whether α or β rays are used to produce the ions. Negative ions show only one mobility. CO_2 ions gave curves which, within experimental error, agree with those for air, indicating one negative and two positive ions, but the time of transition to the final positive stage is somewhat shorter for CO_2. These results are best explained by assuming that in these cases ionization involves merely the detachment of an electron from a molecule, leaving a positive mono-molecular ion which soon attaches itself to a neutral molecule forming the final somewhat unstable bimolecular positive ion, while the electron almost immediately joins a neutral molecule forming a stable negative mono-molecular ion. Dissociation seems to play only a small part. It is concluded that single molecules singly charged, positively or negatively, all have about the same mobility which is independent of mass and molecular volume, and that a singly charged cluster of two or more molecules, not forming a single molecule, has a smaller mobility.

IN earlier articles,[1] results were given showing the existence of an initial and final positive ion in air ionized by alpha rays. Evidence was also obtained showing that the initial ion transforms into the final ion. The half value transition period has recently been determined in this laboratory by Grummann and was found to be of the order of 1/50 sec. The mobility of the initial positive ion is the same as that of the negative ion, namely 1.87 cm/sec/volt/cm, and the final positive ion has a mobility the same as that normally found for the positive air ion namely 1.36 cm/sec/volt/cm.

The resolving power of the apparatus used was not sufficient to separate the two ions when present, for example, in the air at the same time. The reason for the low resolving power was evidently the transition which took place after the initial ion entered the electric field. To obviate this, it was necessary to reduce the time interval required by the ions to pass through the field.

[1] **Erikson,** (a) Phys. Rev. **17,** 400 (1921); (b) **Phys. Rev. 18,** 100 (1921); (c) Phys. Rev. **20, 117** (1922).

With this in view, the apparatus was reconstructed in accordance with Fig. 1. *A* and *B* are two plates 5×15 cm and are 3.5 cm apart. They are kept at a difference of potential by means of the battery *G*. In order to secure a uniform field, wires whose potentials vary in steps are placed at the sides of the space between *A* and *B*. These wires are connected at *C* to plates 2 cm wide, placed parallel and 0.5 cm apart.

The ions were produced by means of alpha rays from polonium placed at *D* and sufficiently far back to insure the presence of both the initial and final positive ions in about equal number at *E* where they enter the field between the plates *A* and *B*. When plate *A* is positive the positive

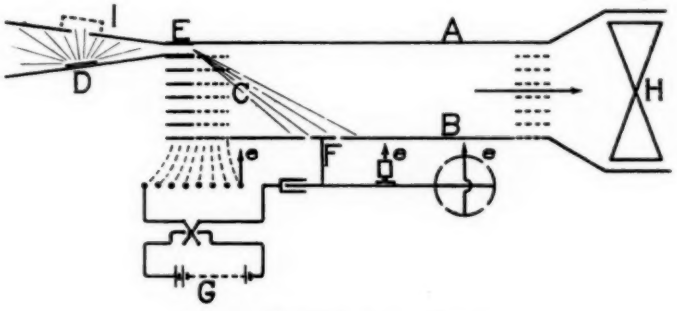

Fig. 1. Diagram of apparatus.

ions are repelled to plate *B* and at the same time are carried down stream with the air drawn through the apparatus by means of the fan *H*. The current received by the strip *F* for different values of the potential between *A* and *B* was determined. By plotting the current against potential the ionic spectrum is obtained.

In order to increase the resolving power it is necessary to make the time interval required by the ions to pass from *E* to *F* so short that the amount of transition of the initial ion into the final ion in this interval is negligibly small. This was accomplished by constructing a fan $4\frac{3}{4}$ inches in diameter, having eight blades set at angles of about 20°. The fan was given a speed of about 5000 r.p.m. by means of a belt, pulleys, and a 1/4 h.p synchronous motor having a speed of 1800 r.p.m. This gave an air velocity of about 2000 cm/sec. and therefore an interval of .002 sec. from *E* to *F*. In order to force the ions from plate *A* to plate *B* in this interval a correspondingly high difference of potential had to be used. The results obtained with ions due to alpha rays, are shown graphically in Fig. 2. *A* is the curve obtained for the negative ion and *B* the curve for the two positive ions. Part *C* of the positive curve is for the initial positive ion and part *D* is for the final positive ion.

It is seen that the maxima for the negative ion and initial positive ion correspond to about 3350 volts. This means that the negative and the initial positive ions have the same mobility. The maximum D for the final positive ion corresponds to about 4550 volts, giving a mobility ratio between the initial and final positive ions of 1.36 which corresponds to the mobility ratio normally found for the negative and positive air ions.

The widths of the curves for the negative and initial positive ions are such as may be accounted for by the fact that the measurements are made at an angle with the direction of motion of the ions, by the repulsion

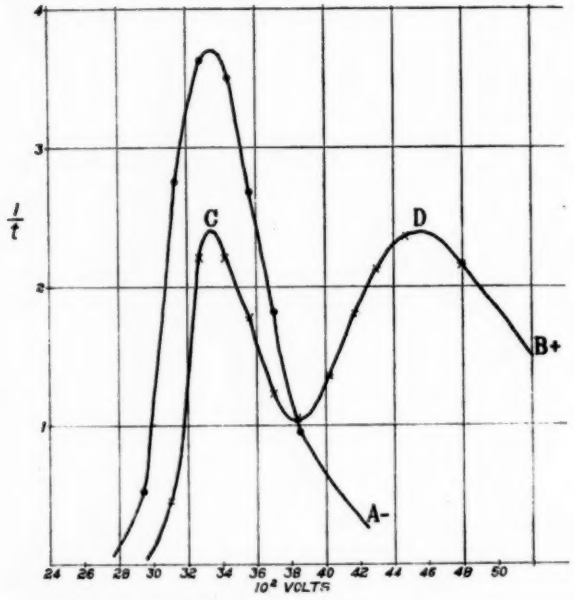

Fig. 2. Results with ions due to alpha rays.

between the ions, and by air turbulence. The width of the curve for the final positive ion cannot, however, be entirely accounted for in this manner. The effect in this case is as if a loading and unloading of the final ion is going on.

In order to determine whether the nature of the ions produced depends upon the ionizing agent, the above experiment was repeated using β rays. A source of β rays, obtained from decayed emanation tubes, was placed at I, Fig. 1. The funnel was surrounded by sheet lead so that the ionization was confined to the air passing into the apparatus at E. The distance between the plates A and B was somewhat smaller, hence the voltages required were lower than for the curves of Fig. 2. The results are shown by the curves in Fig. 3. The curves in Fig. 4 were obtained for ions pro-

duced by alpha rays from polonium as in the case of Fig. 2 but with conditions as identical as possible with those of Fig. 3. It is seen that the initial and final positive ions are present whether the ions are due to α or β rays and that their mobility ratio is normal. The average age of the ions in the case of the α rays, due to the position of the polonium plate, is a little less than in the case of the β rays, and therefore relatively more of the initial positive ions are present. But the similarity of the curves Figs. 3 and 4 indicates that there is no essential difference in the results of the ionizing process in the case of these two rays.

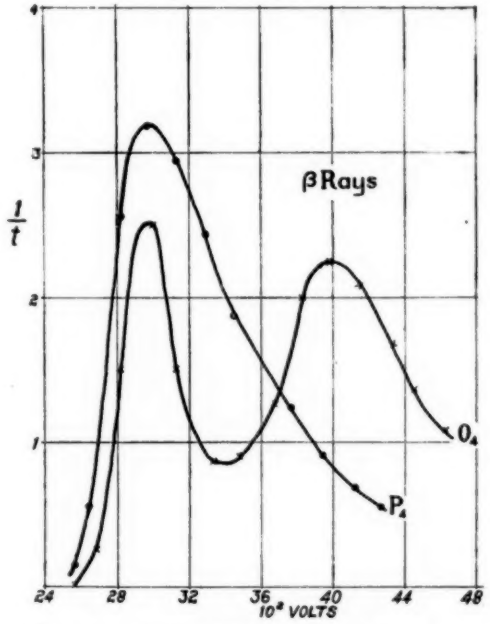

Fig. 3. Curves with ions due to beta rays.

As to the nature of the initial and final positive ions as well as the negative ion, an analysis may be made in terms of the following two assumptions:

(a) The ionizing process involves simply the removal of an electron from the molecule, otherwise leaving the molecule intact.

(b) The ionizing process consists in removing an electron as in (a) and in addition dissociating the molecule.

Assumption (a) leads to the following results. After the electron is removed from a molecule, it remains free for but a short time. This free state has been observed by Wellish, Loeb and others. The electron soon attaches itself to a neutral molecule forming a negative ion, one molecule

large. The remainder of the molecule which lost an electron in the ionizing process forms a positive ion, one molecule large. This positive ion has the same mobility as the above negative ion since their charges and volumes are equal. This is, therefore, the initial positive ion. The transition consists in the initial ion attaching itself to another neutral molecule thus forming a positive ion two molecules in size. This constitutes the final positive ion.

Experiment indicates that a negative atom or molecule does not readily attach itself to another neutral atom or molecule of its own kind. In

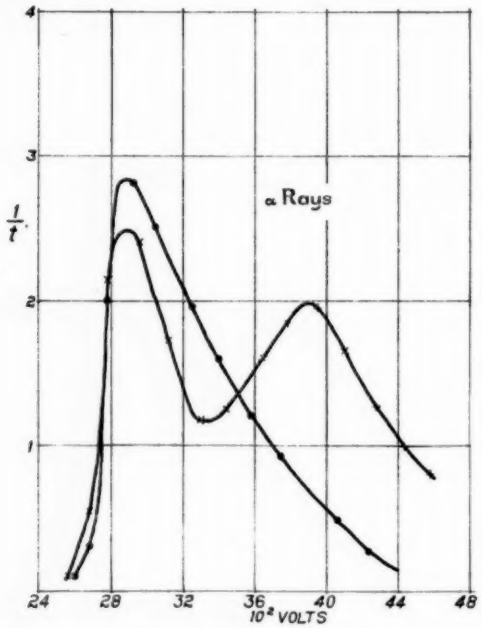

Fig. 4. Curves with ions due to alpha rays, obtained under the same conditions as those of Fig. 3.

this work the constancy of the negative ion and its aversion to union with other bodies, have been very marked. This is perhaps to be expected as such a union would have to take place in the presence of an excess of electrons. The union of a positive atom or molecule with a neutral atom or molecule on the other hand means the sharing of a valency electron by two positive charges, a process which is probable and which is suggested by experimental results.

Assumption (b) leads to the ions resulting from (a). In addition the dissociation may be assumed to result in $(O+O^+ + e^-)$ and $(N+N^+ + e^-)$ where e^- stands for an electron. If the electrons unite with some of the

neutral atoms produced as well as with neutral molecules, two negative ions, one and two molecules large, will result from (b). The positive atoms may unite with neutral molecules and it is thus seen that assumption (b) may give rise to four positive ions, one, two, three and four atoms large.

Of the two assumptions, (b) is the less likely. If all the ions resulting from (b) were present in appreciable numbers, experiment would detect them. Furthermore, if dissociation takes place it would be reasonable to expect a difference in the results from α and β rays, whereas experiments show that no difference exists.

In an earlier article[1c] it was shown analytically that a mobility ratio such as exists between the initial and final positive ions means that the slower ion is twice as large as the other. This also favors assumption (a).

The writer, therefore, feels that (a) gives the best interpretation of the experimental results. On this basis the negative ion and the initial positive ion are each one molecule large and the final positive ion is two molecules large.

If it is further assumed that the final ion may attach itself to another molecule forming a cluster of three molecules the parts of which are so loosely tied together that they are quickly disintegrated through thermal impact, and if it is assumed that even the final two molecule ion is sometimes disintegrated by the more violent thermal impacts, an explanation of the greater spreading of the curve for the final positive ion is obtained.

There is, however, no justification for the complete rejection of (b). That dissociation to a certain extent takes place, especially in the case of the α ray, is experimentally established. The rejection of (b) must be in degree only. That the other ions predicted above and resulting from dissociation are present can hardly be denied. A sufficiently sensitive method should detect them.

The justification for the omission of double charges in the above analysis is based on results by Millikan, Gottschalk and Kelly[2] which showed that no double charged ions are produced in air by α rays.

The above results are for air taken from the room. In a separate experiment the apparatus was placed in a closed vessel. Results were obtained using dry and also saturated air. No effect due to moisture was observed. This, of course, is what should be expected as the above process is molecular. The heavy ions formed by the water vapor are carried down stream and do not enter into the measurements.

[2] Millikan, Phys. Rev. **15**, 157 (1920)

Carbon Dioxide Ions

To test the above conclusions, carbon dioxide gas was passed through the funnel *DE*, Fig. 1. The ions are then produced in CO_2 and enter at *E* where they are drawn out of the CO_2 sheet and pass, through the air entering at *C*, to the plate *B*. This gives an opportunity to determine the mobility of CO_2 ions in air. The CO_2 entered the apparatus from a large tank. This tank was filled from a commercial supply cylinder. No attempt was made to purify the gas.

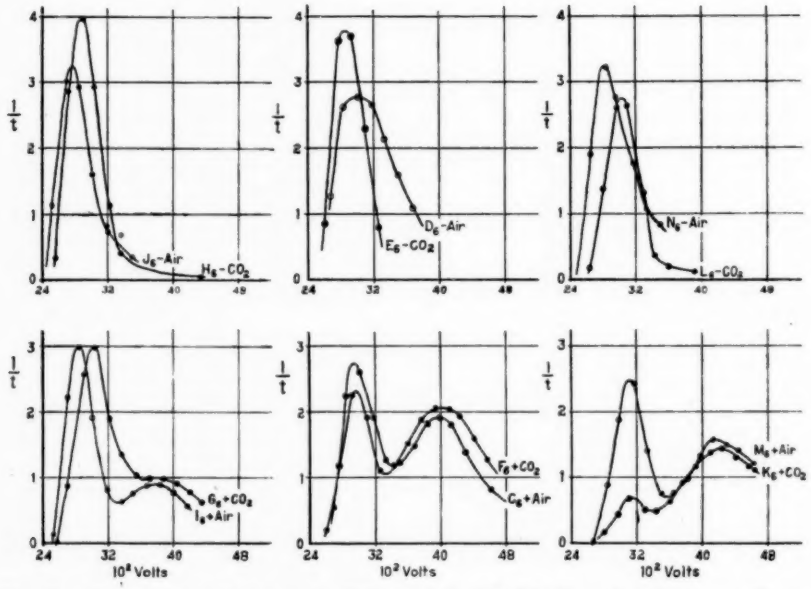

Fig. 5. Comparison of curves for CO_2 ions in air with those for air ions. Upper figures are for negative ions; lower figures for positive ions.

The results obtained are given in Fig. 5. The upper horizontal series is for the negative ions and the lower for the positive ions. The curves for the CO_2 ions have full dots. Accompanying each CO_2 curve is a curve showing the results obtained using air in place of CO_2, the conditions otherwise being as nearly identical as possible. The first vertical set from the left is for ions of an average age of about .005 sec. the second for .02 sec. and the third for about .06 sec.

It is thus seen that the negative CO_2 ion has the same mobility as the negative air ion, that only one ion is present, and that it undergoes no change with age. The lack of exact superposition is due to experimental variations such as slight changes in the air velocity. This is born out by repeated observations on the same ion.

This negative CO_2 ion is undoubtedly formed, as in air, by an electron, freed by the ionizing process, attaching itself to a molecule of CO_2, thus forming an ion one molecule large but containing three atoms. If this is correct then the fact that the negative air ion and the negative CO_2 ion have the same mobility means that the mobility of a natural structure such as a molecule is determined primarily by its charge and that the difference in the molecular volumes is not sufficient to give rise to a detectable difference in mobility. The difference in mass in this case is of small consequence, as is shown by the fact that heavy bodies such as actinium active deposit ions have very nearly the same mobility as the air ions.

A comparison of the curves in the lower series, Fig. 5, for the positive CO_2 ions and the positive air ions, also shows a close similarity. There is in CO_2 as in air, an initial positive ion and a final positive ion. The curves show however that the transition period of the initial to the final is less in the case of CO_2.

The interpretation in this case, on the basis of the above discussion, would be that the initial CO_2 ion is the remainder of a CO_2 molecule which lost an electron in the ionizing process and therefore is one molecule large. This ion being one molecule large has the same mobility as the negative air and CO_2 ions. This initial ion soon attaches itself to a neutral CO_2 molecule thus forming an ion two molecules large. The difference in volume of a positive air ion two molecules large and a positive CO_2 ion two molecules large is not sufficient to give rise to a detectable difference in mobility as is shown by the fact that the maxima correspond to the same voltage. If the above is a correct interpretation the situation may be summarized as follows: All single molecules having equal charges have approximately the same mobility. The mobility of an ion is not a function of its mass. However, any attachment which does not give rise to a natural molecular structure causes a change of mobility.

The writer is indebted to Mr. C. Dane for constructing the apparatus and to Professor John T. Tate for helpful cricitisms.

PHYSICAL LABORATORY,
UNIVERSITY OF MINNESOTA,
May 4, 1924*

*Received July 17, 1924.—*Ed.*

ELECTRON EMISSION FROM ADSORBED FILMS ON TUNGSTEN

By K. H. Kingdon

Abstract

Electron emission from tungsten filaments covered more or less completely with adsorbed films.—(1) *Complete film of oxygen.* The emission corresponds to the equation $i=AT^2e^{-b/T}$ where $A=5\times10^{11}$ amp/cm² deg.²; $b=107{,}000°$. It was necessary to supply oxygen continuously to keep the film complete. (2) *Thorium film covering a fraction θ of a thoriated tungsten filament.* The data obtained with three tubes agree with the empirical expression

$$i_\theta=[a_1{}^\theta+a_2{}^{(1-\theta)}-1]A_0T^2e^{-[b_1\theta+b_2(1-\theta)]/T} \qquad (1)$$

where a_1 and a_2 are the numerical values of A for a complete film of Th on W and for pure W respectively, expressed in terms of the dimensional unit $A_0=1$ amp/cm²deg.², and b_1 and b_2 are the respective values of b. The present experiments give $a_1=7$, $b_1=31{,}200°$; from the results of other workers, $a_2=60$, $b_2=52200°$. (3) *Caesium films on tungsten covered with oxygen.* Complete films of Cs were not obtained, but the results indicate $A_{Cs}<0.003$ amp/cm²deg.² and b_{Cs} slightly less than 8300°. Such low values, together with the values for an oxygen film, substituted in Eq. (1) give a curve which shows a maximum emission for $\theta=0.993$ instead of the expected 1.00. Various experiments on the effect of varying the pressure of Cs vapor and on the effect of evaporating Cs from the surface confirm this conclusion, and also the variation of A and b with θ. (4) *Caesium films on tungsten.* The maximum emission is computed to be for $\theta=0.987$. (5) *Effect of adding nitrogen to fully activated thoriated tungsten* is to increase the emission about five fold at 1400°K. A pressure of 0.1μ is sufficient. The effect seems to be due to a change in the A value.

IN this paper are described several separate experiments relating to electron emission from adsorbed films of oxygen, thorium and caesium on tungsten.

I. The Electron Emission from a Complete Film of Oxygen on Tungsten

The tube used contained a loop of tungsten wire 0.0102 cm in diameter. The anode was divided into two parts so that the emission from the lower part (area 0.145 cm²) of the filament could be measured separately. This was done to avoid the cooling effect of the leads. The currents were measured with an electrometer.

Preliminary measurements showed that the filament temperature must be at least 1500°K to make the electron emission great enough (10^{-13} amp.) to measure conveniently. At these temperatures the rate of evaporation of oxygen from the filament was such that it was impossible

to take a temperature characteristic of the emission before the fraction of the surface covered with oxygen had changed. Accordingly, a bulb containing an intimate mixture of BaO_2 and $KMnO_4$ was heated in an oil-bath to a temperature of about 160°C, and oxygen was thus supplied to the system at a steady rate and consumed by the filament. This, of course, produced a steady decrease in the diameter of the filament which was allowed for as far as possible by measurements of resistance, the temperatures being corrected accordingly. At the end of the experiments the filament temperature was about 10° higher for a given heating current than it had been at the beginning. The oxygen passed through a liquid-air trap before reaching the tube.

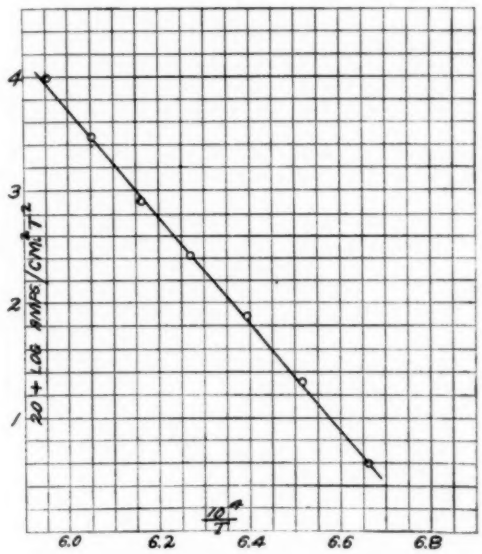

Fig. 1. Electron emission from a tungsten filament completely covered with oxygen.

Measurements were made at rates of supply of oxygen which would have increased the pressure in the system at rates of 0.22, 0.52, 0.95 μ (0.001 mm) per minute if the oxygen had not been consumed by the filament. Runs made at these three rates of supply all had about the same slope, although as a different temperature scale was used for each run there were slight variations in the emission due to errors in temperature. The approximate constancy of the emission at different rates of supply of oxygen shows that the filament was always completely covered with oxygen. Fig. 1 shows the data from one of these runs. From this, the constants in the electron emission formula

$$i = AT^2 e^{-b/T} \qquad (1)$$

were found to be

$$A = 5 \times 10^{11} \text{ amp./cm}^2\text{deg}^2;$$
$$b = 107{,}000°.$$

II. The Variation of the Constant A for a Thoriated Tungsten Filament with the Fraction of the Surface Covered with Thorium

By first flashing at 2800°K and then holding at 2100°K for a few minutes, a monatomic film of thorium may be formed on the surface of a tungsten filament containing a small percentage of thoria.[1] To secure a steady thoriated electron emission the tube is preferably immersed in liquid air to get rid of deleterious gases which attack the thorium layer, or else is supplied with some getter to achieve the same end. The activating process may be stopped at any point, and the electron emission from the tungsten surface partly covered with thorium, studied. If measurements are made at temperatures of about 1500°K, the amount of thorium on the surface remains constant, and activation only recommences when the temperature is raised to about 2000°K. The electron emission constants of the partially covered surfaces may therefore be determined.

The measurements to be described were made with tungsten wire 0.0104 cm in diameter, containing about 1 percent thoria. This was used in three tubes. In two (tubes 80 and 156) the filament was about 12 cm long and was bent into a loop. This was surrounded by a gauze cylinder divided into two parts so that the emission from the lower part of the loop (containing about 4 cm of wire) could be measured separately. The cooling effect of the leads was thus eliminated, and the part of the filament used was all at constant temperature. In the third tube (tube 102) the filament was a straight wire 12 cm long, surrounded by three collinear nickel cylinders so that the emission from the center 2.7 cm of the filament could be measured separately. The tubes were given the customary high-vacuum exhaust treatment and were used on the pumps. Tube 80 contained caesium as a getter, the bulb being at 40°C. The filament was at a high enough temperature to keep the caesium off. Both parts of the gauze cylinder were kept at +30 volts. Tube 156 also contained caesium, but was used immersed in liquid air. The upper section of the gauze cylinder was kept at −100 volts and the lower at +100. It was found necessary to heat the gauzes after immersing the tube in liquid air, so as to get the caesium off and to prevent a flow of photo-electrons from the negative to the positive gauze. Tube 102 did not contain caesium but was

[1] Langmuir, Phys. Rev. **22**, 357 (1923)

used immersed in liquid air. All three cylinders were usually kept at +150 volts.

The filament temperatures were determined from the heating currents. For each state of activity of the filament a temperature T characteristic of the electron emission i was taken, and a plot of log i against $1/T$ was made. The slopes of these lines diminished by $2T$ give the values of b in the electron emission equation (1), and hence A can be found. We will denote the fraction of the filament surface covered with thorium by θ, and let A_θ and b_θ be the corresponding values of A and b. Langmuir[1] has shown that b_θ is a linear function of θ, involving b_W the constant for a pure tungsten surface, and b_{Th} the constant for a tungsten filament completely covered with thorium, and is given by

$$b_\theta = \theta b_{Th} + (1-\theta) b_W \tag{2}$$

The present experiments show that b_{Th} is about 31,200°, while from the work of Davisson and Germer[2], and Dushman,[3] b_W is about 52,200. It is, therefore, possible to calculate θ for every b_θ. The present experiments[4] give $A_{Th}=7$ amp./cm^{2}deg^2 while Davisson and Germer, and Dushman give $A_W=60$. Fig. 2 shows some values of A_θ obtained with each of the tubes. The experimental error was rather large. In particular with tube 156 it was noted that the values of A_θ in the region from $\theta=0.1$ to 0.6 were rather erratic, whereas those from $\theta=0.6$ to 1.0 were much more consistent. It may be that when partly covered with thorium the filament is better able to adsorb residual gases which change the electron emission constants. Each set of points shown represents one complete set of consecutive runs in which the activity of the filament was increased in steps from the lowest to the highest value. It was never possible to de-activate the filament so completely by flashing to a high temperature (2800°K) that its emission was as low as that from pure tungsten.

The values of A_θ in Fig. 2 may be represented by an empirical formula, which also, as will be seen later, is in agreement with another phenomenon observed in the study of electron emission from adsorbed films of caesium. Let us express the A's in terms of the dimensional unit $A_0=1$ amp/cm^2 deg^2. Then the thorium-tungsten data may be represented satisfactorily by the empirical formula

$$A_\theta = [7^\theta + 60^{(1-\theta)} - 1] A_0 . \tag{3}$$

[2] Davisson and Germer, Phys. Rev. **20**, 300 (1922)
[3] Dushman, Phys. Rev. **21**, 623 (1923)
[4] See also Dushman, Phys. Rev. **23**, 156 (1924)

The curve in Fig. 2 is a plot of this expression. In general, if a_1 and a_2 are the numerical values of A for the complete adsorbed film and for the underlying layer respectively, we have

$$A_\theta = [a_1^\theta + a_2^{(1-\theta)} - 1]A_0 . \tag{4}$$

It should be emphasized that this formula is only satisfactory when a_1 and a_2 are expressed in terms of the particular dimensional unit $A_0 =$ 1 amp/cm^{2}deg^2. This might be interpreted as meaning that there is some

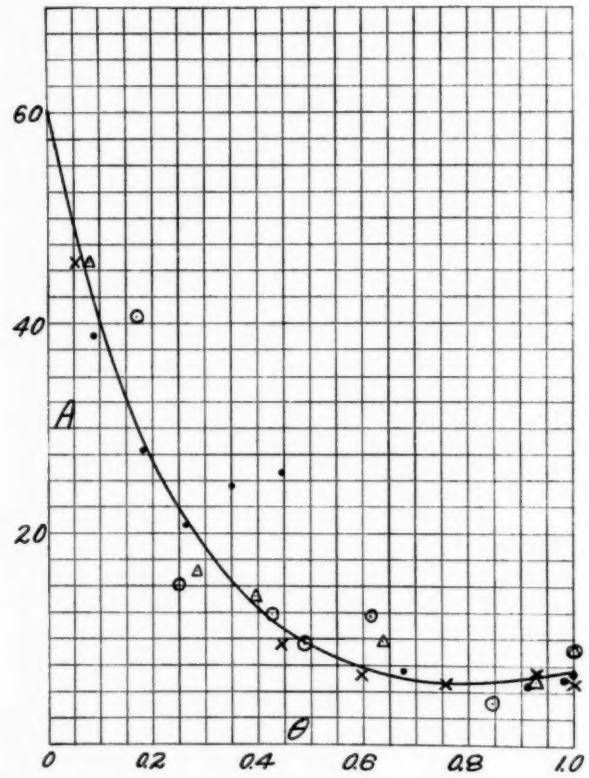

Fig. 2. Values of A for a tungsten filament of whose surface a fraction θ is covered with thorium.

theoretical constant approximately equal to A_o which is of fundamental importance for electron emission. However, little weight can be attached to this on account of the purely empirical character of the expression and on account of the large experimental error. The artificial nature of expression (4) makes it seem likely that this is not the true expression for A_θ but merely one which approximates to the true expression in the cases studied. However, this was the only formula which could be found to

represent the data of Fig. 2, and also the experiments described in section III on the electron emission from adsorbed films of caesium.

Substituting from (4) and (2) in Eq. (1) we obtain

$$i_\theta = [a_1\theta + a_2^{(1-\theta)} - 1]A_0T^2e^{-[b_1\theta + b_2(1-\theta)]/T} \qquad (5)$$

We shall discuss the bearing of this equation on some other cases of electron emission from composite surfaces.

The A factor in Eq. 1 may be regarded as proportional to the current which could escape from the filament if the work-function were zero, and is a measure of the density of the electron atmosphere just outside the surface of the filament. This might lead one to expect that in an expression for the A factor appropriate to a composite surface, θ might enter as a linear multiplier. Such an expression for A_θ is, however, unsatisfactory, and it appears necessary to introduce θ as an exponent as in Eq. (4). This apparently indicates that the presence of neighboring like atoms in the adsorbed film increases the contribution of electrons from a selected atom to the electron atmosphere just outside the surface.

III. The Variation with Caesium Vapor-Pressure of the Electron Emission from Adsorbed Films of Caesium

One point brought out by Eq. (5) is that if a_2 is very large compared with a_1, then even though b_2 is several times b_1 the electron emission from the surface is not at a maximum when $\theta = 1$, but perhaps when $\theta = 0.99$; the decrease in i_θ due to the increase in the b term is more than balanced by the increase due to the change in the A term. Evidence that this actually occurs is furnished by some experiments on the electron emission from adsorbed films of caesium.

Summaries of the electron emission phenomena due to adsorbed films of caesium have been published previously,[5] and a more complete paper (with Dr. Langmuir) is to appear soon. It has been shown that in a bulb containing caesium at 30°C and a tungsten filament, the caesium continually condenses on the filament and forms an adsorbed layer which gives a maximum electron emission of about 10^{-4} amp./cm² at a filament temperature of 700°K. At higher filament temperatures the caesium fails to cover the surface as completely, and the emission decreases.

A large increase in the maximum emission may be obtained by first treating the filament with oxygen. After flashing the filament to 2700°K in vacuum for a short time, it is heated at about 1900°K in oxygen at a pressure of about 0.02 mm for a few seconds. (Somewhat similar results are obtained if the oxygen is merely allowed to come in contact with the

[5] Langmuir and Kingdon, Phys. Rev. **21**, 380 (1923); Science **57**, 58 (1923)

clean, cold filament). The excess oxygen is then pumped out, and caesium distilled in. Some caesium is presumably adsorbed on the filament, but the electron emission which may be obtained at temperatures of from 700°K to 1000°K is very small. If, however, the filament is heated for a few seconds at from 1200° to 1600°K, on returning to the lower temperatures it will be found that the emission has increased many fold and is of the order 0.35 amp./cm^2 at 1000°K with the bulb at 30°C. The heating at from 1200° to 1600°K probably frees the surface of excess oxygen and of adsorbed deleterious gases such as CO. The remaining oxygen is probably held on as negative oxygen ions, and these ions adsorb the caesium more strongly than a tungsten surface does. With the bulb at 30°C the emission is at a maximum at a filament temperature of about 1000°K. At higher filament temperatures the caesium evaporates from the filament faster than it can be renewed by condensation from the vapor in the bulb, and the emission decreases.

At lower filament temperatures (600−700°K) the electron emission, strangely enough, is smaller the higher the pressure of caesium vapor in the tube. This effect occurs both for the caesium-tungsten emission and for the caesium-oxygen-tungsten emission. It is not due to any cooling effect of the caesium vapor on the filament, as the pressures are far too small. It seems too definite and steady an effect to be due to changes in residual gas pressure with bulb temperature. A set of curves for the caesium-oxygen-tungsten emission over the temperature range where the surface is largely covered with caesium is given in Fig. 3. It will be seen that a change in bulb temperature from −185° to +60°C decreased the emission at 625°K 80 fold. The general course of these curves may be accounted for by Eq. (5) if A for a complete film of caesium on oxygen is very small while A for a complete film of oxygen on tungsten is very large. The b for an oxygen film is, of course, several times greater than that for a caesium film. At the high bulb temperatures and low filament temperatures the surface is practically completely covered with caesium, and the emission is small on account of the small A term. As the bulb temperature is lowered a very small fraction of the filament surface is bared of caesium and the increase in the A term increases the emission in spite of the decrease due to the increase in b. The same argument shows that at a constant bulb temperature the slight decrease in the amount of caesium on the surface at the higher filament temperatures gives the curves too steep a slope, and this slope is not even an approximate measure of b on account of the large variation in A. The only curves from which any reliable estimates of the electron emission constants for a

caesium-oxygen-tungsten filament can be made are those taken with the tube immersed in liquid-air. Here there is no continual condensation of caesium on the filament, and the rate of evaporation of the adsorbed layer is so small at 600 to 700°K that a temperature characteristic may be taken without changing the condition of the surface appreciably. Such runs give the values of the constants in Eq. (1) as $A = .003$ amp./cm²deg²; $b = 8300°$. As a little oxygen or tungsten was undoubtedly exposed, b is a little higher and A is almost certainly much larger than the value which would characterize a complete film of caesium on oxygen on tungsten. However, as an approximation, we may take the values for a com-

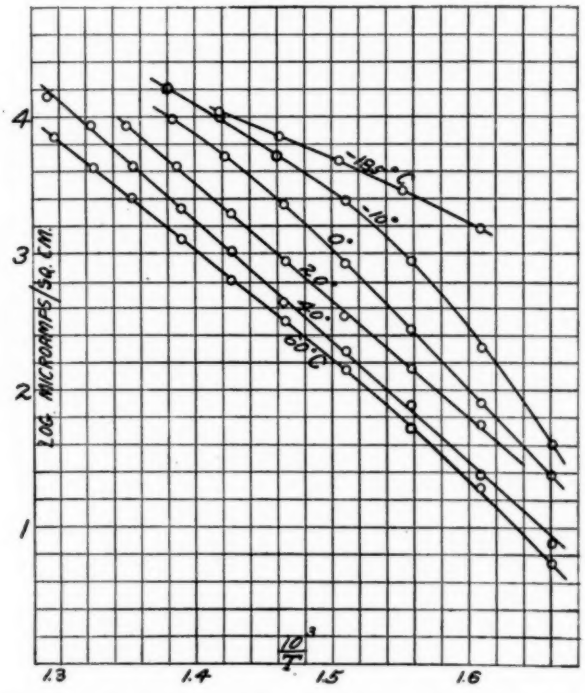

Fig. 3. Variation with bulb temperature of the electron emission from a Cs-O-W filament.

plete caesium film to be $A = .001$ amp./cm²deg², $b = 8300°$. The constants for a complete film of oxygen on tungsten are $A = 5 \times 10^{11}$ amp./cm²deg², $b = 107000°$. Choosing a temperature of 625°K and substituting these values in Eq. (5) we get the curve of Fig. 4 marked Cs-O-W. This shows that at $\theta = 0.99$ the electron emission is about 60 times that at $\theta = 1$. An equation such as (5) is therefore capable of explaining the decrease in electron emission observed at the higher pressures of caesium vapor.

If, when caesium is removed from the surface, tungsten is exposed rather than oxygen, we may substitute the A and b appropriate to tungsten into Eq. (5) and obtain the Cs-W curve of Fig. 4. Here the emission is also at a maximum when the surface is not quite completely covered with caesium, and experimentally it is found that the Cs-W emission shows a decrease with increasing bulb temperature at low filament temperatures similar to that shown by the Cs-O-W emission.

It may be that the small emission obtained just after treating the surface with oxygen (see above) is due to the fact that the adsorbed film of caesium is then too complete, and the flashing at 1200° to 1600°K is

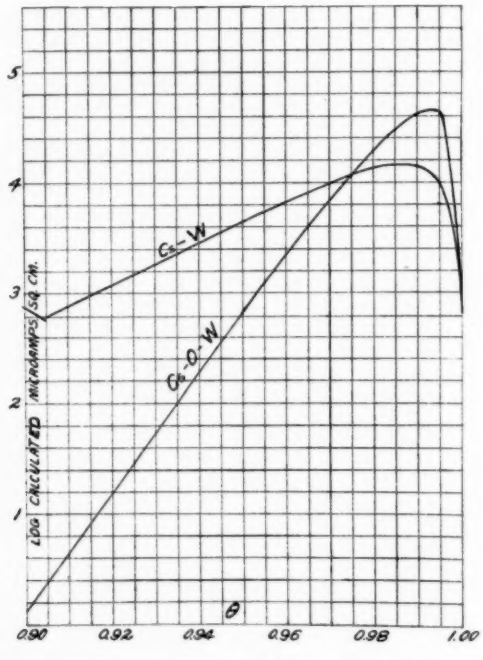

Fig. 4. Electron emission calculated from Eq. (5).

necessary to remove some of the oxygen binder so that the surface is not so completely covered with caesium and a little oxygen or tungsten is exposed. There is, therefore, an optimum amount of caesium on the surface which will give the largest electron emission.

On the other hand, the values of the constants for the thorium-tungsten case discussed in section II are such that Eq. (5) shows the emission to be a maximum when $\theta = 1$. This is in accordance with experiment.

Further evidence that the emission from a Cs-O-W filament is a maximum when $\theta < 1$ is given by the curves of Fig. 5. The tube was

immersed in liquid-air with the filament current off. Time was measured from the instant of starting the filament current. In this tube the emission was measured from the center 4 cm of a 30 cm filament of 1.15 mil tungsten, so that this part of the filament reached its final temperature rapidly. Fig. 5 shows that the emission first increases as a little caesium evaporates from the filament, and then decreases when too much has been lost. The tube was warmed up to room temperature between each run to allow caesium to recondense on the filament. The bulb temperature at which this condensation took place made no difference. The time changes in the emission are shown for several different filament temperatures.

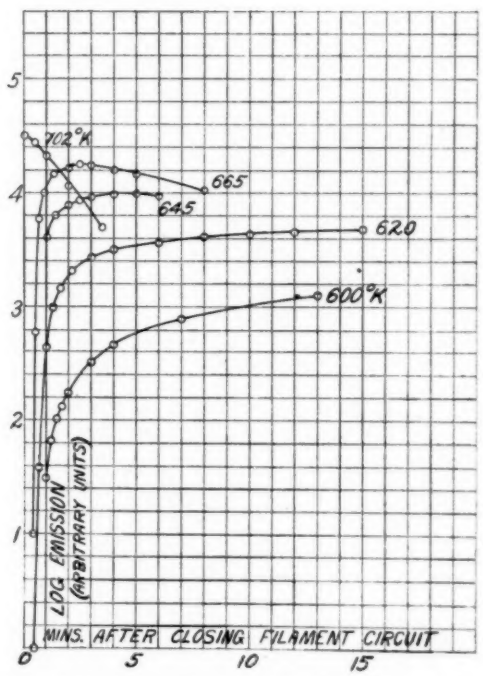

Fig. 5. Changes in electron emission from a Cs-O-W filament as caesium is evaporated from the surface.

Further experiments on the Cs-O-W emission with this tube immersed in liquid-air give some support to Eq. (4). With the filament in its optimum electron-emitting state the bulb was immersed in liquid-air and a temperature characteristic of electron emission was taken. This gave $A = 0.003$ amp./cm^{2}deg^2, $b = 8300°$ in Eq. (1). A little of the adsorbed caesium was then evaporated, and the A and b for the filament in this new state found. This was repeated for as many different states of activity

as possible. The resulting values of A and b are plotted as crosses in Fig. 6. The values in the lower state of activity are subject to large errors as the filament temperature necessary to obtain a measurable electron emission was so high that it was difficult to obtain a sufficient number of observations before the amount of caesium on the surface had changed appreciably by evaporation. The curve marked Cs-O-W is a plot of Eq. (4) using $a_{Cs}=0.001$, $b_{Cs}=8300°$, $a_{Ox}=5\times10^{11}$, $b_{Ox}=107000°$, and calculating b_θ from an equation similar to (2). The equation represents the experimental points satisfactorily, but it is unfortunate that the measurements cannot be carried out at lower states of activity as well.

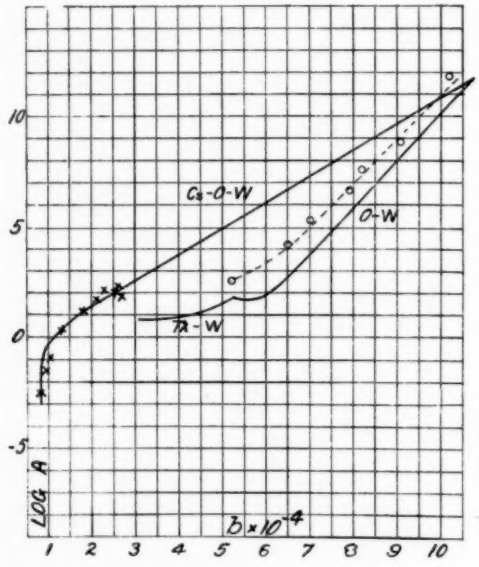

Fig. 6. Comparison of observed values of A and b with those calculated from Eq. (4).

In Eq. (4) if a_1 is very much larger than a_2, then for all values of θ except those nearly zero, the value of the term in brackets will be determined by a_1^θ. That is, log A_θ will be a linear function of θ. Now from (2), b_θ is also a linear function of θ, and therefore log A_θ is a linear function of b_θ. Richardson[6] in fact has pointed out that there is a linear relation between log A and b for a tungsten filament contaminated with various gases, probably always containing oxygen or water vapor. The data quoted by Richardson from Langmuir[7] are plotted as circles in Fig. 6, after reducing A to amp./cm$^2T^2$, and b to degrees in Eq. (1). The line marked *O-W* is a plot of Eq. (4) using the values of A and b for oxygen and tungsten and calculating b from (2). The experimental points lie

[6] O. W. Richardson, The Emission of Electricity from Hot Bodies, 2nd ed., p. 135
[7] Langmuir, Phys. Rev. **2**, 450 (1913)

above the curve, which is for the most part linear. Under the experimental conditions, the amount of oxygen on the filament would be less at high temperatures than at low. This change in the condition of the filament would give too large values of b and therefore of A, and accounts satisfactorily for the discrepancy. It will be noticed that the slopes of the experimental points and of the *O-W* line are about the same.

IV. The Effect of Pure Nitrogen on the Electron Emission from a Completely Activated Thoriated Tungsten Filament

These measurements were made with tube 80 described in section II. The nitrogen used was taken from a commercial tank and was not purified before reaching the tube except by passing through a liquid-air trap. The caesium in the tube, however, completely freed the nitrogen of traces of oxygen before it reached the filament. Table I gives some data showing the effect of nitrogen.

TABLE I

Tube temperature	Filament temperature	Nitrogen pressure	Anode voltage (V_c)	Anode current (i_c) (60 = 10^{-6} amp.)	State of filament
25°C	1455°K	0μ	30	37000	Completely activated
−184		0		35000	
25		0		37500	
25		7		180000	
−184		2.5		180000	
30	1268	0	10	1050	Completely activated
30	1268	15	10	5600	
30	1455	0	10	3.5	Partially deactivated
30	1455	15	10	2.6	

The electron emissions given are those from the lower part of the filament loop of tube 80 (area 0.131 cm²) as described in section II. The first part of the table shows that at $V_c = 30$ the presence of nitrogen increased the emission about five fold. This increase occurred whether the tube was at 25°C or at −184°C, showing that the presence of caesium had nothing to do with it. The second part of the table shows that the increase also occurs at $V_c = 10$, showing that ionization of the nitrogen is not the essential cause of it. It was necessary to lower the filament temperature in this run to avoid space-charge limitation of the emission. The increase in emission occurred as soon as the nitrogen was admitted. The third part of the table shows that the increase did not occur when the thorium layer had been largely removed from the filament surface.

The three temperature characteristics of Fig. 7 were taken at the different pressures of nitrogen marked on the curves and show that the

effect increases only slowly with pressure. The filament was in the completely activated state. The curves converge at the top on account of space-charge limitation of the emission.

Finally the nitrogen was all pumped out with the filament cold. When a good vacuum had been reached, the filament was heated. The emission was much above normal at first and slowly decreased, taking several minutes at 1455°K to fall to somewhere near the value for a thoriated surface. The increase in emission was doubtless due to an adsorbed film

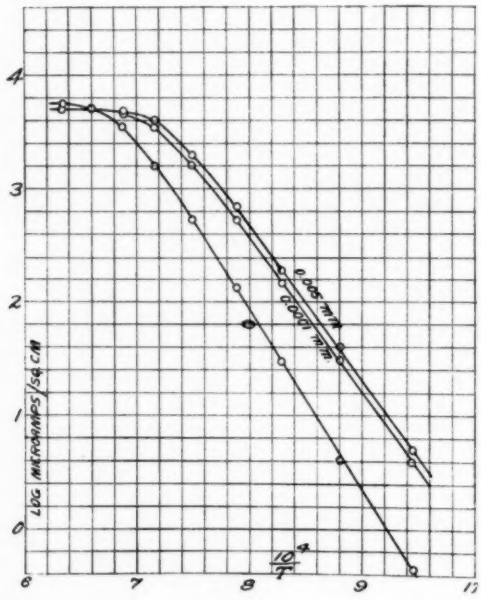

Fig. 7. Effect of nitrogen on electron emission from a thoriated tungsten filament.

of nitrogen on the filament surface. It seems hardly likely that nitrogen would decrease the work function for a thoriated surface, and the increased emission was probably due to an increase in the A term of Eq. (1).

It may be noted in passing that the emission from an adsorbed film of caesium on tungsten is also increased considerably when a little nitrogen is admitted to the tube.

The examples discussed above therefore furnish some cases where the electron emission from a composite surface is increased by adding an electronegative component to the surface. They may all be accounted for formally by an equation of the type of (5).

RESEARCH LABORATORY,
GENERAL ELECTRIC COMPANY,
SCHENECTADY, NEW YORK.
June 14, 1924

SOME EFFECTS OF GAS UPON THE RESISTANCE AND RESISTANCE-TEMPERATURE COEFFICIENT OF SPUTTERED PLATINUM FILMS

By F. W. Reynolds

Abstract

Effects of oxygen and heat treatment on the resistance and temperature coefficient of resistance of sputtered Pt films.—Films 8 mm square were each sputtered in air at .02 mm on a blank kept at any desired temperature T up to 450°C by means of a heating coil. Resistance temperature curves made in a vacuum of 1μ of Hg at temperatures below T are reproducible straight lines. For "thin films" (resistance <500 ohms) the coefficient is positive and increases with ageing at high temperatures, approaching the value for bulk metal. For "very thin films" (resistance >500 ohms) the coefficient is negative but becomes positive by exposure to O_2 while hot. Heat treatment alone will not cause a reversal in the coefficient. The effect of oxygen at room temperature on thin films sputtered cold is to decrease the resistance slightly, while if the films are sputtered hot and then cooled the effect is a slight increase. The resistance of very thin films when exposed to O_2 at a temperature above a minimum (80 to 200°) depending on the film, increases very rapidly and would soon become infinite, but if cooled decreases again in time and soon reaches a value below the initial resistance. Other gases tried, H_2, He and CO_2 had practically no effect. It is suggested that the low values of the temperature coefficient are due to H_2 absorbed during sputtering and that the effects of the O_2 are partly due to chemical action with the H_2 and partly to absorption of the O_2.

THE various properties of sputtered platinum films such as; conductivity, resistance-temperature coefficient, and thermo-electric power are not the same as for the metal in bulk. Furthermore, these properties of sputtered films have been found to be dependent upon their previous history and are not permanent. Koller[1] studied the time change in resistance of these films and found that the presence of gas had a marked effect. He developed a combination theory of adsorption and agglomeration to account for the observed facts.

Longden,[2] Patterson,[3] Swann,[4] and others have reported variations in the resistance-temperature coefficient of these films. They found that the coefficient becomes smaller with decreasing thickness, passes through zero, and for very thin films is negative. Their data on the variation of

[1] L. R. Koller, Phys. Rev. **18,** 221 (1921)
[2] A. C. Longden, Am. Jour. Sci. **9,** 407 (1900)
[3] J. Patterson, Phil. Mag. **4,** 652 (1902)
[4] W. F. G. Swann, Phil. Mag. **28,** 467 (1914)

resistance with temperature were taken with the films exposed to air and were neither consistent nor reproducible.

The purpose, in part, of the present investigation was to make a more detailed study of the effects of gas upon the resistance and resistance-temperature coefficient of these films and to find some method for obtaining reproducible results.

Apparatus and Procedure

The usual type of sputtering apparatus was used with a few changes and additions. Platinum heating coils were placed beneath the blanks on which the films were deposited. This permitted the simultaneous deposition of two films beneath the same cathode and at different temperatures between that of the room and 450°C. Wires sealed in the sputtering jar enabled temperature and resistance readings to be taken in the original sputtering vacuum. The copper-advance thermocouples used were made of fine wire (No. 40 B & S) and were fastened to the blanks with a thin layer of alundum cement.

The films were deposited on glass, mica, and quartz at various temperatures in residual air and at a pressure of 20 μ of Hg. A 1 kw transformer supplied the potential of 15 kv which was completely rectified with a specially constructed high voltage synchronous commutator. The maximum current density at the cathode was .00005 amp. per cm^2. The blanks on which the metal was deposited were prepared about as described by Richtmyer and Curtiss.[5] In sputtering the thick Pt terminals, which were found more satisfactory than Au, the mask was raised about 1 mm above the blank. The resulting deposit formed a graded terminal for contact with the film and was found to have a negligible resistance. Pt foil was used for making electrical contact between the thick sputtered terminal and clamp. The films studied were 8 mm square and uniform in density.

The temperature of films sputtered cold never exceeded 40°C, due to precautions taken during sputtering. Ageing and resistance-temperature data were taken at pressures less than 1μ without exposing the film to air. A trap immersed in liquid air prevented oil and mercury vapors from entering the sputtering jar.

It will be convenient to divide the films studied in two classes, "thin," and "very thin." "Thin films" (8 mm square) are those whose final resistances after heat treatment at 300°C in a vacuum are between 80 and 500 ohms. They have a positive resistance-temperature coefficient

[5] F. K. Richtmyer and L. F. Curtiss, Phys. Rev. **15**, 465 (1920)

and are reasonably stable in resistance when heated in air. "Very thin films" are those whose final aged resistances are greater than 500 ohms. They have a negative coefficient and will become infinite in resistance if heated in air to 200°C. The thickest films used (80 ohms) absorb less than 40 percent of the incident light whereas a film having a resistance of a few thousand ohms is scarcely visible.

Experiments With Thin Films ($R < 500$ ohms)

Resistance. If these films are exposed to O_2 while hot there occurs a permanent decrease in resistance or ageing effect. The term ageing refers to a permanent decrease in resistance of a film with time. This method of ageing films is more effective than using either gas or heat alone and requires less time.

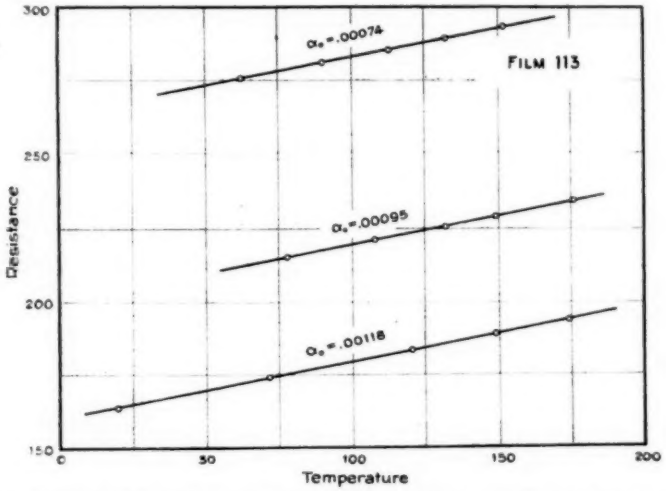

Fig. 1. Reproducible resistance-temperature data for one film, taken in a vacuum before and after ageing and at temperatures below the maximum sputtering and ageing temperatures, respectively.

Resistance-temperature coefficient. All sputtered Pt films except those classed as very thin have positive resistance-temperature coefficients. If the film has been sputtered cold it will require ageing for several hours at a higher temperature than that at which data will be taken. If sputtered hot reproducible data may be taken at once below the maximum temperature. Fig. 1 represents data taken on a film deposited hot. The upper curve was taken immediately after sputtering at 200°C, α_0 being the apparent resistance-temperature coefficient. This curve could be repeated over a period of several days provided the film remained in a vacuum and the temperature was not allowed to exceed 200°C. The

lower curves represent data taken on the same film after ageing by heating to higher temperatures. It should be noted that the graphs are linear and approximately parallel.

The advantage of sputtering a film hot is that it will yield reproducible data *below* this temperature without further ageing. In general the higher the temperature at which a film is sputtered or aged the nearer α_0 approaches the value of the bulk metal.

Experiments With Very Thin Films (R>500 ohms)

Resistance. Fig. 2 illustrates the effect of admitting O_2 and increasing the temperature of one of these films. The resistance of this film in a vacuum at room temperature was 13,000 ohms. O_2 was admitted at *A*

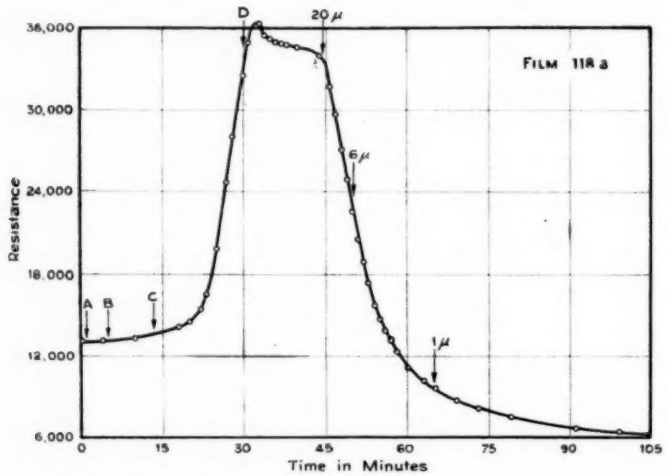

Fig. 2. Changes in resistance due to O_2 and heat treatment.

and caused a small increase in resistance. If the film had been left at room temperature there would have been little further increase in resistance with time. However, at *B* the heater current was started and at *C* the temperature of the film reached a constant value of 90°C. The resistance then began to increase and the rate soon became 2500 ohms per minute. Leaving the temperature constant at this value would have caused infinite resistance. In order to determine if the effect of gas and heat treatment were reversible the temperature was lowered at *D* and the pumps started. The film then aged to less than half its initial value. This film was initially sputtered at 160°C and was stable below this temperature while in a vacuum, hence the above ageing effect was not due to heat alone but to the O_2 admitted.

Fig. 3 shows the effect of temperature upon the rate of increase in resistance of a very thin film when exposed to O_2. At *A* O_2 was admitted to 20 cm pressure while the temperature was 115°C; at *B* the temperature was raised to 132°C; at *C* the temperature was lowered to 115°C; at *D* the temperature was raised to 132°C; at *E* the temperature was lowered to 100°C; at *F* the heater was turned off and the pumps started (the small increase in resistance at *F* was due to leakage of air through pumps on starting); and at *G* the pressure had reached about 5μ. It is obvious from the above that the rate of increase of resistance, when a film is exposed to O_2, can be largely controlled by regulating the temperature.

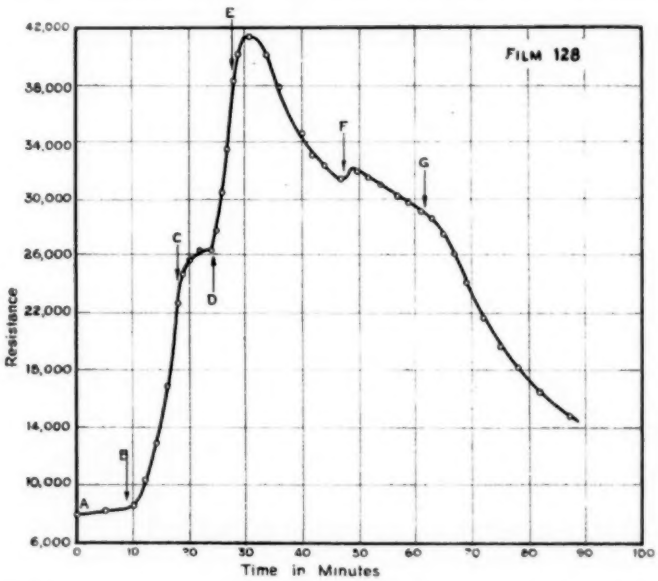

Fig. 3. Effect of temperature upon the rate of change of resistance when exposed to O_2.

The temperature at which the resistance begins to increase rapidly and also the rate of increase depend upon the film. It may vary from 80°C to 150°C for different films, but a temperature of 200°C is sufficient in any case to cause infinite resistance when a very thin film is exposed to O_2. H_2 and *He* under similar conditions caused only a slight increase in resistance which may have been due to traces of O_2 present.

Resistance-temperature coefficient. Very thin films initially have a negative coefficient which can also be reproduced below the maximum sputtering temperature. Fig. 4 shows data for one of these films immediately after sputtering. This film was deposited at 190°C; the points taken during cooling are enclosed by circles. The triangles enclose

points taken during a subsequent heating. The temperature was then raised and maintained for several hours at about 240°C causing ageing and a decrease in the slope to that of the lower curve, which was taken on cooling.

After treatment with O_2 and ageing in a vacuum the coefficient becomes positive. Fig. 5 illustrates the reversal of the coefficient of a film from negative to positive by this method. The circles on the curve A enclose points taken during the initial cooling, and the triangles represent data during a subsequent heating. The film was then exposed to O_2 while hot

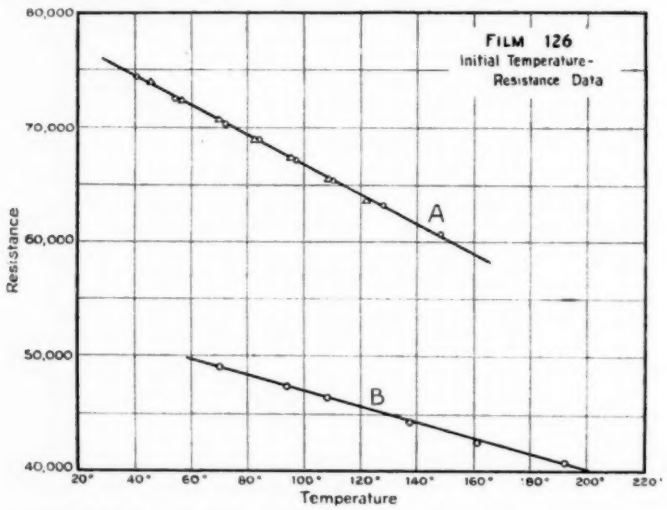

Fig. 4. Reproducible resistance-temperature curves for a very thin film. A, initial curve after sputtering at 190°C; B, after ageing at 240°C.

and finally aged for several hours in a vacuum. Reproducible data were then taken which showed that the film now had a positive resistance-temperature coefficient. Admission of O_2 again to this film resulted in a small increase in resistance which was reversible with decrease in pressure. The resistance-temperature coefficient, however, remained permanently positive.

Effects of Gas on Ageing at Room Temperature

Films deposited cold. The greatest rate of ageing occurs immediately after sputtering when the pumps, continuing to operate, decrease the pressure from 15μ to less than 1μ. A part of this initial decrease, for the thicker films, is due to cooling but the larger part is due to lowering of the gas pressure.

Fig. 6 shows the effect of admitting O_2 during the initial ageing of a film. This curve is typical of all films deposited cold and not heated. The sudden decrease in resistance shown here does not occur when H_2, He, or CO_2 is admitted under similar conditions. This ageing is therefore not due merely to pressure variation.

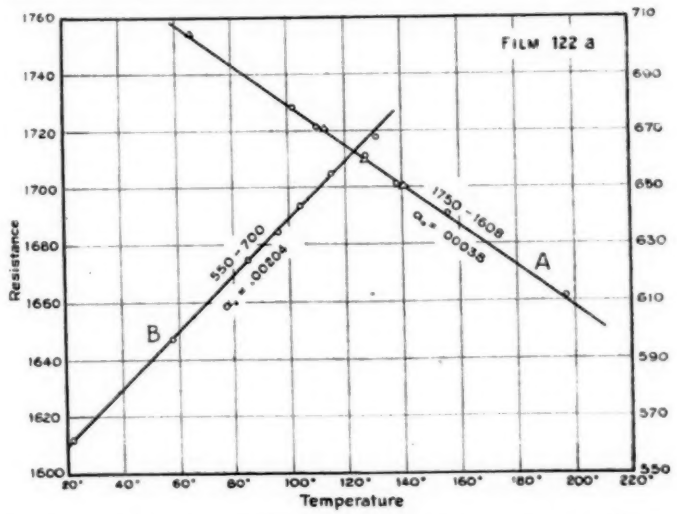

Fig. 5. Reversal of coefficient from negative to positive. A, initial curve; B, curve after exposure to O_2 and heat treatment.

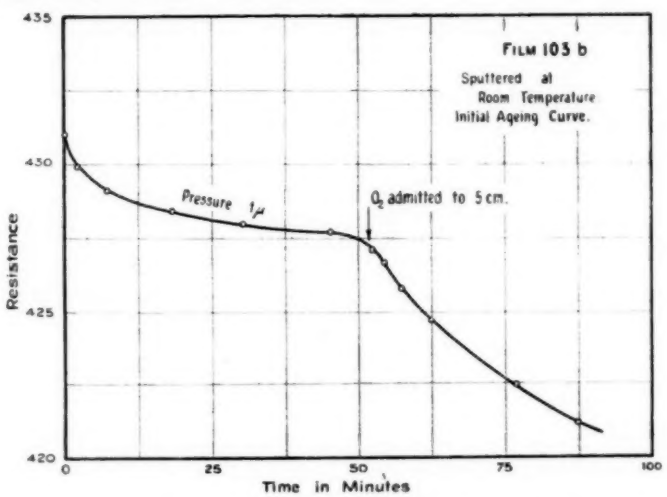

Fig. 6. Initial ageing of a film sputtered at room temperature, showing effect of admitting O_2.

Films deposited hot or subsequently heated. If films are deposited at a temperature of 60°C or higher and are then allowed to cool to room

temperature, admission of O_2 causes a few percent increase in resistance. Films deposited cold exhibit the same properties as those deposited hot if they are heated in a vacuum for a few minutes. In general these films age and behave towards various gases like those described by Koller.[1] It is evident therefore that most of his films were sputtered at temperatures considerably above that of the room.

Discussion

The above experimental facts can be qualitatively explained on the assumption that sputtered platinum films contain absorbed H_2. This view is consistent with the work of Holmes[6] who found the thermoelectric power of Pt films to differ from that of the bulk metal in the same way as bulk metal containing absorbed H_2 differs from gas free metal. This absorbed H_2 should increase the specific resistance of sputtered Pt as it is known to do for the bulk metal. Consequently resistance changes in a film maintained at constant temperature are an indication of a changing gas content. A simple agglomeration or sintering theory will not explain the behavior of the class of films represented in Fig. 2.

The decrease in resistance of a film resulting from the admission of O_2 at room temperature, according to the present view, is due to a partial 'clean-up' of the H_2 previously absorbed during the sputtering. This would be predicted from the work of Koller[1] who showed that freshly sputtered Pt or the Pt cathode itself (immediately after sputtering) are active catalysts and will cause combination of H_2 with O_2 *at room temperature* with explosive violence.

Films which have been sputtered hot should differ in two important respects from those deposited cold. First, they should contain less H_2 and second, they should be activated due to being heated in the presence of H_2 and O_2 as described by Langmuir[7] in the case of bulk Pt. Bulk Pt after such activation will occlude measurable amounts of O_2 and other gases.

Unless the temperature of a very thin film exposed to O_2 is lowered before the resistance becomes infinite the increase in resistance will not be reversible. This fact suggests that the water vapor which is being formed very rapidly within the film escapes with sufficient violence to rupture it. The adsorption-agglomeration theory proposed by Koller[1] to explain the infinite resistance is not in agreement with the fact that these very thin films show no tendency to pass through a minimum when

[6] R. M. Holmes, Phys. Rev. **22**, 137 (1923)
[7] I. Langmuir, Amer. Chem. Soc. Jour. **40**, 1361 (1918)

heated to 450°C in a vacuum. Furthermore, it has been found that the resistance of a film may increase to several megohms by exposure to O_2 and yet decrease to its initial value with decrease of pressure and temperature.

The effect of gas upon the resistance-temperature coefficient is in general agreement with the work of Dellinger.[8] He showed that impurities in metals caused an increase in their specific resistance and a corresponding decrease in their coefficient. Furthermore, he found that the additional resistance caused by the impurity did not vary with temperature.

Swann's[4] theory of the conductivity of thin films does not take into consideration any of the above variations in the conductivity or resistance-temperature coefficient due to changes in gas content. Furthermore, an inspection of his data shows that a large part of the variation in resistance which he attributed to temperature was due to O_2 and consequently was not reproducible.

In conclusion, the writer desires to take this opportunity for expressing his appreciation to Prof. F. K. Richtmyer for helpful suggestions and kindly interest throughout the investigation.

CORNELL UNIVERSITY
May 8, 1924

[8] Dellinger, Bur. Stand. **7**, 71 (1911)

HALL EFFECT IN A CONDUCTOR DUE TO ITS OWN MAGNETIC FIELD

By W. van B. Roberts

Abstract

If there is at each point in a conductor an electric intensity proportional to the vector product of the magnetic field and current density, there should be a difference of potential between points at different distances from the axis of a cylindrical conductor carrying a current. Rather than attempt to measure this, a qualitative confirmation of the existence of the effect was sought by use of a cylindrical specimen of bismuth having a long section of small diameter (3 to 4.8 mm) between two larger end sections (12.5 mm). When 60 cycle alternating current was sent through the specimen, the mean potential differences between the surface of the small section at the point M and two points A and B on the surface of the larger sections at each end, was measured by means of a tuned electro-dynamometer connected from M to the balance point on a semi-circular conductor connecting A and B, at which the 60 cycle potential differences were balanced out. This Hall effect has a double frequency because it does not reverse with the current. The resulting deflections were from .1 to .3 times the theoretical upper limit, therefore in good qualitative agreement. That they were not due to thermo-electric effects was proved by the absence of the effect when an alloy with zero Hall coefficient was substituted, as well as by other tests. It is concluded that the Hall effect is always present in wires carrying currents and should cause a slight increase of resistance at high current densities.

Theory

BOTH the Hall effect and the Corbino effect are consistent with the following hypothesis: At any point in a conductor there exists an electric force e_H which is proportional to the resistivity ρ of the material multiplied by the vector product of the current density I and magnetic field H at that point. Thus the Hall field is at right angles both to the lines of flow of current and to the magnetic field. Expressed as an equation,

$$e_H = c\rho[IH] . \qquad (1)^*$$

The question naturally arises, is there not some Hall effect in every wire carrying a current, due to the magnetic field of the current itself, or is it only an additional magnetic field that produces the effect? A very simple imaginary experiment indicates the former. Imagine a long cylindrical conductor divided up into a great number of long thin wedges so that the cross-section would be as shown in Fig. 1. If each wedge be insulated from every other by a negligibly thin space, the magnetic

* The constant of proportionality c is not always absolutely constant. In bismuth, for example, the value of c is less in very strong magnetic fields than in weak ones.

field produced when the ends of the wedges are connected to the same battery, will be a family of circles. Now, pick out any one wedge. Because of the magnetic field produced by the rest of the wedges there will be a potential difference between the edge of the wedge and the part on the circumference. By symmetry, this must be true of all the wedges. Hence the circumference of the conductor is an equipotential, but its potential is different from the potential of the point where the axis cuts its plane. As there should be no reason for the current to travel in a spiral along the conductor, it should make no difference whether the wedges are insulated from each other or only divided in the imagination. However, it was thought worth while checking this conclusion experimentally.

Fig. 1

Fig. 2

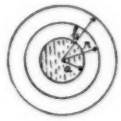

Fig. 3

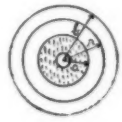

Fig. 4

The potential differences to be expected in a number of different cases, are as follows: (practical units, amperes, volts, gauss, etc., are used throughout)

Case I. Solid cylindrical conductor. Fig. 2. At a distance r from the axis,

$$H=(2C/10r)\ (r^2/b^2)$$

where C is the total current and b is the radius of the cylinder. Substituting in Eq. (1),

$$e_H=c\rho I(C/10)\ (2r/b^2) \qquad (2)$$

The potential difference between axis and circumference will then be the integral of $e_H dr$ from 0 to b, or $V_H=c\rho IC/10$. Now ρI is the potential gradient along the conductor, so ρIC is the number of watts dissipated in heat per cm length of the conductor, which we will call W. Thus finally, $V_H=cW/10$.

Case II. Hollow cylindrical conductor, inner radius a (Fig. 3). In this case $H=(2C/10r)\ (r^2-a^2)/(b^2-a^2)$, so

$$V_H=(cW/10)\left\{1-2\left[a^2/(b^2-a^2)\right]\log_e(b/a)\right\}.$$

The function in brackets depends only upon the ratio a/b and to a rough approximation falls linearly from the value 1 that it assumes when $a/b=0$ to zero when $a/b=1$. Fig. 5A shows a graph of this function.

Case III. Hollow cylindrical conductor, with return current inside and coaxial, to avoid incalculable effect of return current. (Fig. 5) In

this case $H=(2C/10r)-(2C/10r)(r^2-a^2)/(b^2-a^2)$ and the potential difference between inside and outside of the pipe will be

$$(cW/10)\{2\ [b^2/(b^2-a^2)\ ]\log_e(b/a)-1\}\ .$$

The bracketed function is plotted in Fig. 5B. It increases rapidly as a/b becomes small, but a/b is limited by the necessity for a finite size for the return conductor.

Case IV. Conductor of varying cross-section. (Fig. 6) By taking the line integral of e_H around the small element formed by adjacent stream lines and the orthogonals, we find curl $e_H=\partial/\partial s(c\rho IH)+\psi c\rho IH$ where ψ is the curvature of the orthogonal to the stream lines. Hence there will be small circulating currents superposed upon the normal current. If the

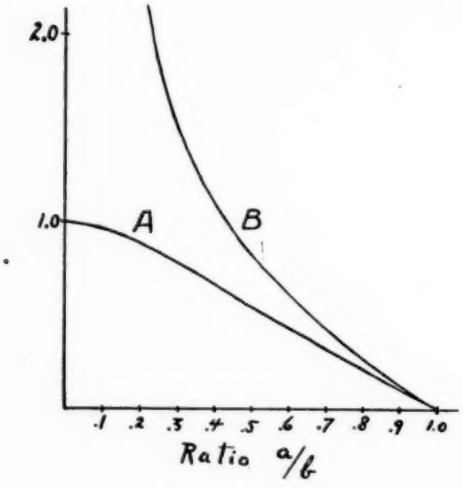

Fig. 5

intensity of the superposed current is i, then we have curl $(\rho i)=$curl e_H. Integrating curl e_H from the axis to the surface, between sections of the conductor which have stream lines approximately parallel, we obtain $c_2W_2/10-c_1W_1/10$. Referring to Fig. 6, c_1 and W_1 are the values in the narrower section, and c_2 and W_2 the values in the thicker section. The integration is done in two steps. First integrating along a stream line,

$$\int \text{curl}\ e_H du\ ds=\int[(\partial/\partial s)c\rho IH+\psi c\rho IH]duds=\int[\delta(c\rho IH)]du$$
$$+\int(c\rho IH)\delta du=\int\delta(c\rho IHdu)=c_2\rho_2I_2H_2du_2-c_1\rho_1I_1H_1du_1\ ,$$

since $\psi\, duds=\delta\, du$, the change in du in the distance ds. The values are those obtaining on the stream line at the limits of integration. Then making use of the fact that u may be replaced by r where the stream lines are parallel

we have $H=(2C/10r)\ (r^2/b^2)$, and integrating with respect to r (c and ρ being supposed constant across the cylindrical sections) we get $c_2\rho_2 I_2 C/10$ or $c_2W_2/10$. Likewise, at the other section we get $-c_1W_1/10$. This result is the same as the line integral taken by the use of the formula of Case I, going along the axis (which contributes nothing, being a stream line), then out radially through the thicker section (which contributes $c_2W_2/10$ by Case I), then along the surface of the conductor (which contributes nothing, being a stream line), then inward radially to the axis through the narrow sect on (which contributes $-c_1W_1/10$ by Case I).

Thus, although it might appear that the Hall effect should not cause any alteration of the relative potentials of points A and B in F g. 6 because the line integral of e_H along the surface from A to B is zero, yet there will be an alteration due ind rectly to the Hall effect, because of the resistance drop along that path of the circulating current that must flow in response to the existence of the closed line integral of e_H. The exact proportion of the total voltage (developed by Hall effect) that is available by tapping at A and B is not easy to calculate.

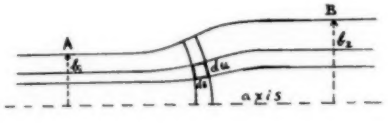

Fig. 6

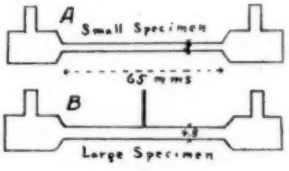

Fig. 7

Outline of Experiment

After a careful consideration of the dimensions of the cylinders that would have to be used if a quantitative measurement using the arrangements of Cases I, II or III were to be tried, and of the chances of the cooling system being adequate to prevent thermo-electric currents that would be difficult to separate from the Hall effect, it was decided that it would be more feasible to seek only the qualitative confirmation of the theory that could comparatively easily be obtained from a modification of the arrangement of Fig. 6.

Bismuth was chosen to work with on account of its large Hall coefficient.[1] A specimen was cast in a graphite mould, 3 mm in diameter and 65 mm long, with sections 12.5 mm in diameter at each end, provided with projections so that contact could be made where the junction would not be heated. Fig. 7 shows the specimen to scale. The current was led in and out of the bismuth by copper wires 3 mm in diameter. A

[1] Albert K. Chapman, Phil. Mag., **32** (Sept. 1916)

hole was drilled in each end of the specimen, and the end of the copper was tinned and heated and pushed into the hole, the hot solder readily alloying with the bismuth. Connection was made to the projecting portions in a similar manner. Current was supplied by a 30 to 1 ratio step-down transformer. Alternating current was used to discourage thermo-electric effects as much as possible. As they both depend upon the instantaneous value of W, the Hall effect and thermo-electric currents both have double frequency components, but the latter should show mostly the constant component, while the former should show just as great a double frequency as the constant component.

The schematic arrangement is shown in Fig. 8. The field due to the semicircle (of radius 60 cm) is fairly well compensated for by proper choice of the resistance of the smaller semicircular shunt (about 3.5 cm radius). The instrument indicated by the arrow is capable of measuring alternating voltages of either 60 cycles or 120 cycles exclusively. The sliding contact S is adjusted to a position where no 60-cycle current flows. This is also the proper position to balance out any other frequencies

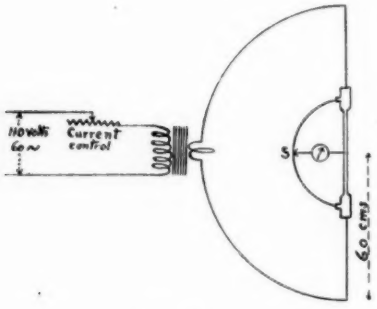

Fig. 8

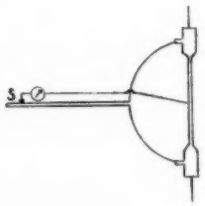

Fig. 9

that may be supplied by the transformer. If, however, Hall effect is present, currents of both zero and 120 cycles will flow through the instrument, being independent of the direction of the exciting current. A sheet of water from a fan-shaped nozzle was kept on the bismuth to keep down thermo-electric currents and prevent unbalancing at S due to unequal heating of the two halves of the bismuth. The adjustment at S is so critical that instead of a small semicircle, the arrangement of Fig. 9 was used. Thus, there was about 6 feet of wire for the slider to work on, and even then an adjustment to better than 1 mm was necessary.

Another difficulty lay in currents induced in the circuit of the detecting instrument by the magnetic fields due to the iron of the transformer and to the main current. These were eliminated by connecting two coils of

wire (one of five turns, the other two turns, both of 3″ diameter) in series with the detecting instrument. The five-turn coil was placed about a foot from the transformer and was adjusted so as to balance out its field when the secondary was open-circuited. The other was placed further from the transformer but near the main current, and could be adjusted so as to eliminate induction due to the current. The procedure was as follows: First the detecting arrangement was fixed to detect a 60-cycle frequency only, and the deflection reduced to zero by adjustment of the slider S and the two compensating coils. Then the detector was made sensitive only to 120 cycles and the deflections observed and plotted against watts per cm. The deflections were of the predicted order of magnitude. To be sure that these deflections were really due to Hall effect, three checks were employed. (1) Runs were made with a rapidly flowing stream of water and then with a much slower stream. The results were so nearly the same that thermo-electric currents could not be responsible for any very large proportion of the deflections. (2) The leads to the amplifier were reversed right at the amplifier input. This reversed the sign of the deflection, which would not have been the case if the 120-cycle current had been generated inside the amplifier as an harmonic of a 60-cycle input. (3) A duplicate specimen was cast of bismuth alloyed with 2 percent tin. This alloy has approximately zero Hall coefficient.[2] Replacing the pure bismuth by this specimen, everything else being unchanged, observations were taken as before, but this time no deflections of the same order of magnitude were observed. Hence, it seems certain that the previously observed deflections were really those predicted by the hypothesis $e_H = c\rho[IH]$.

To make doubly sure, the experiment was repeated with slight modifications. Again duplicate specimens were used, one of c.p. bismuth and the other of 2 percent tin alloy, but this time the contact to the center of the narrow part was not the phosphor-bronze knife edge previously used, but a thin rod of bismuth less than 1 mm in diameter cast integral, as shown in Fig. 7B. The diameter of the specimen being increased to 4.8 mm, this projection should disturb the stream lines very little, and since all junctions of dissimilar metals are well away from the main current, they can be kept at the same temperature. The other difference is that the detecting instrument was left adjusted to detect only 120 cycles throughout, the balance for 60 cycles being more quickly and easily got by means of a telephone receiver. Probably due to unequal cooling effect on the two halves of the bismuth rod, this balance was

[2] Albert K. Chapman, loc. cit.[1]

not always quite independent of current. So a balance was made by ear (without looking at the deflection) after each change in current, and then the deflection was read. Again the pure bismuth sample gave deflections of the expected magnitude, while the alloy gave none to speak of.

Sample observations with both small and large specimens are given in Tables I and II and in Fig. 10.

TABLE I

Sample observations on small size specimens[2]

Current in amperes							
bismuth specimen:	22	32	40	48	56	64	72
alloy specimen:	not much less than for bismuth						
Heat developed in watts/cm[3]							
bismuth specimen:	.035	.09	.15	.23	.32	.43	.65
alloy specimen:	greater than for bismuth						
Deflections in cm							
bismuth, water running slowly:	.04	.10	.17	.24	.34	.45	.61
alloy specimen:	.00	.10	.07	.03	.1	.1	.1

TABLE II

Sample observations with large size specimens[4]

	current (amp)	heat (watts/cm)	deflection (cm)	reversed deflection[5]	upper limit predicted
bismuth specimen	20	.32	.09	.0 cm	.16
(resistance	34	.92	.15	−.06	.46
.0008 ohms/cm)	43	1.46	.21	−.12	.73
	53	2.24	.29	−.20	1.12
	61	2.97	.35	−.24	1.48
	64	3.27	.48	−.28	1.63
	80	5.22	.69	−.52	2.61
	96	7.4	.95	−.75	3.7
	117	10.5	1.40	−1.05	5.2
alloy specimen	58	5.5	.01		
(resistance	61	6.0	.01		
.0016 ohm/cm)	64	6.5	.02		
	69	7.6	.02		

DETECTING ARRANGEMENT

The deflection instrument used was a Leeds and Northrup electrodynamometer which gave a deflection of 2.5 mm when 1 milampere was put through both coils in series. To measure 120-cycle currents, 100 milamperes of 120-cycle current were supplied to the fixed coil, and the

[2] These readings were made with a single balancing out of the 60 cycle current at the beginning of each run.

[3] The resistance of bismuth specimen was about .002 ohm/cm, while that of alloy specimen was about twice as much.

[4] Each reading was taken after a 60 cycle balance had been made by ear.

[5] Deflection when input to amplifier is reversed.

current to be measured was put through the moving coil. As a steady torque would not result unless the two currents were absolutely synchronous, it was necessary somehow to use the second harmonic of the 60-cycle source that supplied the main current through the bismuth. This was obtained by reversing the function of the "push-pull" vacuum-tube amplifier. This is shown in the schematic circuit of Fig. 11.

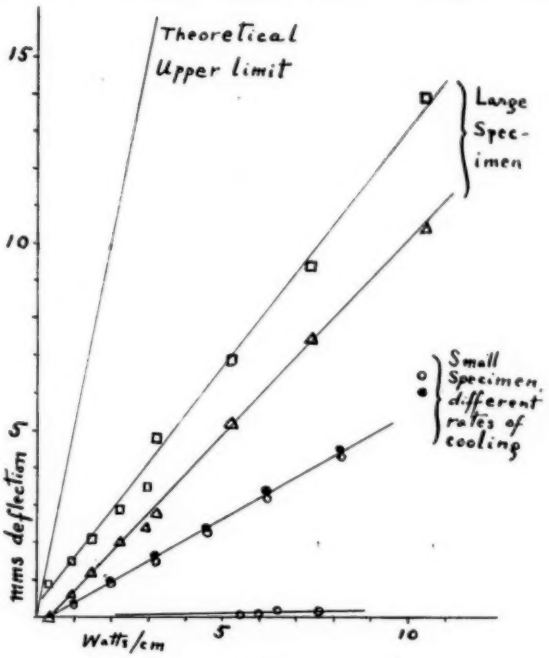

Fig. 10

Now in addition to being synchronous, the two currents in the electrodynamometer coils should be in phase. Considering the phase of the current in the moving coil as fixed, the other current could be brought into phase by shifting the phase of the input voltage to the circuit of

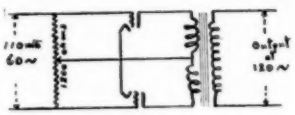

Fig. 11

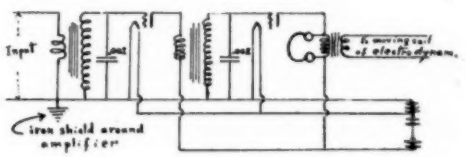

12

Fig. 12. A simpler process is to have two phases 45° apart available for this input. A 45° shift of the 60-cycle input causes a 90° shift in the 120-cycle output as will be proved below. By measuring the two deflec-

tions obtained with the two stationary coil currents 90° different from each other, we deduce the deflection that would be observed if the currents in the two coils were in phase, by taking the square root of the sum of the squares of the two deflections.

Returning to analyze the action of the 120-cycle generator, assume that the plate circuit current of a vacuum tube is represented by a power series of the grid potential variations. On one grid we impress sin pt and on the other $-\sin pt$, so the plate circuit currents are $\sin pt+\sin^2 pt+\ldots$ etc. and $-\sin pt+\sin^2 pt-$ . . . etc. and the flux in the iron core of the output transformer will contain only the even harmonics, the odd ones being cancelled out by the similarity of the primary windings. The sliding contact on the high resistance across the input allows this balance to be effected. When balanced, 100 milamperes at 120 cycles can be put through the stationary coil and considerable current at 60 cycles through the moving coil, without causing any deflection. Suppose now that the phase of the input is shifted an angle φ. The input is then $\sin (pt+\varphi)$ and $\sin^2 (pt+\varphi)$ becomes a constant $+\cos (2pt+2\varphi)$, showing that the phase of the second harmonic advances twice as fast as the phase of the input. The complete circuit of the 120-cycle generator is shown in Fig. 13, which

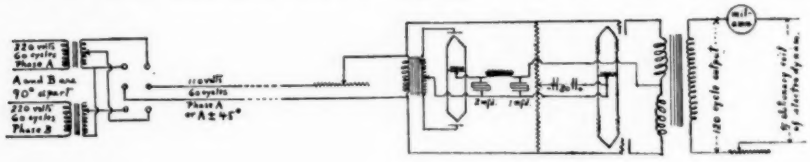

Fig. 13

includes the arrangement for phase shifting. The windings that light the filaments are low tension windings on the same core as the step-up winding that supplies the high tension. This transformer is the Radio Corporation of America model UP-1368 and the choke is their model UP-1626, and the rectifier tubes are their UV-216. The amplifier tubes are Western Electric VT-2 or E tubes, with suitable resistances in the filament leads. The output transformer is a Western Electric W-230, 6,000:50.

The sensitivity of the electro-dynamometer not being sufficient, an amplifier was used ahead of it. Two cheap audio-frequency interstage transformers were used, one as input and one as output. Only the secondary, which is designed to work into a vacuum tube, was used for the input transformer, a special primary of 45 turns with midtap being used to come nearer to matching the impedance of the circuit attached to it. The output transformer, on the other hand, has a special secondary

wound with the intention of matching the impedance of the moving coil. However, there was not room to get enough turns on to do this, and no attempt was made to overcome this imperfection, as the amplifier was sufficiently sensitive anyway. The circuit is shown in Fig. 12. The middle transformer is an "Amertran." The tubes are Cunningham 301-A's. The small .002μf condensers helped stabilize the amplifier and increased the amplification of low frequencies.

The calibration of the detecting system was made by passing 50 milamperes of 120-cycle current through a standard .01 ohm resistance. The input of the amplifier was connected across this, so that a known voltage of 5×10^{-4} volt was applied. The electro-dynamometer coils were connected, in *parallel*, to the output of the amplifier, and a 4 mm deflection resulted. As the impedance of the moving coil was 17 ohms and that of the stationary coil 32 ohms (both nearly pure resistance), and as 1 milampere in each coil gives 2.5 mm deflection, we can calculate the currents that give 4 mm. Call the stator current i_s and the rotor current i_r. Then $32\ i_s=17\ i_r$ and $i_s\times i_r=4/2.5$. These equations give $i_s=.92$ and $i_r=1.73$, approximately.

Now if only the moving coil had been connected to the output transformer, it would have received not less than 1.73 milamperes and not more than 2.65, according to the impedance of the transformer. Taking 2 as a tentative value, we summarize by saying that 5×10^{-4} volt input gives 2 milamperes output. Now we know that we are actually using 100 milamperes in the stationary coil instead of .92, so the deflection would be $(100/.92)\times4$ or 430 mm. Hence, a deflection of 1 mm corresponds to $5\times10^{-4}/430$ or 1.16×10^{-6} volt input under actual operating conditions.

That this is enough sensitivity to detect the Hall effect in bismuth, is seen by putting in the value of c which is in the neighborhood of 7×10^{-5} for weak fields. The total generated Hall voltage is thus about $.7\times 7\times10^{-5}\times(W_2-W_1)/10$ or $5\times(W_2-W_1)\times10^{-6}$ volt (effective value), which might give a barely observable deflection for $W_2-W_1=1/10$ and could give 25 mm for $W_2-W_1=5$. These are, of course, upper limits, as only a fraction of the generated voltage can be picked off the outside of the specimen.

Before leaving the subject of the electro-dynamometer, it should be mentioned that the coils had to be connected together to prevent deflections due to static electrical charges, and had to be adjusted exactly at right angles, or current in the stator induced current in the rotor, tending to pull it to right angles. This same effect introduces a restoring force that adds to the restoring force due to the twist of the suspension. Since

the sensitivity of the amplifier was measured in the absence of this effect, the currents in both coils being small, some correction must be made. Experiment shows that the restoring torque due to 100 milamperes in the stator is only one-tenth that of the suspension. The correction is most easily made by changing our statement that 1 mm deflection $=1.16\times10^{-6}$ volt input, to 1 mm $=1.05\times10^{-6}$ volt input.

Discussion of Results

It will be noticed that the small specimen gave less deflection per watt than the large one. This may possibly be because connection to the amplifier had less effect on reducing the potential differences in the case of the larger lower resistance specimen, or it may be because the supply of bismuth gave out and the larger specimen was cast of a new c.p. lot.

Another peculiarity is that the deflections run uniformly larger when the connections to the amplifier are such that the harmonic (of any 60-cycle unbalance) generated by the amplifier adds to the Hall effect. This might be due to the unidirectional torque produced by the interaction of higher harmonics in the two dynamometer coils, or it may be explained as follows. In balancing out the 60-cycle current there is a small range where the 60-cycle hum cannot be heard on account of the much louder 120-cycle noise. If the connections to the amplifier are such that the Hall effect 120-cycle current and the harmonic of any 60-cycle unbalance are in phase, then the slider is set at a minimum for both frequencies. But if the amplifier connections are reversed, then the slider is apt to be set a little to one side of the true balance point, not enough to make the 60-cycle note audible through the 120-cycle noise, but just enough to let the amplifier produce a small amount of 120-cycle harmonic which in this case is 180° out of phase with the Hall effect and hence gives the illusion that a better balance is obtained a trifle off the proper point. If this explanation is correct, the larger deflections should be the best values. If some unidirectional torque is the cause of the difference then a mean of the two sets of values would be best. It makes no difference which alternative is chosen as far as the general conclusions that may be drawn go.

The fact that the deflections plotted against watts/cm give fairly straight lines does not prove anything, for thermo-electric currents or harmonics generated in the amplifier would give deflections behaving the same way; but the independence of rate of cooling, the change in sign of the deflections with reversal of connections to the amplifier, the vanishing of the deflections w th the addition of 2 percent tin, and the satisfactory

quantitative agreement with the predicted order of magnitude of the deflection, seem to establish the existence of the effect quite decisively. The comparison of observed deflections with the predicted upper limits indicates that the arrangement used makes available between the external contacts a few tenths of the total generated Hall voltage.

If the Hall effect causes circulating currents wherever the expression for curl e_H (derived in Case IV) is not equal to zero, and the energy loss due to these currents varies as the fourth power of the main current, then the measured resistance of a conductor would be of the form $R+a\,I^2$ and give the possibility of detecting an apparent increase in resistance where the current density is very high. This may have something to do with the increase observed by Bridgman[6] at densities of about a million amperes per square centimeter.

I wish to thank Prof. E. P. Adams, who suggested this experiment, for his interest throughout.

PALMER PHYSICAL LABORATORY
PRINCETON UNIVERSITY.
May 7, 1924

[6] P. W. Bridgman, Proc. Amer. Acad. **57,** (April, 1922)

TORQUE ON A CYLINDRICAL MAGNET THROUGH WHICH A CURRENT IS PASSING

By John Zeleny and Leigh Page

Abstract

The torque acting on a vertical magnet, free to rotate about its axis, when an electric current is sent into the magnet by means of a horizontal arm attached at the central portion of its length and taken out along the axis, is usually ascribed either to the action of the field of the magnet on the current in the horizontal arm or to the action of the field of the current in the magnet on the poles of the magnet. But with a symmetrically magnetized magnet the latter torque reduces to zero whereas the action on the horizontal arm is opposite to the torque actually observed. The predominating torque which is overlooked is that resulting from the action of the magnetic flux through the magnet on the entering current sheet. *Theoretical equation.* It is shown that if a current enters along the peripheral surface of a symmetrically magnetized cylindrical magnet, the total torque is $iN/2\pi$ where i is the c.g.s. current flowing and N the flux cutting the current sheet. The same relation holds when the magnetization is not symmetrical if the current enters the magnet in a symmetrical manner through a peripheral ring of the surface. If the current enters a magnet through the whole base over which there is a uniform magnetic induction, then the torque is $iN/4\pi$. *Experiments* made with a symmetrically magnetized magnet with the current entering the magnet from a salt solution at peripheral rings at various places along the length of the magnet and leaving at the axis, verify the formula deduced. The same formula was found to agree also with experimental results obtained when a brass cylinder in the field of a solenoid replaced the magnet, showing that poles are without effect. The torque on a magnet when the current entered through a side arm was found to be the less the longer the side arm.

MANY books in physics describe a modification of Ampère's experiment in electromagnetic rotation in which a vertical bar magnet of circular cross section free to rotate about its axis of symmetry has attached to it near the center a horizontal conducting arm the end of which dips into a circular trough of mercury concentric with the magnet. If a current entering the magnet through the mercury trough and conducting arm passes out along the axis of the magnet, a torque is experienced which may be sufficient to cause the magnet and attached arm to rotate. The phenomenon is the inverse of unipolar induction.

Various explanations of the rotation have been given of which some are incomplete and others incorrect. It is clear that two torques are involved, (1) the torque exerted by the field of the magnet on the current circuit, and (2) the torque exerted by the current circuit on the poles of the magnet. The first of these may be subdivided into L_i the torque

on the portion of the circuit inside the magnet, L_i' the torque on the attached arm and L_i'' the torque on the portion of the circuit which is mechanically free from the magnet. Obviously the rotation of the magnet is due to the combined action of these torques (1) and (2), with the exception of L_i''. As will appear later, in the cases to be considered, each of the torques (1) and (2) vanishes individually, and the rotation is due to the fact that only the parts L_i and L_i' of the first torque operate on the magnet.

Some authors[1] have ascribed the rotation solely to the torque L_1' exerted on the current in the arm by the field of the magnet. As a matter of fact the rotation is in the opposite sense to that of this torque and the rotation is more pronounced the shorter the arm. For the torque on the arm opposes a greater torque L_1 on the current passing through the material of the magnet. The latter torque has generally been overlooked in explaining the phenomenon.

Other writers[2] attribute the rotation to the torque L_m exerted by the current on the poles of the magnet. While this explanation leads to a rotation in the sense actually observed, and may in certain cases yield a quantitative value of the torque which is approximately correct, it is misleading in that it fails to take account of the other torques which are operative. It will be shown that as a matter of fact no current circuit whether it passes in part through the magnet or no, can exert a torque on a symmetrically magnetized bar.

As the experiment is one which has evidently led to some misapprehension, it has seemed worth while to develop the theory involved and to describe some experiments which were performed to check the theory. In the initial theoretical discussion the current is supposed to enter the magnet along the periphery of a circular cross-section and to flow out along the axis at the top. Thus the horizontal arm may be supposed to be replaced, as is sometimes done, by a conducting apron dipping into a mercury trough along the whole of its circular periphery.

Mathematical Theory

First consider a magnet without an attached conducting apron (Fig. 1). A symmetrical sheet of current[3] enters the magnet along the periphery

[1] A. L. Kimball, College Text Book of Physics, 462, 1917; Brooks and Poyser, Electricity and Magnetism, 347, 1912.

[2] O. D. Chwolson, Traité de Physique **4**, 794, 1913;
A. Winkelmann, Handbuch der Physik **5**, 435, 1908;
Müller-Pouillets, Lehrbuch der Physik **5**, 674, 1914.

[3] The sheet is symmetrical with respect to the axis of the magnet though the distribution of current in the sheet may not be symmetrical.

of the circular section AB and passes out along the axis at N. The torque consists of two parts, the torque L_i exerted by the field due to the magnet on the current sheet i passing through the magnet, and the torque L_m exerted by the field produced by the current on the magnet.

Torque L_i Exerted by the Magnet

To compute the first of these torques consider the small portion of the symmetrical sheet extending from C to D. Put $d\lambda$ for the slant distance CD and $\mathbf{p}$ for the radius of the circular section of the current

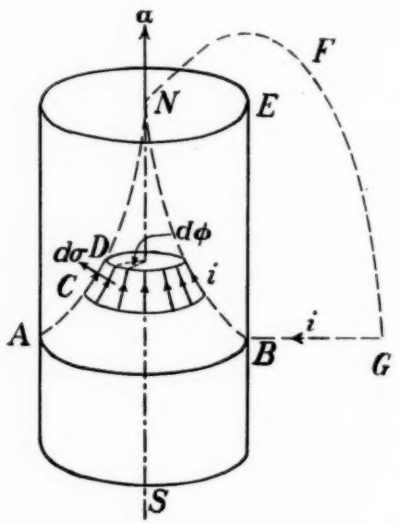

Fig. 1

sheet. Then, as the average field strength inside the magnet is the magnetic induction $\mathbf{B}$, the force $d\mathbf{K}_i$ on the element of the current sheet subtending the azimuth $d\phi$ is

$$d\mathbf{K}_i = \frac{di}{d\phi}\, d\phi\, d\lambda \times \mathbf{B},$$

and if $\mathbf{a}$ is a unit vector in the direction of the axis, the torque about this axis is

$$dL_i = \frac{di}{d\phi} d\phi\, (\mathbf{a}\times\mathbf{p}) \cdot (d\lambda \times \mathbf{B}) = \frac{di}{d\phi}\left[\{d\phi\, (\mathbf{a}\times\mathbf{p})\} \times d\lambda\right] \cdot \mathbf{B}\,.$$

But the expression inside the brackets is just a directed element of area $d\sigma$ of the current sheet. Hence

$$dL_i = \frac{di}{d\phi}\, \mathbf{B} \cdot d\sigma\,. \qquad (1)$$

The following two cases are of especial interest.

Case I. The distribution of current in the sheet is symmetrical. Then

$$di/d\phi = i/2\pi,$$

and integrating (1) with respect to ϕ

$$\delta L_i = (i/2\pi)\ (N_1 - N_2), \tag{2}$$

where N_1 and N_2 are the total upward fluxes through the cross sections at C and D respectively. It is to be noted that (2) holds for a symmetrical distribution of current in the sheet no matter how asymmetrical the magnetization of the magnet and the distribution of the lines of induction may be. If the current leaves the magnet along the axis, the total torque is

$$L_i = iN/2\pi, \tag{3}$$

where N is the flux through the section AB, and i the current in c.g.s. units.

Finally, if the current sheet enters through an apron attached to the magnet, the same formula holds provided N is understood to denote the flux through the periphery of the apron. As the flux outside the magnet is oppositely directed to that in the interior, the effect of the apron is to diminish the torque. In the limiting case of an apron of infinite cross section the torque obviously vanishes.

If the current spreads through the magnet instead of flowing in a sheet of infinitesimal thickness, the single current sheet considered above must be replaced by a family of sheets having common peripheries. As Eq. (3) holds for each sheet individually it holds for the ensemble of sheets.

Case II. The magnet is symmetrically magnetized. Then, if B_n denotes the component of $\mathbf{B}$ perpendicular to the current sheet

$$\mathbf{B} \cdot d\sigma = B_n p d\lambda d\phi$$

is constant, and (1) leads to

$$\delta L_i = B_n p d\lambda \int \frac{di}{d\phi} d\phi = (i/2\pi)\ (N_1 - N_2)\ . \tag{4}$$

Therefore Eq. (3) gives the torque on a current sheet passing through a symmetrically magnetized bar no matter how asymmetrical the distribution of current in the sheet may be. This expression for the torque holds equally well if the current is not confined to a single sheet of infinitesimal thickness, for whatever the distribution of current in the magnet may be, it may be represented by a family of symmetrical current sheets in each of which there exists a symmetrical or asymmetrical distribution of current. Furthermore, if a current element such as CD in the figure

does not lie in the plane determined by C and the axis of the magnet, the force on the component of the current at right angles to this plane passes through the axis and therefore contributes nothing to the torque.

Hence it is clear that, if the magnet is symmetrically magnetized, the torque produced by a current all of which enters at the point B is the same as if the current entered uniformly around the periphery AB. If the current enters through an arm dipping into a mercury trough as in the usual experimental arrangement, Eq. (3) gives the torque provided N is taken to mean the flux through a circle of radius equal to the distance of the end of the arm from the axis of the magnet.

The Torque L_m Exerted by the Current

It will now be shown that the torque L_m exerted by the current on the magnet vanishes for each of the two cases which have been discussed. Let ρ be the pole strength per unit volume of the magnet.[4] Consider an annular ring of constant cross section ds coaxial with the axis $\mathfrak{a}$ of the magnet. Let H_ϕ be the component of the field due to the current tangential to the ring. Then the tangential force on the portion of the ring which subtends the angle $d\phi$ is

$$dK_m = \rho p H_\phi d\phi ds,$$

and the torque exerted by this force is

$$dL_m = \rho p^2 H_\phi d\phi ds. \tag{5}$$

Case I. The distribution of current in the sheet is symmetrical. Then H_ϕ is constant around the periphery of the ring, and equal to $2i/p$ if the current passes through the ring, or zero if the current does not pass through the ring. Therefore integrating (5) with respect to ϕ,

$$\delta L_m = p H_\phi \int \rho \, p d\phi \, ds \equiv 2i\delta m. \tag{6}$$

where δm is the total pole strength in the ring and i is the current passing through the ring. Summing up over the entire magnet

$$L_m = 2\, i \Sigma \delta m, \tag{7}$$

where $\Sigma\delta m$ is the total pole strength in that portion of the magnet lying above and outside the current sheet, considered as cut away from the rest of the bar. The portion of the magnet below and inside the current sheet is not involved because the field due to the sheet vanishes at all points in this region. Now the algebraic sum of the pole strengths on any isolated body is zero. Therefore the torque vanishes. It is to be noted that the magnet has not been assumed to be symmetrically magnetized. So long as the distribution of current in the sheet is symmetrical the

[4] As a surface distribution may always be included in the general volume distribution there is no need of treating the surface poles separately.

torque which it exerts on the magnet vanishes no matter how asymmetrical the magnetization may be.

Case II. The magnet is symmetrically magnetized. Consider the effect of a closed current filament $BNFG$ on an annular ring. As ρ is not a function of ϕ, the integration of (5) around the ring gives

$$\delta L_m = \rho p ds \int H_\phi p d\phi = 4\pi i \rho p ds = 2i\delta m \tag{8}$$

if the ring encircles the current, or zero if it does not. Summing up over the whole magnet, the total torque due to the action of the current filament on the magnet vanishes. As this is true of every current filament, it is clear that no circuit can exert a torque about the axis of symmetry of a symmetrically magnetized bar, whether the circuit passes through the magnet or no. Provided the symmetry of magnetization is not destroyed by inductive effects, no steady outside field can produce a torque on a symmetrically magnetized bar, for any such field is, in the last analysis, due to closed current circuits.

As the torque exerted by the current on the magnet vanishes in each of the cases which have been discussed, the total torque is that exerted by the field of the magnet on the current passing through the magnet and through any apron or arm which may be attached thereto. This torque is given by Eq. (3).

If the current enters near the middle of a uniformly magnetized bar which has a radius small compared to its length, the flux N appearing in the equation for the torque is nearly all due to the intensity of magnetization I, and hence, to a fair degree of approximation,

$$L = (i/2\pi)\,(\pi a^2)\,(4\pi I) = 2i\pi a^2 I = 2im\ . \tag{9}$$

This formula has been given by E. Hagenbach[5] who, however, obtains it by considering only the torque between the current and the pole at the end of the magnet. In the case under consideration, however, the torque exerted by the current on the north pole at the end of the bar, the torque on the effective poles surrounding the entering current sheet, and the torque on the current due to the field of the magnet, are respectively $2im$, $-2im$, and $2im$, to the degree of approximation considered above. Therefore the result obtained by Hagenbach is correct for this particular arrangement, although his method of deduction is misleading.

A slight variation of the cases considered heretofore is obtained by allowing the current to enter uniformly through the base of the magnet

[5] Hagenbach, Drude's Annalen **4**, 238 (1901)

and pass out along the axis. Assuming that the magnet is symmetrically magnetized and that B is constant over the base, (3) gives for the torque.

$$L_i = \frac{iB}{a^2}\int_0^a p^3 dp = \frac{iN}{4\pi}, \tag{10}$$

where a is the radius of the base and N the total flux through it. In this case the torque is half as great as when the current enters around the periphery of the base.

The fundamental formula (3) for the torque may be obtained very simply for the case of a symmetrically magnetized bar, from the expression for the induced electromotive force in the inverse phenomenon of unipolar induction. For if the magnet rotates with angular velocity Ω when the current i passes through it, conservation of energy requires that

$$Ei = Ri^2 + L\Omega, \tag{11}$$

where E is the impressed electromotive force, R the resistance of the circuit and L the frictional torque. As the back electromotive force due to the rotation is $\Omega N/2\pi$, the current is given by

$$Ri = E - \Omega N/2\pi. \tag{12}$$

Substituting in Eq. (11), Eq. (3) for the torque is obtained. Conversely the principle of conservation of energy may be invoked to obtain the induced electromotive force appearing in the phenomenon of unipolar induction from the expression (3) for the torque.

Experimental Test

Case I. Current enters magnet through a peripheral ring. The apparatus used to measure the torque acting on a magnet when an electric current entering its periphery passes along its length is shown diagrammatically in Fig. 2. A cylindrical magnet C, 10 cm long and 1.432 cm in diameter, was suspended by a phosphor-bronze strip A with its lower end immersed in a solution of copper sulphate contained in a glass vessel E. The current passed through an insulated wire S to the copper disk H, through the copper sulphate solution to the magnet, up the magnet and suspension and out at R. To limit the area of the magnet through which the current entered it from the solution, the lower portion of the magnet including the bottom was covered with a coating of paraffin wax. The part of the magnet through which the current entered was varied in the experiments by changing the height to which the magnet was coated with wax and by raising or lowering the vessel E so that the solution covered a small length of the uncoated surface. For example the dotted lines in the figure show the magnet coated to the level F, allowing the current

from H to enter the magnet through the narrow annular area extending from F to the surface of the liquid. Comparatively small currents, not exceeding 0.05 amp., were used and the electrolytic action at the surface of the exposed portion of the magnet did not present any difficulties. The annular area through which the current passed into the magnet was merely made larger than would otherwise have been necessary so as to reduce the electrolytic action per unit area. The use of a salt solution for making the electrical contact with the magnet eliminates almost completely the frictional forces which are so troublesome when mercury or metallic contacts are used The resultant torque acting on the magnet was measured in each case by the deflection (obtained with aid of the mirror B) given to the magnet against the restoring couples of the suspension A and that resulting from the action of the earth's magnetic field owing to a lack of perfect symmetry of the two poles of the magnet about its axis. The torque required to turn the system through a unit angle was determined by the usual method from the moment of inertia of the system and its period of oscillation. It was assumed that the restoring torque due to the earth's magnetic field as well as that due to the torsion in the suspension is proportional to the angular displacement; this is nearly the case for the small angles used and moreover the portion of the restoring torque arising from the magnetic action was much the smaller of the two.

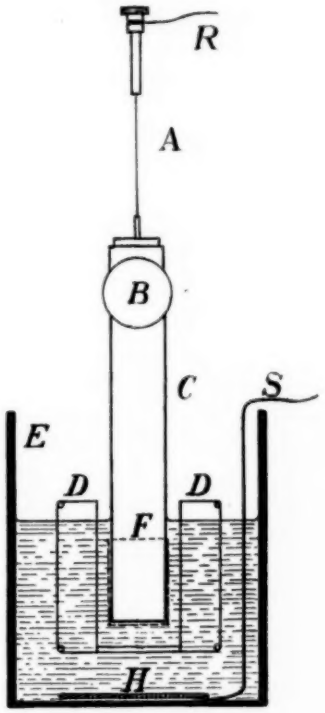

Fig. 2. Apparatus.

The use of a solution for the contact with the magnet introduces one complication. The current passing radially through the liquid toward the magnet interacts with the magnetic field of the magnet and as a result the liquid is set into rotation about an axis coincident with the axis of the magnet. This rotation produces a drag upon the magnet whose torque is opposed to that resulting from the other forces and may in reality be 15 per cent or more of the total torque acting. The rotation of the liquid was effectively stopped by introducing into the solution two pairs of

baffle plates, one pair of which, *DD*, is shown in the figure, the other pair being at right angles to those shown. The plates were made of copper; they were usually left bare and the current passed partly through them on its way to the magnet, but in some cases the plates were covered with paraffin wax without noticeable effect. The baffle plates were supported from the top of the vessel *E* by rods which are not shown.

Two different magnets of approximately the same size and having masses of 128 gm and 130 gm respectively were used. The magnets were magnetized by placing the steel bars in a symmetrical position between the poles of a large electromagnet, and it is believed that the magnetization was nearly enough symmetrical about the geometric axis to satisfy the condition considered in the theoretical part of this paper, since when suspended the magnets were only slightly acted upon by a permanent magnet brought near. The magnetic flux through different transverse sections of the magnets was measured by means of a Grassot fluxmeter in series with a flat coil of wire, the calibration of the fluxmeter having been verified by the aid of a standard solenoid inductance. The flux had to be remeasured from time to time since the magnets were newly magnetized and not very retentive so that the magnetization diminished somewhat with time. The way in which the flux through a section of the magnet varied with the location of the section along the magnet is shown by the curves in Fig. 3, where the abscissas represent the distance of the section from the bottom of the magnet and the ordinates the corresponding values of the flux. It is seen that at the center of the magnet (5 cm) the flux is nearly four times as large as at the end. The flux cutting the current sheet in the magnet could thus be easily changed by simply letting the current sheet enter the magnet at different distances from the bottom. The current did not enter along a peripheral line, but entered through a short cylindrical area which in some cases had a height of as much as 5 mm. The curves in Fig. 3 show that the flux through a section passing through the lower edge of this area at the lower portion of the magnet about 35 per cent smaller than the flux through a section at the upper edge of the area. For a distance equal to the width of the cylindrical area it is seen, however, that the flux changes approximately in a linear manner, and so in computing torques, the flux taken was that passing at a section situated half way between the top and bottom of the cylindrical ring through which the current entered. This cannot be far wrong because the average current density was doubtless very nearly the same at different elevations on the cylindrical strip. Deflections were taken in each case for both directions of the current. The observed deflections

were found to be proportional to the current and to the magnetic flux cutting the current sheet.

The experimental and theoretical results are compared in Table I for the case in which the current sheet entered the magnet through a ring-shaped surface formed by two planes normal to the axis of the magnet.

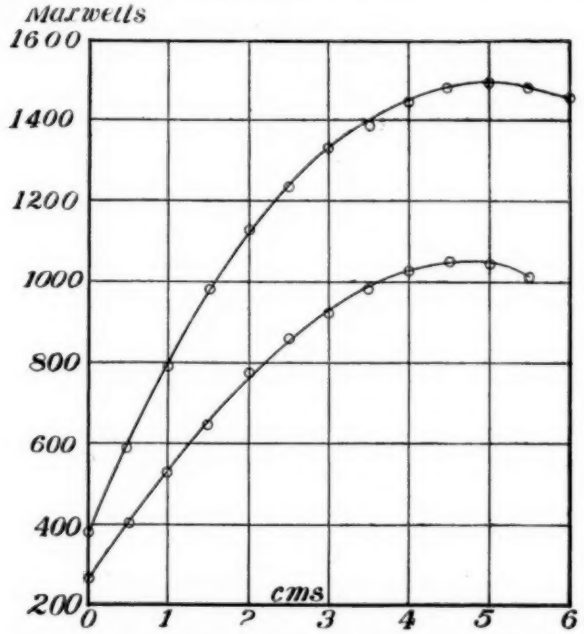

Fig. 3. Flux through a section of the magnet as a function of distance from the bottom section.

The symbols at the head of the columns in this table, and in Table II as well, have the following meaning.

I = current passing through the magnet.

w = width of the cylindrical area through which the current entered the magnet.

d = distance from the bottom of the magnet to the lower edge of the above area; i. e. the height to which the magnet was coated with non-conducting wax.

N = magnetic flux in maxwells through a section of the magnet at the center of w.

L(obs.) = the torque acting on the magnet in dyne cm as computed from the observed deflection.

L (calc.) = the torque acting on the magnet in dyne cm as calculated by the theoretical formula $IN/20\pi$, the current now being expressed in amperes.

A and B refer to the two magnets respectively.

The subscripts to B signify the use of different suspensions which changed the sensitivity of the system.

Comparing the results in the last two columns for the first nine experiments it is seen that there is a good agreement between the observed values of the torque acting on the magnet and those computed by Eq. (3),

the theoretical values being on the average about two percent higher than the observed values. This order of accuracy is perhaps all that could be expected. From other experiments to be described later it is believed that this tendency of the observed values to fall below the theoretical ones is not due to a drag produced by a remnant rotation of the solution.

TABLE I

Observations with magnet symmetrically magnetized.

Expt. No.	Magnet	I (amp.)	w (cm)	d (cm)	N (maxwells)	L(obs.) (dyne cm)	L(calc.) (dyne cm)
1	A	0.050	0.2	0	360	0.286	0.287
2	A	0.050	0.5	4.5	1045	0.797	0.832
3	B_1	0.050	0.4	0	440	0.350	0.350
4	B_1	0.050	0.2	1.8	1050	0.805	0.835
5	B_1	0.050	0.25	4.2	1450	1.18	1.16
6	B_2	0.050	0.5	0	330	0.263	0.263
7	B_3	0.050	0.3	1.8	940	0.726	0.750
8	B_2	0.050	0.5	5.1	1300	1.00	1.03
9	B_3	0.020	0.5	5.1	1300	0.403	0.413
10*	B_2	0.050	0	0	330	0.112	0.132

* In this experiment the current entered the magnet through its base.

A magnet symmetrically magnetized was suspended with the lower end in a solution and arranged so that the current entered the solution through a copper cylinder concentric with the axis of the magnet, and then passed into the magnet through a peripheral ring area, as has been described. The torque was now measured, and then the copper cylinder was moved to one side so that its axis no longer coincided with the axis of the magnet. The current now entered the magnet asymmetrically, but this change produced no appreciable effect upon the resultant torque acting on the magnet.

Case II. Current enters magnet through its base. Some experiments were made in which the current entered the magnet through its base. The wax was removed from the magnet and the solution allowed to touch its bottom surface only. In the theoretical result obtained for this case the torque is given by Eq. (10), $L=IN/40\pi$, on the supposition that the flux density is uniform over the whole base where the current enters. The actual distribution of the flux over the base in the magnet used was not determined, but one of the results obtained is given under item 10 of Table I. This experimental value is about 15 percent below that given by theory for the ideal case. Some readings taken under these same conditions with magnet A during the preliminary stages of this work showed the torque when the current entered through the base only, to be very nearly half that observed when the current entered only through a

peripheral ring at the bottom of the magnet, as theory shows should be the case if the flux density were uniform over the base.

Case III. Current enters magnet through a side arm. A side arm was attached to the magnet normal to its length and half way between the two ends. The end of the arm was bent at right angles and immersed in a cup of copper sulphate. The current entering the cup by a fixed wire passed through the side arm into the magnet and then out through the suspension in a way similar to that shown in Fig. 2. The arm was gradually shortened and measurements were made of the total torque acting on the magnet for arms of different lengths.

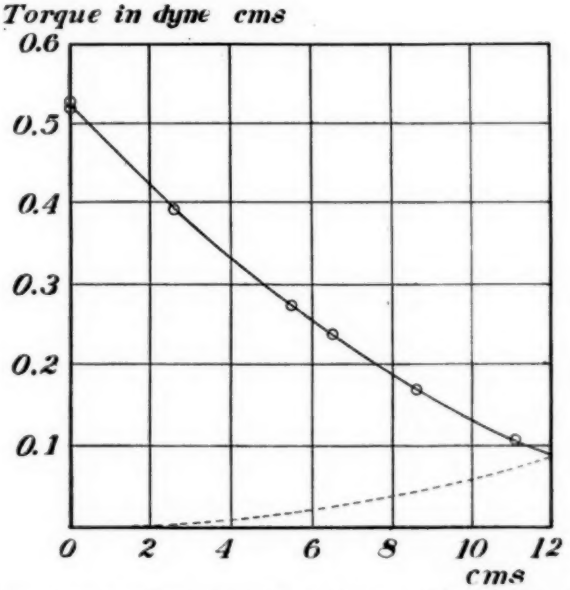

Fig. 4. Torque as a function of length of side arm through which current was introduced.

The results are given in Fig. 4 where the ordinates of the full line curve give the observed torques in dyne cm, corresponding to the lengths of the attached arm in cm as represented by the abscissas, the same current of 0.020 amperes being used throughout. The result for an arm of zero length was obtained with the current entering the magnet from a copper sulphate solution through a central cylindrical ring area, as was done in Case I. It is seen that the effect of the side arm is to diminish the torque acting and that the longer the arm the smaller the total torque. The flux outside of the magnet due to the magnet, being opposite in direction to the flux inside, produces a torque where it acts on the current

in the arm, which opposes that arising from the current sheet inside of the magnet. With an arm 11 cm long the resultant torque was only about one fifth of the value without an external arm.

With arms of this length consideration must be given to the vertical component of the earth's magnetic field (and the field due to other magnetic bodies near by), since at this distance from the magnet the earth's field is greater than the field due to the magnet. In the experiments described the north pole of the magnet was uppermost and accordingly the two above fields were in the same direction outside of the magnet, and it was their combined effect that opposed the torque arising from the flux inside the magnet. If a long side arm is to be used in an arrangement of this kind for producing rotation, there is an advantage in having the south pole of the magnet the upper one. With the south pole up, the resultant torque should reach a minimum and then increase whereas with the north pole uppermost the resultant torque should become zero and then reverse in direction as the length of the arm is further increased. Values of the torque arising from the earth's field alone have been computed for arms of different lengths and plotted as a broken line in Fig. 4. The torque due to the field of the magnet alone is found for any arm length by adding the ordinates of the two curves. The curve showing the effect of the earth's field is only approximately correct, since the work was done in a laboratory and the actual field at the place was not determined.

It is evident from these experiments alone that the torque producing rotation in a magnet, under conditions which are now under consideration, cannot be ascribed to the action of the flux from the magnet on the current in the arm.

Case IV. A brass cylinder replaces magnet. The following experiments prove that the poles of a symmetrical magnet contribute nothing to the torque acting upon it when a current flows along a portion of its length.

In the apparatus of Fig. 2 the magnet was replaced by a brass cylinder 10 cm long and 1.266 cm in diameter. A magnetic flux along the length of the cylinder was produced by means of a current in a vertical solenoid, 45 cm long and 5 cm inner diameter, in the center of which the cylinder was suspended. To permit deflections to be read, the cylinder had a wire rigidly fastened to it at the center of one end, and this extended beyond the upper end of the solenoid and there carried a mirror. The suspension was also fastened to this wire. The lower end of the cylinder was immersed in a copper sulphate solution and baffle plates were used as before. The magnetic flux passing through the cylinder was computed from the

strength of the current in the solenoid. The flux was naturally very nearly constant over all sections of the cylinder and it was not necessary to restrict as much as previously the area through which the current entered the sides of the cylinder. The flux in this case was in the same direction outside of the cylinder as inside, and accordingly the torque acting on the liquid was in the same direction as that acting on the magnet, and the drag of the rotating liquid on the magnet when no baffle plates were used tended to increase the deflections, whereas this effect was in the opposite direction when a magnet was used. The bottom of the cylinder was kept coated with paraffin wax to prevent entry of any current through this surface. As in the case of the magnet the theoretical values of the torque were computed by formula (3), $L=IN/20\pi$. The results obtained are given in Table II, in which the letters have the same meaning as in Table I.

TABLE II

Results with brass cylinder

Expt. No.	I (amp.)	w (cm)	d (cm)	N (maxwells)	L(obs.) (dyne cm)	L(calc.) (dyne cm)
1	0.050	2.0	0	64	0.050	0.051
2	0.100	2.0	0	32	0.049	0.051
3	0.200	2.0	0	32	0.099	0.102
4	0.300	2 0	0	32	0.149	0.153
5	0.100	1.0	2.5	30.4	0.048	0.048

It is seen that the observed torques are proportional to the product IN, and that there is very good agreement between the observed and the calculated torques given in the last two columns. As there are no magnetic poles present in this case, and the observed torques agree with those computed by the same formula that was found to represent the experimental results when a magnet was used, it follows that the magnetic poles in the latter case contributed nothing to the torque. It will be noticed that the calculated torques are slightly larger on the average than the observed ones, as was the case with the suspended magnets. Since the effect of any remnant rotation of the liquid should tend to increase the deflection in one case and to decrease it in the other, it is thought that the small difference noted cannot arise from this effect. Perhaps it is due to the superficial viscosity of the solution being able to overcome a small torque.

Case V. Current entering and leaving the magnet along its axis. A cylindrical magnet 10.2 cm in length and 1.5 cm in diameter was suspended in a vertical position as before by a phosphor-bronze strip

attached at the center of the north pole end of the magnet. A small peg attached to the center of the lower end was immersed in a small cup of mercury or of copper sulphate. The magnet had a hole 8.4 mm in diameter bored through its center at right angles to its length. From the upper wall of this hole a small metallic point projected down for a short distance along the axis of the magnet. A small brass rod with a cavity on one side which was filled with a drop of mercury or copper sulphate was placed into the hole in the magnet so as not to touch the sides but with the metallic central point dipping in the drop of liquid. The suspended magnet was thus free to move about a vertical axis and the arrangement permitted a current to be sent axially either from one end of the magnet to the other or from the center to either end.

When a current of 0.1 amp. was sent from one end to the other no perceptible deflection of the magnet was observed, and none is indicated by theory. However, when a current of 0 02 amp. was sent from the central axial contact to either end of the magnet, an average torque of 0.73 dyne cm was observed. The direction of this torque was clockwise, as viewed from above. This is the same direction as that of the torque which acts when a current enters axially at the north pole of a symmetrically magnetized magnet and emerges along the periphery of the magnet at the center of its length.

The total flux through the central portion of the present magnet was 1650 maxwells, and hence, had the magnet been symmetrically magnetized, the torque as computed by Eq. (3) for the conditions cited above would have been only 0.52 dyne cm.

It should be noted too that the effect of the current in the rod by which the current is led into the center of the magnet should be to produce a torque on the magnet opposite to that observed. However, the transverse hole through the center of the magnet produces at that portion of the magnet a very unsymmetrical magnetization and without detailed knowledge of the nature of this magnetization it is not possible to compute the magnitude of the torque and even its direction is not readily predicted. The experiment, while not readily explained, is an interesting example of the effect of an unsymmetrical distribution of magnetization.

Two more experiments with this magnet will be described. When the bottom of the magnet was covered with paraffin wax and the magnet immersed in a copper sulphate solution to a height of 7 mm, the torque observed with a current of 0.02 amp. flowing from the suspension at the top of the magnet to the peripheral ring at the bottom was 0.165 dyne cm whereas the torque computed by Eq. (3) ($N=545$) is 0.158 dyne cm,

showing that the unsymmetrical magnetization at the center of the magnet did not greatly influence the resultant torque.

When the lower end of the magnet was covered with paraffin wax to a height of 2.5 cm and immersed in copper sulphate to a total depth of 3 cm and when a current of 0.02 amp. flowed from the solution up to the center, the torque observed was clockwise, as viewed from above, and of magnitude 0.26 dyne cm, whereas a torque in the same direction and of magnitude 0.73 dyne cm was found when the current entered through the suspension at the top of the magnet and emerged at the contact at the center of the magnet. The flux N through a central section of the peripheral area in contact with the solution was 1210 maxwells, so that when the current entered from below, the computed anti-clockwise torque due to the entering current sheet alone was 0.38 dyne cm. The effect at the center was therefore opposed to this since the resultant was a clockwise torque of 0.26 dyne cm.

We wish to acknowledge our indebtedness to our assistant, Mr. H. O. Stearns, for aid with the experimental part of the paper.

SLOANE LABORATORY,
YALE UNIVERSITY.
July 14, 1924

DIELECTRIC ANOMALIES IN ROCHELLE SALT CRYSTALS

By Joseph Valasek

Abstract

Residual charge and fatigue effects for Rochelle salt condenser.—The throw of a ballistic galvanometer connected to a condenser with Rochelle salt crystal as dielectric depends on the time of charging and the time of discharging. It increases to a maximum as the charging time is increased to 2 sec. (for crystal plates .15 cm. thick) and then decreases slowly, reaching for a time of 24 hours a value about half the original. The decrease of the throw for .03 sec. charging, due to fatiguing for 24 hours at 100 volts, was found to be nearly independent of the temperature from −15°C to +20°C. The first increase is probably due to residual charges which are easily displaced to a more or less definite limit and which account for the high dielectric constant in this temperature range. The subsequent decrease is due to a fatigue effect which may be likened to an electrolytic polarization of the internal displacement current. These effects are associated with the water of crystallization, since dessication decreases them while previous soaking in alcohol accelerates them. To explain the limited temperature range of the effects it is supposed that at −20°C there is a loosening of the water ions enough to permit a slight motion of about 10^{-9} cm with reference to the Rochelle salt molecules, while at temperatures above +25°C further loosening allows electrolytic conduction to increase greatly.

Thermal changes in Rochelle salt.—There is apparently an evolution of heat starting at 24°C and persisting to 54°C where a very strong absorption of heat takes place.

ROCHELLE salt crystals have some unusual dielectric properties between −20°C and +25°C, that is, in the range of greatest piezoelectric activity. Many of these have already been described.[1] For example, at 0°C the specific inductive capacity for the ă crystallographic direction apparently reaches the extremely high value of 800 as determined by measurements of the ordinary charge by a ballistic galvanometer. If the discharging time is limited to 0.03 sec. by means of a Helmholtz pendulum, this value is reduced to 700. If, again, measurements are made with an oscillating circuit at two million cycles the dielectric constant is, according to Frayne,[2] about 80. The high values at low frequency are not due to ordinary conduction because this is much too small below 30°C to give over 0.1 percent of the total charge. In this connection it is also significant that the specific inductive capacity *decreases* between 25°C and 30°C, while the conductivity as measured by an electrometer shows a ten-fold *increase*. The explanation is rather

[1] Valasek, Phys. Rev. **17**, 475 (1921) and **19**, 478 (1922)
[2] Frayne, Phys. Rev. **21**, 348 (1923)

that the residual charge and the internal conduction effects are very large, contributing up to 90 percent of the total dielectric constant at low frequencies.

There are several theories to explain residual charges. Maxwell[3] has suggested a non-uniform, layered dielectric. Von Schweidler[4] has suggested two theories, one of them based on motion of ions as in a very dense gas, and the other on the assumption of over-damped bound charges. A very successful approach to the subject of residual charge, leading to satisfactory equations but to no definite picture of the mechanism, is through analogy with residual elasticity.[5]

All these theories lead to the conception of a residual charge current which flows for some time whenever there is a change in the potential difference between the plates of the condenser. The integral of this current over the time of charge or discharge gives the quantity to be added to the corresponding "free" charge. A very important conclusion about the manner of variation of the residual charge current, which has been the object of much experimentation, is the so-called "super-position principle" of Hopkinson.[6] It states that any variation in the electric field produces a variation in the anomalous current which is independent of the field or the dielectric displacement already existing. This principle will now be applied to the special case where the variation in the field is equal to the field itself, namely in simple discharging of the condenser.

Let $f(t)$ represent the residual charge current while the condenser is being charged. This is some monotonically decreasing function probably the sum of two or three exponentials.[7] Let the time of charging be t_1 and let the instant of discharging be the time origin. The residual current on charging, if continued, would be $f(t_1+t)$. The change in voltage being equal and opposite to the charging voltage, there will be superposed on this current, one equal to $-f(t)$. The residual charge current on discharge will therefore be equal to $-f(t)+f(t_1+t)$. Now if δ is the time that this current flows through the galvanometer, the discharge will be greater by the integral of this current from zero to δ. That is, if R is the contribution of the residual charge current to the discharge, then (calling the current positive) it follows that

$$R=\int_0^{\delta}[f(t)-f(t_1+t)]dt=F(t_1,\delta) \qquad (1)$$

[3] Maxwell, Electricity and Magnetism, I, §§ 328-330.
[4] Von Schweidler, Ann. der Phys. **24**, 711 (1907)
[5] Wagner, Ann. der Phys. (4), **40**, 817 (1913)
[6] Hopkinson, Phil. Trans. **167**, 599 (1877)
[7] Jaquerod and Mugeli, Arch. des Sci. **4**, 10 (1922)

Now since $f(t)$ is monotonically decreasing, it follows that R must increase for increases in either δ or t_1. The first conclusion is easily verified experimentally with Rochelle salt, for the residual charge effect is very large and accounts for the difference between the ordinary specific inductive capacity and that obtained with short charging times or high frequencies.

The conclusion that R increases with t_1 is, however, not found to hold for charging times greater than several seconds. When the time of charging is increased beyond this, the discharge is found to become much smaller. This may be supposed due to a fatigue of the dielectric. While the crystal is being fatigued by the application of a field of a certain sign, one finds on reversing the field for a moment that the total discharge as well as the part due to residual charge increases for this opposite direction of charging. This effect has been observed only between $-20°C$ and $+25°C$ where the crystal is piezo-electrically active.

The object of this article is to describe experiments on these dielectric anomalies and to show their relationship to each other and to the piezo-electric effect.

Experimental Procedure

The crystal plates were all cut from a large perfect crystal which was kindly furnished by W. R. Whitney of the General Electric Company. The faces were in most cases perpendicular to the å crystallographic axis since in this direction the effects it was proposed to study are the greatest. The plates were usually about 0.15 cm thick, the electrode area being about 2 cm^2. After considerable experimentation it was found that amalgamated tinfoil electrodes squeegeed on polished surfaces of the crystal gave the most constant results. The crystal plates used were not dessicated or otherwise treated unless specifically stated, the electrodes being usually attached to the clear crystal immediately after polishing on a ground glass. While the observations were being made the crystal was kept in an air-tight tube containing KOH. This proved to be the most satisfactory arrangement for eliminating electrical leakage due to moisture without causing dehydration of the crystal.

The tube containing the crystal was immersed in a Dewar flask in order that the observations could be taken at various constant temperatures. The charging and discharging throws of the crystal condenser were measured by means of a Leeds and Northrup high sensitivity ballistic galvanometer. The times of charging and discharging were controlled by means of a set of switches operated by a Helmholtz pendulum. The apparatus was calibrated by means of a standardized Gerdien air con-

denser which could be substituted by opening the tube without changing any of the external connections.

Dielectric Fatigue

Below −20°C and above +25°C Rochelle salt has quite normal electrical properties, the hysteresis[8] vanishing and the other anomalies not being unusual. Between −20°C and +25°C the dielectric properties show peculiarities and the crystal is piezo-electrically active. In this temperature interval the dielectric constant is very large, as though a new type of polarization were created at −20°C, causing the increase in the dielectric constant and being responsible for practically the entire piezo-electric effect.

The polarization produced by these loosely bound charges appears to be rather sluggish in response to any field or force which may be applied to the crystal. This is the residual charge effect, the discharges of the condenser becoming larger when longer times of discharging are used. When, however, the time of *charging* is made longer, the discharges for a constant time of discharging become smaller for charging times greater than about one second in case of a plate which has been in alcohol for two days. This is the fatigue effect. Untreated crystals also show fatigue but it does not appear as soon. Observations of these effects are given n Table I.

Table I

Observations showing residual charge and fatigue effects
Discharging time 0.03 sec.; temp. 20°C; field 900 v/cm.

Charging time	Discharge (untreated)	Discharge (alc. 2 days)
0.03 sec	2.15	3.12
0.15	2.34	3.51
0.50	2.46	3.55
2.0	2.49	3.43
6.0	2.48	3.29
30	2.50	3.04
180	2.47	2.70
1200	2.33	2.25
3600	———	2.00
5800	1.94	———

For short times of charging the discharges are seen to increase as they should according to the superposition principle. The smaller discharges for the longer times of charging are attributed to a dielectric fatigue which is related to the internal conduction.

When fields of 900 or 1000 v/cm are applied for several hours, the discharges of the condenser are reduced by an amount which depends on the fatigue already existing. In order to know the exact state of the

[8] Valasek, Phys. Rev. **19**, 479 (1922)

fatigue, it is best to apply a potential (e.g. 100 volts) for at least 24 hours before making any observations. The fatigue is then definite and the results are reproducible.

A fatigue of this kind is found to diminish the discharge $\Delta\sigma$ for the same direction of charging and to increase it for discharges from the opposite direction. If now the opposite field $-E$ is applied for an increasing time t, there is recovery of the low values and a decrease of the high values in an approximately exponential manner. These results are illustrated by Fig. 1.

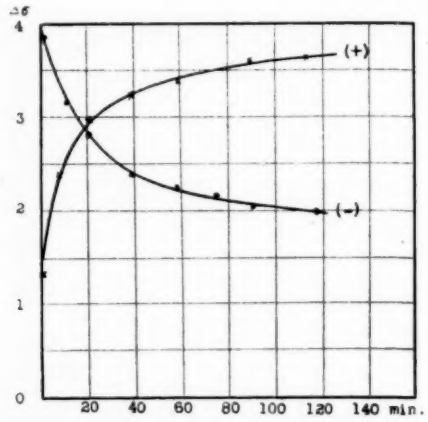

Fig. 1. Fatigue and recovery of Rochelle salt condenser after charging for 24 hr with +100 volts, then applying −100 volts.

It is interesting to note that if one compares the fatigued values of the discharges for various short increasing discharging times it is found that the positive and negative values are nearly proportionately increased. This is illustrated by Table II, where the negative discharge is over twice the positive due to fatigue, yet the ratios of the discharges for 0.03 and for 1 sec are nearly the same. This shows that the residual charge effect is the same in both cases.

TABLE II

Charging time 10 hours

Discharging time	+Discharge	−Discharge	Ratio
0.03 sec	1.63	3.54	2.17
0.08	1.67	3.60	2.16
0.17	1.71	3.72	2.18
0.48	1.76	3.90	2.22
1.0	1.88	4.12	2.19

The hysteresis loop of the charge σ and the field E is a fatigue effect of the kind described above. The observations are taken by a method

analogous to one described by Ewing[9] for obtaining magnetic hysteresis loops. Each observation of $\Delta\sigma$ is taken after a number of reversals in the field, by making the final change of ΔE from either the $+E$ or the $-E$ reached on the last reversal, with the crystal connected across the galvanometer. The value of ΔE is increased until it amounts to an entire reversal. The short time that the maximum field is applied just before the measurements are made fatigues the crystal and it does not return to the normal state on discharge but recovers gradually at a rate depending on the field and the time of application. The hysteresis loop can thus be made larger by taking the observations after a longer pause at the maximum fields. These effects are greatest when the crystal is treated with alcohol.

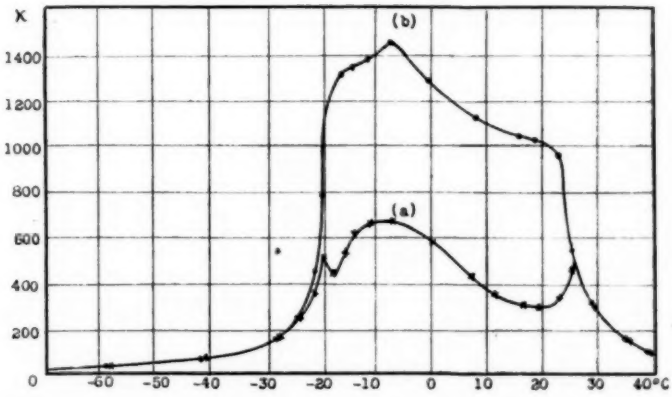

Fig. 2. Temperature variation of fatigue after charging for 24 hr with + 100 volts. Average dielectric constants for discharges (a) from + 100 and (b) from − 100 volts, for a discharging time of .03 sec.

Fatigue is observed only at temperatures between −20°C and +25°C and it is clearly related to the fatigue one observes in the piezo-electric response. The variation with temperature is illustrated in Fig. 2. The observations were taken after the crystal had been fatigued for 24 hours at +100 volts. The average rate of heating was about ten degrees per hour. The ordinates for curves (a) and (b) represent the average dielectric constants for discharges from +100 and −100 volts respectively and for a discharging time of 0.03 sec. Between −15°C and +20°C the two curves are approximately parallel, showing that the change in the dielectric constant due to fatigue is independent of temperature in this range. Besides the differences in the heights of the two curves, one notices the

[9] Ewing, Magnetic Induction, 358.

peaks at $-20°C$ and at $+25°C$ on one of them.[10] These are only observed when the time of charging is short, fatigue tending to make them more pronounced. They show the appearance of the type of variation of specific inductive capacity that Frayne[11] observed at high frequencies. At optical frequencies there are no peculiar variations in the indices of refraction of the crystal at these temperatures.[12]

Internal Conduction

The nature of the relation between the polarization and the field, as well as the very high dielectric constant of Rochelle salt, indicates the presence of charges which are in a sense intermediate between the ordinary bound and free charges. They are easily displaced to a more or less well defined limit beyond which the displacement becomes difficult. The internal currents produced by them are restricted to small regions inside the crystal. A distinction between this internal conduction and the actual conduction is shown most strikingly above $+25°C$ where the actual conduction increases exponentially with the temperature, while the abnormally high dielectric constant due to internal conduction decreases. The fatigue effect may be likened to an electrolytic polarization of the internal current which is probably confined to the Rochelle salt molecule and is perhaps due to the water of crystallization.

Among the reasons for attributing the internal conduction to the water of crystallization is the fact that when the crystal is dehydrated by means of phosphorus pentoxide, the high dielectric constant is greatly reduced, and with complete dessication there are no longer any transitions at $-20°C$ and $+25°C$. The conductivity increases with temperature but not as rapidly as before.

After the crystal has been immersed in alcohol, different effects are observed. The piezo-electric activity is fully six times as great as before. The specific inductive capacity is also increased but not in as great a proportion. Even by the use of tinfoil electrodes attached by means of shellac dissolved in alcohol, the capacity deflections may be doubled or tripled. These deflections decrease after the shellac dries but there is some permanent improvement. The effect of alcohol can be best studied by using amalgamated tinfoil electrodes since they can be readily stripped off and attached again in exactly the same way after the crystal has been

[10] These maxima are very different in origin from the second maximum noted by the writer (Phys. Rev. **19**, 485, 1922) which was merely due to the improvement of an imperfect contact when the conductivity of the crystal increased.

[11] Frayne, Phys. Rev. **21**, 355 (1923)

[12] Valasek, Phys. Rev. **20**, 644 (1922)

kept in alcohol for a time. After two days immersion the capacity deflections are about doubled for the ordinary charges (1 sec. discharging time for example), the discharges not being changed as much for shorter times. This is for the unfatigued crystal. Fatigue causes a change in the relative increases of the discharges for the two directions and discharging times. The results are shown in Table III which also shows the relative persistence of the effects.

TABLE III

	+Discharge		−Discharge	
	.03 sec.	1 sec.	.03 sec.	1 sec.
Untreated	1.63	1.88	3.54	4.15
Alcohol 2 days	1.83	4.60	7.08	12.10
2 days later	2.11	4.07	7.70	11.10
24 days later	2.22	3.69	5.85	8.08

The observations in the table are all taken after an application of +90 volts for 24 hours. Accordingly the values in the columns headed + are smaller and those headed − are larger than normal, due to fatigue. Two discharging times are used, namely 0.03 and 1 second in order to indicate the magnitude of the residual charge effect. A comparison of these will show that the residual charges are greatly increased by the alcohol; in fact, the increase in specific inductive capacity seems to be wholly due to increased residual charges. The relative amount of fatigue is also increased, showing that alcohol affects whatever is responsible for the anomalous dielectric action of Rochelle salt, this being most probably the water of crystallization.

In order to test for the presence of electrolytic polarization layers or space charges, a platinum wire probe was sealed into the crystal, one third the distance from one of the plates, and connected to a string electrometer. Unless the temperature was very steady for at least an hour a potential difference of several volts was indicated even though the plates were earthed. This was due to the so-called "false" pyro-electric effect resulting from the thermo-elastic stresses set up by temperature gradients in the crystal. The resulting internal potentials produced fatigue effects. Perhaps the variations that have been observed in the dielectric anomalies of quartz and other crystals may be due to such effects.

The probe measurements showed that there are no unsymmetrical polarization layers in Rochelle salt. There is, however, a symmetrical variation from a linear potential drop through the crystal. It is not known whether there are equal potential jumps at both plates or a continuous variation in potential as in quartz.[13]

[13] Joffe, Ann. der Phys. **72**, 4 (1924)

It would be of interest to inquire whether it is possible to account for the high dielectric constant of Rochelle salt on the basis of the water of crystallization without requiring greater displacements of the ions than the distances between molecules. To do this one must know the maximum polarization. The polarization gradually approaches saturation which is, however, never reached because the crystal breaks when the field exceeds about 25,000 volts per centimeter. The maximum polarization obtainable is less than 15,000 e.s.u./cm^3. There are four molecules of water for every molecule of Rochelle salt. In a crystal lattice, each molecule of water may be regarded as equivalent to three ions, two H^+ and one O^{--}. Suppose that the restoring force per unit displacement per unit charge is the same, then $P_{max}=16\ Ne\xi_{max}$, where P is the polarization, e is the electronic charge, and ξ is the displacement. From the density and molecular weight of Rochelle salt and the mass of the hydrogen atom, it is found that there are $N=3.76\times10^{21}$ molecules per cubic centimeter. From this value of N one finds that the average distance between molecules is 3×10^{-7} cm, whereas the formula above gives $\xi_{max}=5\times10^{-10}$ cm. There is accordingly no contradiction with the assumption that the water of crystallization furnishes the ions for the internal conduction and that these ions do not move out of the molecule.

With reference to the possible interpretations of the critical temperatures of $-20°$ and $+25°$C it has been said that the former is the temperature at which the ions of the water of crystallization are loosened sufficiently to give rise to internal conduction. The temperature may be called in one sense a melting point of the water of crystallization. However, it was not possible to detect any absorption of heat at this point with a sensitive differential thermocouple. Above $+25°$C the internal conduction ions are gradually freed so that they may migrate through the crystal; the conduction increases approximately in an exponential manner until at $+54°$C the crystal goes through a transition point and is converted into a moist granular mixture of the single tartrates of sodium and potassium with water. A differential thermocouple indicates an apparent evolution of heat starting at $+24°$C and persisting to $+54°$C where a very strong absorption of heat takes place.

UNIVERSITY OF MINNESOTA,
DEPARTMENT OF PHYSICS.
April 22, 1924

THE RELATION BETWEEN THE MECHANICAL AND PIEZO-ELECTRICAL PROPERTIES OF A ROCHELLE SALT CRYSTAL

By Frank C. Isely

Abstract

Stress-strain curves for a Rochelle salt crystal for 16 to 36°C.—A crystal cut so as to give maximum piezo-electric response under compression, was mounted so that a known force was applied to the center of a brass block resting on the top, and the corresponding strain was measured to within 10^{-6}mm by means of an optical extensometer described by S. R. Williams. *Variation with piezo-electric charge.* When the load is applied, the initial strain is less than the final strain by an amount proportional to the initial piezo-electric charge, the difference varying with the temperature and reaching a maximum for 22.25°, the temperature of maximum piezo-electric response. For a stress of 2225 gm/cm², the strain with the charge is less than the "no charge" strain by an amount 0.7×10^{3} per coulomb per cm²; for this stress the initial and final strains were 9.5 and 13.4×10^{-5}, the corresponding moduli being 2.32 and 1.62, both times 10^{10} dynes. The final strain is independent of temperature; it is not proportional to stress, being 7.5×10^{-5} for 1 kg/cm² and 12.5×10^{-5} for 2 kg/cm².

Introduction

DURING the last few years much work has been done in studying the piezo-electric properties of the Rochelle salt crystal. This work has been especially directed toward determination of the quantity of charge, the hysteresis effect with an applied electromotive force,[1] and the optical properties[2] at various temperatures. There also has been some work in determining the usefulness of the crystal for signal[3] and seismographic[4] use, and in the control of the steadiness of oscillating circuits.[5] But in all this work nothing has been published on the correlation of the mechanical change in length with the charge produced by a given stress.

Apparatus

The block of crystal used was cut as shown in Fig. 1 in order that the maximum piezo-electric effect would be secured. The usual method of cutting with a wet string was used after which the block was smoothed and polished with emery and water and then with ground glass and

[1] Valasek, J., Phys. Rev. **17**, 475 (1921); **19**, 478 (1921); **20**, 639 (1922)
[2] Valasek, J., Phys. Rev. **20**, 639 (1922)
[3] Anderson, Reports to the National Research Council, March and April 1918.
[4] Wood, Bull. Seismological Soc. Am. **11**, March 1921.
[5] Cady, W. G., Report to the National Research Council, May 1918.

water. After getting the block in shape it was coated with asphaltum cement, made of powdered asphaltum gum and benzine. This cement altered in no way the crystalographic structure of the crystal and reduced

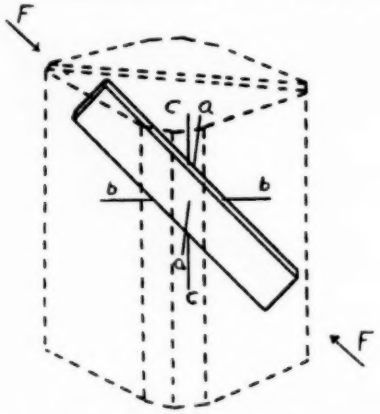

Fig. 1. Showing direction of cutting the crystal.

to a minimum the change in vapor tension.[6] A piece of tinfoil was also cemented to each side of the crystal, from which wires were led to the galvanometer.

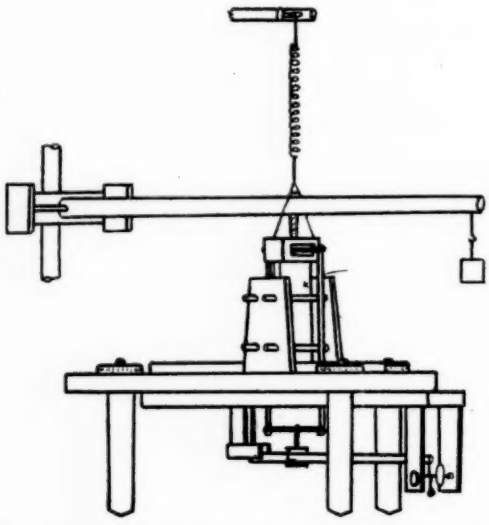

Fig. 2. Apparatus for obtaining strain-stress curves for Rochelle salt.

The crystal was cemented to a brass block, which in turn was bolted to a rubber base, Fig. 2. A small brass block, with a conical hole in the center in which rested a needle point fastened to the upper part of the

[6] Valasek, J., Phys. Rev. **17**, 476 (1921)

saddle, was placed on the crystal. From the center of the lower part of the saddle a small wire passed down to the stirrup of an optical extensometer, which was made according to a description by S. R. Williams.[7] It consists essentially of a six to one lever arm and a fine wire passing from the longer arm down to and around a steel pivot to a weight. The pivot, at the point of contact with the wire, was about a millimeter in diameter, and had jewel bearings. In calibrating the instrument it was found possible to measure a change in length as small as a tenth of the

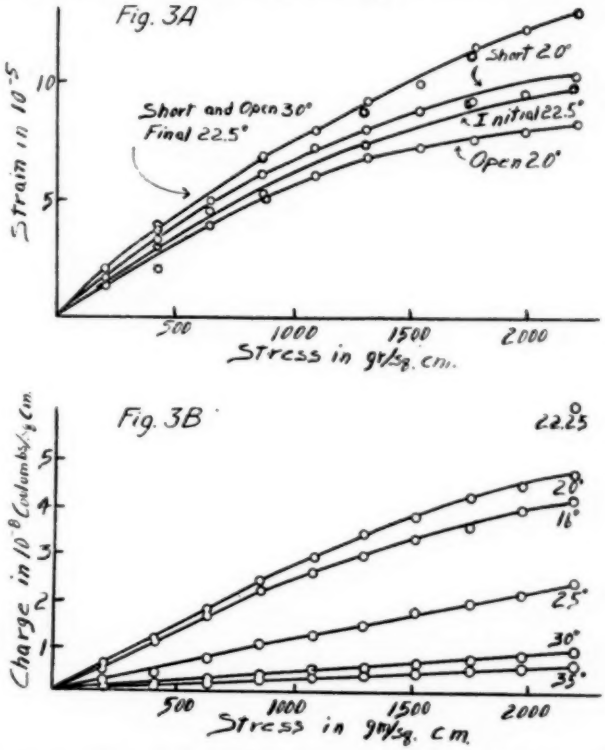

Fig. 3A. Strain-stress curves for temperatures 20°, 22.5° and 30°.
Fig. 3B. Charge-stress curves for temperatures 16° to 35°.

wave-length of sodium light with an error of less than 1 per cent. The stress was applied by gently putting weights on the lever arm. A spring was used to compensate for the initial stress due to the lever arm and extensometer.

The charge was measured by a Leeds and Northrup galvanometer which had a sensitivity of 2241 megohms, a critical damping resistance of 8100 ohms, and a period of 5.85 sec.

[7] S. R. Williams, Jour. Opt. Soc. Am. **7**, Nov. 1923.

Temperature control was secured by surrounding the crystal with a double walled cylindrical tin tank of water, in which a coil of copper tubing, carrying tap water, was submerged, and also by placing a nitrogen light bulb over the glass cover to the tank, care being taken that the light rays did not fall directly on the crystal. Thus any temperature from 16° to 35° could be maintained.

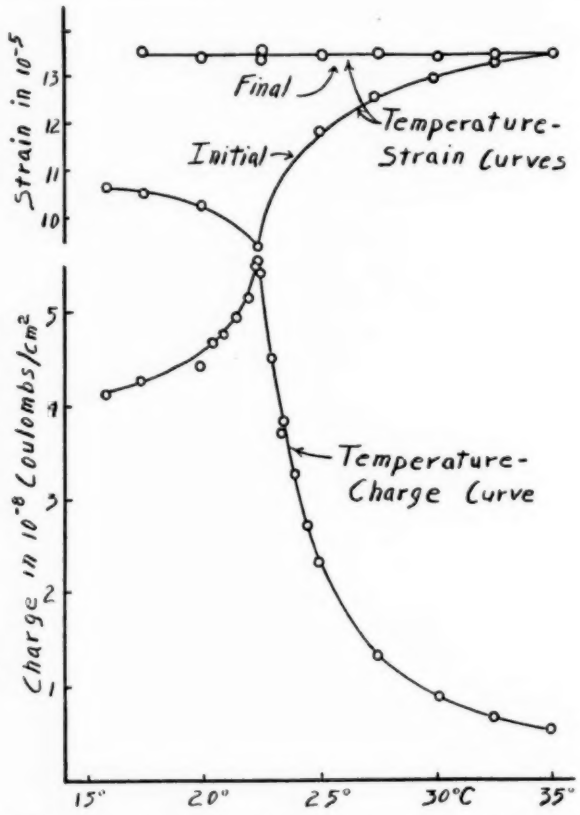

Fig. 4. Strain and charge as functions of temperature, for a constant stress of 2225 gm/cm².

Experimental Procedure and Results

In the initial run it was found that great care had to be exercised in applying the stress so as not to alter the position of the brass block, for a very slight change in its position altered the direction of the applied force. A movement to either side of the exact center caused the change in length to be larger because of a bending of the crystal. This central position, found by getting that position for which the extensometer gave minimum

reading, was assumed as the point where the applied force was in direction F, Fig. 1. It was also found that there was a creep of the extensometer reading at most temperatures, this creep lasting about fifteen seconds on short circuit of tinfoil plates and twice that time on open circuit. Unless otherwise stated strain is taken as the initial value, i.e. the value taken for short circuit of the plates.

With the block in this central position, three series of runs were taken. The first series determined stress-strain and stress-charge relations at various temperatures from 16° to 35°, the stresses at each temperature being increased from zero to 2225 gm/cm² in steps of 222.5 gm/cm². A second series determined the initial and final strain under various stresses at a temperature near that for which the crystal gave the maximum piezo-electric response. The third included a temperature-strain and a temperature-charge run, both with a constant stress of 2225 gm/cm². The results are shown in Figs. 3 to 5.

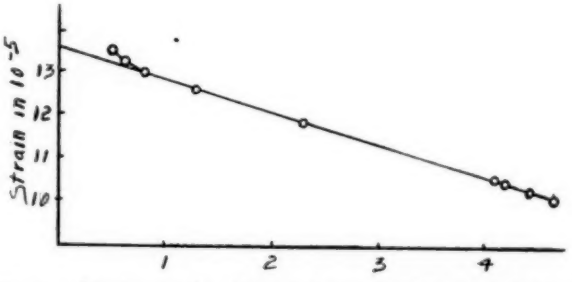

Fig. 5. Strain as a function of charge in 10^{-8} coulombs/cm².

Fig. 3A shows the variation of initial and final values of the strain as a function of stress for various temperatures. "Open" means the initial values on open circuit, and "short" means the initial values on short circuit. There is a difference in these values due to the charge neutralizing itself on short circuit. The final values for a temperature of 22.5° are the same as the final values for 30°.

Fig. 3B shows the variation of charge with stress, for various temperatures. The variations of initial and final values of the strain with the temperature are shown in Fig. 4 and also the variation of charge with temperature, all for a stress of 2225 gm/cm². The final strain is seen to be independent of the temperature. For the temperature of maximum piezo-electric response 22.25°, the initial strain is a minimum. It is evident that the difference between initial and final strain varies with the charge and it is shown in Fig. 5 that the difference is directly proportional to the charge, being equal to 0.7×10^3 per coulomb per cm². For a stress

of 2225 gm/cm^2 at a temperature of 22.25° the initial and final strains are 9.5 and 13.4×10^{-5}, the corresponding moduli being 2.32 and 1.62 respectively, both times 10^{10} dynes.

In closing the author wishes to express his thanks to the General Electric Co. for the crystal used and especially his obligation to Dr. F. E. Kester under whose supervision the work was done.

BLAKE PHYSICAL LABORATORY,
UNIVERSITY OF KANSAS.
May 20, 1924

A MATHEMATICAL TREATMENT OF THE ELECTRIC CONDUCTIVITY AND CAPACITY OF DISPERSE SYSTEMS

I. The Electric Conductivity of a Suspension of Homogeneous Spheroids

By Hugo Fricke

Abstract

Conductivity measurements may give values for (1) the specific conductivity, (2) the concentration or (3) eccentricity of form of the suspended particles of suspensions such as biological tissues, blood and cream. *Mathematical theory.* The following relation is derived: $(k/k_1-1)/(k/k_1+x)=\rho(k_2/k_1-1)/(k_2/k_1+x)$, where k, k_1 and k_2 are the specific conductivities of the suspension, the suspending medium and the suspended spheroids, ρ is the volume concentration of the suspended spheroids, and x is a function of the ratio k_2/k_1 and the ratio a/b of the axis of symmetry of the spheroids to the other axis. For the case of spheres, $x=2$ and the formula reduces to that of Lorentz-Lorentz and Clausius-Mossotti. Curves are given showing the variation of x with k_2/k_1 for various values of a/b. Comparison with experimental data of Stewart for the conductivity of the blood of a dog ($k_2=0$, $a/b=1/4.25$, $x=1.05$) shows excellent agreement for concentration from 10 to 90 per cent. Also the observations of Oker-Blom for two suspensions of sand in salted gelatine, give in each case constant values of x for various concentrations.

A. Introduction

THE present theory has been developed as a basis for experiments concerning the electric conductivity and capacity* of colloids and biological cell suspensions, like blood for instance, which for sometime have been carried out in this laboratory. In this paper we shall consider the electric conductivity of a suspension of homogeneous non-polarizable spheroids; in a second paper, the electric capacity of a suspension of polarizable homogeneous spheroids for a current of low frequency; and in a third, the conductivity and capacity for any frequency, of a suspension of spheroids each consisting of a homogeneous interior surrounded by a thin membrane the conductivity of which is different from the conductivity of the interior. The last calculation includes the case of a suspension of homogeneous polarizable spheroids. A series of measurements illustrating the practical and theoretical applicability of

*A suspension is electrically equivalent to a certain resistance in parallel with a certain capacity. We refer to this resistance and to this capacity when we speak of the conductivity and capacity of a suspension.

the theory will be given in separate papers. Preliminary reports of some of the measurements have already been presented at meetings of the American Physical Society.

An investigation of the conductivity of a suspension may serve as a means of determining the conductivity of the single particles of the suspension. Important knowledge of the state of the suspended particles may thus be obtained, as in the case of protected metallic colloids, and especially in the case of suspensions of biological cells the life of which seems to be associated with the existence of a characteristic semi-permeability of the exterior cell wall and of the different interphases of the cell interior. In connection with the latter case we may refer to the researches of Brooks,[1] of Crile, Hosmer and Rowland,[2] of Osterhout[3] and of many other investigators on the changes of the electric conductivity of bacterial suspensions and of different plant and animal tissues under varying conditions.

The determination of the conductivity of a suspension may also furnish a method for obtaining the volume concentration of the suspension when the specific conductivity of the disperse phase and of the suspending medium is known. This method is used practically in the determination of the volume concentration of the red corpuscles of blood. It seems probable that it may have many other practical applications, as for instance, the determination of the butter-fat of cream.

Finally, the measurement of the conductivity of a suspension may lead to a determination of the structural factors of the suspended phase. This is possible because as we shall see later, for a constant volume concentration the conductivity of a suspension is to a certain extent dependent on the form (but not on the size) of the suspended particles. This is especially marked when the suspended particles are non-conductors, the condition which is of the most practical interest. This method may, for instance, find practical application in soil analysis.

B. Theory of Electric Conductivity of Suspension of Spheroids

The determination of the electric conductivity of a suspension belongs to a very important group of physical problems all of which depend on the solution of Poisson's equation for a two-phase system, including Poisson's

[1] J. Brooks, J. Gen. Physiol. **5**, 365 (1923); Proc. Soc. Exp. Biol. and Med., **19**, 284 (1922)

[2] G. W. Crile, H. R. Hosmer, and A. F. Rowland, Amer. J. Physiol., **60**, 59 (1922)

[3] W. J. V. Osterhout, Injury, Recovery and Death in Relation to Conductivity and Permeability, Phila., 1922; (see Bibliography).

theory of induced magnetism, the Clausius-Mossotti theory for the dielectric constant, the Lorenz-Lorentz theory for the index of refraction, etc. Applied to the case of electric conductivity, the formula to which these theories lead, reads

$$\frac{(k/k_1)-1}{(k/k_1)+2} = \rho \frac{(k_2/k_1)-1}{(k_2/k_1)+2} \tag{1}$$

in which k, k_1 and k_2 are the specific conductivities of the suspension, the suspending and the suspended mediums respectively; and ρ is the volume concentration of the suspended medium. This formula is true theoretically only for the case of a suspension of spheres. The case of a suspension of infinitely well conducting ellipsoids has been treated theoretically by Poisson[4] in his theory of magnetic induction and also by Lampa[5] in his theory of the dielectric constant of a crystal.

According to its theoretical derivation as presented hitherto, Eq. (1) can be expected to hold only for dilute suspensions. The reason for this is that in the given theoretical treatment the electric field around any ussspended particle due to the electric charges on the other particles in the suspension is considered as equal to the average value of this field over the whole space of the suspended medium. For the case of a cubic arrangement of spheres, Lord Rayleigh[6] has shown that the influence of these charges is represented correctly in Eq. (1) only to the first approximation. It seems difficult theoretically to decide whether the formula holds strictly for the case of a random distribution of the suspended particles. That it does is supported by the well known fact that there is usually a very close agreement[7] between the values of the refractive index of a liquid (or dielectric constant, although the agreement here generally is less close)[8] as determined experimentally and as calculated from formula (1) by means of the experimental value of the refractive index for its vapor. Confirmation was obtained for volume concentrations up to 15 per cent by Millikan[9] from his observations of the dielectric constant of emulsions of water in benzol-chloroform. In the following presentation, therefore, we shall take into account the interaction of the suspended particles by means of the procedure employed in deriving formula (1); that is, we shall add to the original field the mean value of the forces due to the charges on the suspended particles throughout the whole space of the

[4] S. D. Poisson, Mem. Acad. Roy. Sci. Inst. France, **5**, 488 (1826)
[5] A. Lampa, Sitz. Math. Nat. Klasse Akad. Wiss. Wien., **104** (IIa), 681 (1895)
[6] Lord Rayleigh, Phil. Mag., **34**, 481 (1892)
[7] W. Brühl, Zeits. Phys. Chem., **7**, 1 (1891)
[8] P. Lebedew, Wied. Ann. **44**, 304 (1891)
[9] R. A. Millikan, Wied, Ann. **61**, 337 (1897)

suspending medium. The exactness of this method is proven by an experimental verification of the formula which we shall derive; to this end we shall in this paper make use of the extensive experimental data which have been accumulated for the electric conductivity of blood.

We shall consider first the general case of a suspension of homogeneous, non-polarizable ellipsoids. The suspension is assumed to be in an electrolytic cell, the dimensions of which are $1\times1\times1$ cm. The potential between the electrodes is V volts; the current i amperes.

Let us consider a single ellipsoid with half axes a, b, c in this suspension. We shall, for the moment, consider a to be parallel to the direction of the electric force. We shall introduce an orthogonal co-ordinate system with its origin in the center O of the ellipsoid and its axes x, y, z parallel to a, b and c (Fig. 1). We shall designate the electric force at an arbitrary

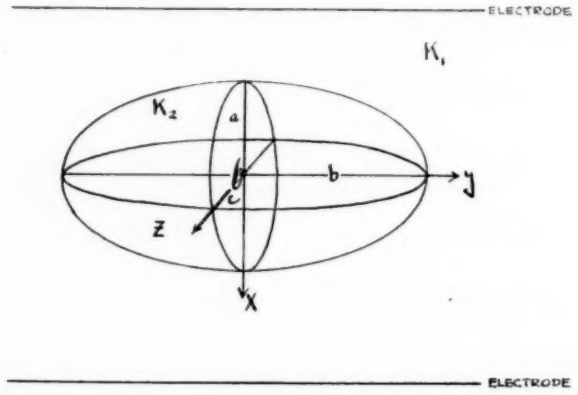

Fig. 1

point of the suspending phase as F; as stated above, this is composed of the original electric force V due to the surface charges on the electrodes and of the mean value of the forces due to the surface charges on the suspended particles throughout the whole space of the suspending medium.

For the purpose of determining the surface charges of the ellipsoid we shall introduce confocal co-ordinates defining these for a point x, y, z as the three values of θ, λ, μ and ν, which satisfy the equation

$$\frac{x^2}{a^2+\theta}+\frac{y^2}{b^2+\theta}+\frac{z^2}{c^2+\theta}=1\,.$$

The potential due to the force F is

$$V_s=-Fx=-F\sqrt{(a^2+\lambda)\,(a^2+\mu)\,(a^2+\nu)/(b^2-a^2)\,(c^2-a^2)}\,.$$

The total potential at a point outside the ellipsoid must be of the form

$$V_{ext} = -F\sqrt{\frac{(a^2+\mu)\,(a^2+\nu)}{(b^2-a^2)\,(c^2-a^2)}}\left\{\sqrt{(a^2+\lambda)} + D\sqrt{(a^2+\lambda)}\int_{\lambda}^{\infty}\frac{d\lambda}{(a^2+\lambda)\,\Delta\lambda}\right\} \quad (2)$$

while at a point inside the ellipsoid

$$V_{int} = -F\sqrt{\frac{(a^2+\lambda)\,(a^2+\mu)\,(a^2+\nu)}{(b^2-a^2)\,(c^2-a^2)}}\,D_1 \,. \quad (3)$$

where $\Delta\lambda = \sqrt{(a^2+\lambda)\,(b^2+\lambda)\,(c^2+\lambda)}$, and D and D_1 are constants which are to be determined by the boundary conditions. The boundary conditions to be fulfilled are

(1) For $\lambda = \infty$, V_{ext} must be equal to the potential of the original field; this condition is fulfilled since the last term becomes zero for $\lambda = \infty$.

(2) At the surface of the ellipsoid ($\lambda = 0$), $V_{int} = V_{ext}$; hence, from Eqs. (2) and (3),

$$D_1 = 1 + D\int_{0}^{\infty}\frac{d\lambda}{(a^2+\lambda)\,\Delta\lambda} \quad (4)$$

Hence

$$\int_{0}^{\infty}\frac{d\lambda}{(a^2+\lambda)\,\Delta\lambda} = \frac{D_1-1}{D} \equiv L_a \,,$$

if we write L_a for the definite integral.

At the surface of the ellipsoid, $N_{ext}k_1 = N_{int}\,k_2$, N_{ext} and N_{int} being the normal forces at the two sides of the surface of the ellipsoid. The equation indicates that no accumulation of electricity takes place at the surface. Using n for the direction of the normal to the surface of the ellipsoid we have

$$N_{ext} = -(dV_{ext}/dn)_{\lambda=0} = -(dV_{ext}/d\lambda)_{\lambda=0}\cdot(d\lambda/dn)_{\lambda=0}$$

and a similar equation for N_{int}.

Consequently our equation of condition becomes

$$+F\sqrt{\frac{(a^2+\mu)\,(a^2+\nu)}{(b^2-a^2)(c^2-a^2)}}\left[\frac{1}{2a} + \frac{DL_a}{2a} - \frac{D}{a^2bc}\right]k_1$$

$$= +F\,D_1\sqrt{\frac{(a^2+\mu)\,(a^2+\nu)}{(b^2-a^2)\,(c^2-a^2)}}\;\;\frac{1}{2a}k_2:$$

$$k_1\left[1+DL_a-2D/abc\right] = k_2\,D_1. \quad (5)$$

From equations (4) and (5) we obtain:

$$D = \frac{(1-k_2/k_1)}{2/abc+L_a(k_2/k_1-1)}$$

$$D_1 = \frac{2}{2+abcL_a(k_2/k_1-1)}$$

We now obtain for V_{int}

$$V_{int} = -F\sqrt{\frac{(a^2+\lambda)(a^2+\mu)(a^2+\nu)}{(b^2-a^2)(c^2-a^2)}} \cdot \frac{2}{2+abcL_a(k_2/k_1-1)}$$

or, going back to the x, y, z co-ordinate system

$$V_{int} = -\frac{2Fx}{2+abcL_a(k_2/k_1-1)}. \tag{6}$$

The values of V_{int} when b or c are parallel to the electric field, are derived by replacing a in Eq. (6) by b or c.

The value of F is determined by the following equation:

$$\int_{ext} F_x\,dx\,dS + \int_{int} F_x\,dx\,dS = V$$

in which F_x is the component of the electric force parallel to x and dS an element of area perpendicular to x, the first integral is taken over the space outside the ellipsoids, the other over the space inside the ellipsoids.

We obtain, using equation (6) and writing

$$\int_0^\infty \frac{d\lambda}{(b^2+\lambda)\,\Delta\lambda} \equiv L_b\,; \quad \int_0^\infty \frac{d\lambda}{(c^2+\lambda)\,\Delta\lambda} \equiv L_c$$

$$V = F(1-\rho)+\tfrac{1}{3}F\rho\sum^{a=a,b,c} \frac{2}{2+abcL_a(k_2/k_1-1)}. \tag{7}$$

In order to find the conductivity k of the suspension we shall divide the space between the electrodes (Fig. 1) into an infinite number of volume elements dS, dx.

By Ohm's law we have

$$k_1 \int_{int} dx \int_{int} F_x\,dS + k_2 \int_{ext} dx \int_{ext} F_x\,dS = i = Vk\,. \tag{8}$$

where the first of the two integrals is taken over the space inside the ellipsoids and the other over the space outside the ellipsoids. This equation is evidently equivalent to

$$k_1 \int_{all} dx \int_{all} F_x\,dS + (k_2-k_1) \int_{ext} dx \int_{ext} F_x\,dS = Vk$$

in which the first double integral is taken over the whole space between the electrodes. We obtain

$$Vk_1+(k_2-k_1)\int dS[(V_{int})_{-x}-(V_{int})_{+x}] = Vk$$

$$Vk_1+(k_2-k_1)\frac{2F}{2+abcL_a(k_2/k_1-1)}\int 2x\,dS = Vk$$

$$k_1+\frac{2k_1(k_2/k_1-1)F/V}{2+abcL_a(k_2/k_1-1)}\rho = k \tag{9}$$

ρ being the volume of the ellipsoids.

This equation corresponds to the case in which a is parallel to the direction of the original field. The equations which correspond to the cases in which b and c are parallel to the original field are obtained by replacing a by b and c.

The equation corresponding to an arbitrary orientation of the ellipsoids is the sum of three equations like (9)

$$3k_1+k_1\rho\sum^{a=a,b,c}\frac{2(k_2/k_1-1)F/V}{2+abcL_a(k_2/k_1-1)} = 3k \tag{10}$$

Combining this equation with equation (7) we obtain

$$\frac{F}{V} = \frac{k_2-k}{(1-\rho)\,(k_2-k_1)}$$

Introducing this value of F/V into equation (10), we obtain finally

$$k = k_1+\frac{\frac{1}{3}\rho}{1-\rho}\sum^{a=a,b,c}\frac{2(k_2-k)}{2+abcL_a(k_2/k_1-1)}. \tag{11}$$

We shall now confine ourselves to the case of spheroids, that is $b=c$. We have the following two integrals in equation (11) to integrate

$$L_a = \int_0^\infty \frac{d\lambda}{(a^2+\lambda)\,\Delta\lambda} = \int_0^\infty \frac{d\lambda}{(a^2+\lambda)^{3/2}\,(b^2+\lambda)}$$

$$L_b = \int_0^\infty \frac{d\lambda}{(b^2+\lambda)\,\Delta\lambda} = \int_0^\infty \frac{d\lambda}{(b^2+\lambda)^2(a^2+\lambda)^{1/2}}$$

We find by partial integration

$$L_a = \frac{2}{ab^2} - 2\int_0^\infty \frac{d\lambda}{(a^2+\lambda)^{1/2}(b^2+\lambda)^2}.$$

The integral

$$ab^2\int_0^\infty \frac{d\lambda}{(a^2+\lambda)^{1/2}(b^2+\lambda)^2} \equiv M$$

can easily be calculated.

$$M\,(a<b) = \frac{(\varphi - \frac{1}{2}\sin 2\varphi)}{\sin^3\varphi}\cos\varphi \quad \text{where } \cos\varphi = a/b\,, \text{ and}$$

$$M\,(a>b) = \frac{1}{\sin^2\varphi'} - \frac{1}{2}\,\frac{\cos^2\varphi'}{\sin^3\varphi'}\log\left(\frac{1+\sin\varphi'}{1-\sin\varphi'}\right), \quad \text{where } \cos\varphi' = b/a$$

consequently by (11),

$$k = k_1 + \frac{k_1\rho\beta}{(1-\rho)}\,\frac{(k_2-k)}{(k_2-k_1)} \tag{12}$$

or

$$\left(\frac{k-k_1}{k_2-k}\right)\left(\frac{k_2}{k_1}-1\right) = \frac{\beta\rho}{1-\rho} = \beta\rho_1 \tag{13}$$

where $\rho = \rho_1/(1+\rho_1)$

and

$$\beta = \tfrac{1}{3}\left[\frac{2}{1+(k_2/k_1-1)\frac{1}{2}M} + \frac{1}{1+(k_2/k_1-1)\,(1-M)}\right]\left(\frac{k_2}{k_1}-1\right)$$

In Figs. 2 and 3 we have plotted β against k_2/k_1 (or k_1/k_2) for different values of a/b.

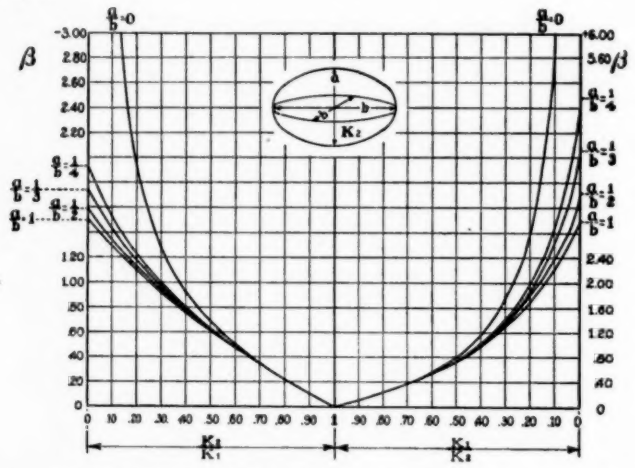

Fig. 2. Graphical representation of β for the case of the oblate spheroid.

The influence of the geometrical factors of the suspended particles is expressed in equation (13) solely in β. Therefore we conclude from the expression for β and from Figs. 3 and 4, that for a constant volume concentration, the conductivity of a suspension is independent of the size of the suspended particles and also nearly independent of the form of the particles when the difference between the conductivities of the suspended and the suspending phases is not very large. This is especially true for

suspensions of prolated spheroids which are less conducting than the suspending medium.

Putting

$$x = -\frac{(k_2/k_1-1)-(k_2/k_1)\beta}{(k_2/k_1-1)-\beta}$$

we obtain from equation (13) the following analogue to equation (1)[10]

$$\frac{(\mathbf{k}/\mathbf{k}_1)-1}{(\mathbf{k}/\mathbf{k}_1)+\mathbf{x}} = \rho \cdot \frac{(\mathbf{k}_2/\mathbf{k}_1)-1}{(\mathbf{k}_2/\mathbf{k}_1)+\mathbf{x}} \tag{14}$$

x is plotted in Figs. 4 and 5.

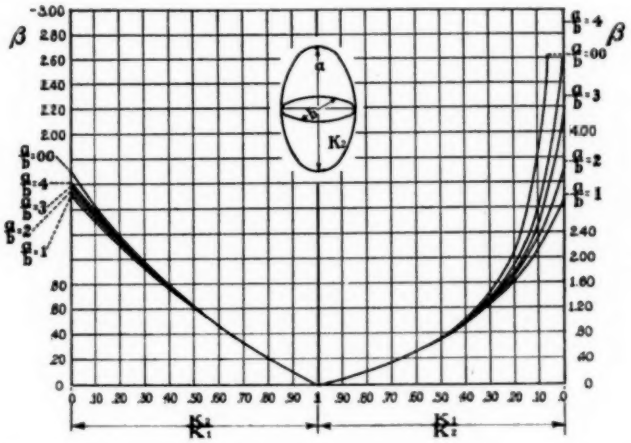

Fig. 3. Graphical representation of β for the case of the prolate spheroid.

For the case of the sphere, $x=2$, making Eq. (14) identical with Eq. (1). For the case when $k_2=0$, Eq. (13) becomes

$$\left(1-\frac{k_1}{k}\right) = \frac{\beta\rho}{1-\rho} = \beta\rho_1 \; ; \tag{15}$$

also

$$x = -1/(\beta+1) \; ; \quad \beta = -(x+1)/x \; , \tag{16}$$

and Eq. (14) becomes

$$-\frac{\rho}{x} = \frac{k-k_1}{k+k_1 x} \; ; \qquad \left[1-\frac{k_1}{k}(1-\rho)\right]x = -\rho \tag{17}$$

C. Comparison of Theory with Experimental Data

In this section we shall apply the formula which we have derived to the very accurate and extensive experimental data for the conductivity

[10] Compare O. Wiener, Abh. K. Sächs. Ges. Wiss. Math. Phys. Kl. **32**, 509 (1912)

of blood which have been accumulated by Stewart,[11] Bugarszky,[12] Fraenckel[13] and others. According to these investigators for a current of low frequency the red corpuscles of blood are perfect insulators so that the ratio of the conductivity of blood to that of its serum is dependent only on the volume concentration of the red corpuscles but independent of the absolute value of the conductivity of the serum. Determinations of this ratio are made for volume concentrations up to 90 per cent. For the

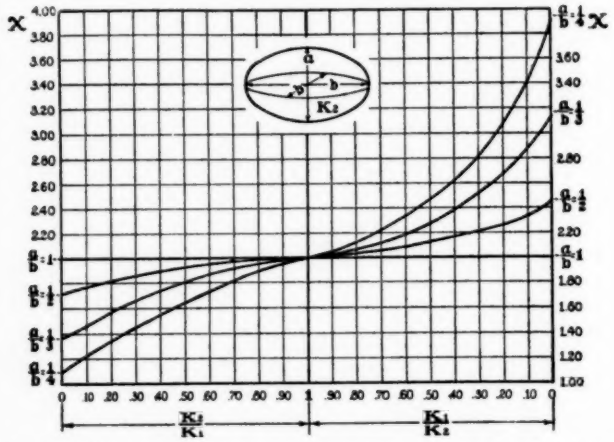

Fig. 4. Graphical representation of x for the case of the oblate spheroid.

same value of the volume concentration, this ratio is very nearly the same for the blood of man, horse, dog and cow.[13] The most exact methods for determining the volume concentration have been used by Stewart and Fraenckel. Stewart has used two independent methods, a colorimetric and Hoppe-Seyler's chemical method. Fraenckel has used Bleibtreu's chemical method. The agreement between the results of Stewart and those of Fraenckel is very good. However, as has been stated also by Fraenckel, one would expect that Stewart's methods would give the most exact results. We shall, therefore, restrict ourselves to a comparison of the results of Stewart with those secured by the formula. In Table I is given a series of measurements made by Stewart (l.c.[11] p. 369) for the blood of a dog. The volume concentration of the normal blood was determined twice by the colorimetric method and twice by Hoppe-Seyler's method. The results were 41.16, 40.72, 41.52 and 40.99 per cent, the average ratio being 40.98 per cent. A series of red corpuscle suspensions of varying volume concentration was made up by concentration or

[11] G. N. Stewart, J. Physiol., **24,** 356 (1899)
[12] S. Bugarszky, Zentr. Physiol., **11,** 297 (1897-98)
[13] P. Fraenckel, Zeits. klin. Med., **52,** 470 (1904)

dilution of the normal blood. The volume concentration for each of these suspensions was determined volumetrically using the value of the volume concentration of the original blood. These volume concentrations are

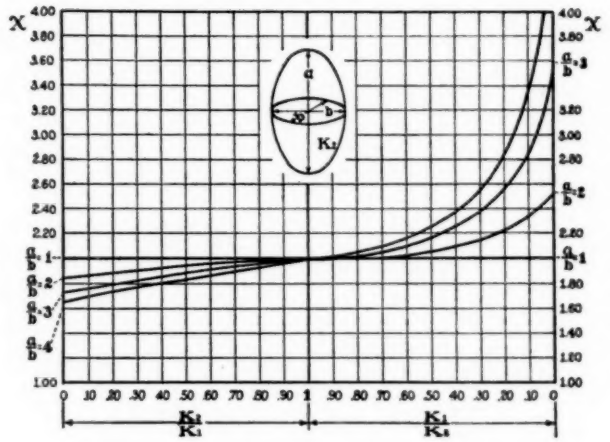

Fig. 5. Graphical representation of x for the case of the prolate spheroid.

given in Table I under ρ (obs.). The ratio of the conductivity of the serum to that of the blood is given under k_1/k.

In applying our formula, we take $k_2=0$, and assume $a/b=1/4.25$; consequently (see Fig. 2) $x=1.05$ and $\beta=-1.95$, and either (15) or (17)

TABLE I

Conductivity of blood of dog

k_1/k	ρ(obs.) (per cent)	ρ(calc.) (per cent)	Difference (per cent)
15.62	90.7	88.2	+2.7
9.08	82.1	80.5	+2.0
6.56	74.5	74.0	+0.7
5.06	67.8	67.5	+0.4
4.14	61.6	61.6	−0.0
3.51	56.1	56.2	−0.2
3.063	51.0	51.4	−0.8
2.726	46.4	46.9	−1.0
2.436	42.2	42.3	−0.2
2.348	41.0	40.8	−0.5
2.225	38.4	38.5	−0.4
1.903	31.9	31.6	−0.8
1.697	26.4	26.3	−0.0
1.539	21.8	21.6	+1.0
1.428	18.1	18.0	+0.5
1.342	15.3	14.9	+2.4
1.232	11.4	10.7	+6.1

may be used to calculate the values of the volume concentration ρ for the observed values of k_1/k. These are given under ρ (calc.). The devia-

tions ρ (obs.) $-\rho$ (calc.) given in the fourth column are probably always within the experimental errors.*

It may be of interest to apply our formula also to some measurements of sand suspensions which have been made by Oker-Blom.[14] and are often cited in connection with work on the conductivity of blood. Two different kinds of sand were used. The suspensions were prepared by adding the sand to a hot salt solution containing 3 per cent gelatine and cooling this mixture to gelatination under continuous rotation. No information is

TABLE II

Conductivity of suspensions of sand

k_1/k(obs.)	ρ(obs.) (per cent)	β	x
2.488	40.	2.22	.820
2.220	36.4	2.14	.876
2.075	33.3	2.15	.870
1.952	30.8	2.14	.876
1.866	28.6	2.17	.854
1.790	26.7	2.17	.854
1.725	25.0	2.18	.848
1.6835	23.5	2.22	.820
	Average values:	2.17	.854

given concerning the form of the sand particles except for the statement that the particles of the sand which were used in the second series of experiments (Table III) were more nearly spherical than those which were used in the first series (Table II). Our theory is therefore best

TABLE III

Conductivity of suspensions of sand

k_1/k(obs.)	ρ(obs.) (per cent)	β	x
1.190	10	1.710	1.410
1.426	20	1.705	1.420
1.734	30	1.712	1.405
2.156	40	1.732	1.367
2.715	50	1.715	1.400
3.613	60	1.74	1.35
	Average values:	1.72	1.392

*The red corpuscles of mammalians according to the most generally accepted data are biconcave in shape but their dimensions especially in the dog have not been accurately measured. The value 1/4.25 for a/b which secures the best agreement in the present case is in good agreement with the observed values for the dimensions. Determinations of the conductivity of the blood of different animals with simultaneous measurements of the dimensions of the red corpuscles will be made in this laboratory; these investigations will include studies of the blood of different non-mammalian vertebrates in which the red corpuscles are approximately ellipsoids.

[14] M. Oker-Blom, Arch. Ges. Physiol., **79,** 510 (1900)

applied by using Oker-Blom's observed values of k_1/k and ρ and calculating the value of x by means of Eq. (17) since $k_2=0$. Our calculated results are given in Tables II and III, one for each of the two kinds of sand used by Oker-Blom The calculated values for x in each case are constant within experimental errors. It hardly seems probable, however, that the sand particles could have been as flat as these values for x would indicate; it is more probable that the large values for x are due to the fact that the sand particles became more or less completely orientated by the rotation. Eq. (14) with a different value for x holds also in this case.

DEPARTMENT OF BIO-PHYSICS,
CLEVELAND CLINIC FOUNDATION,
CLEVELAND, OHIO.
April 9, 1924.

BOOK REVIEWS

Handbuch der Spectroscopie. Volume VII, Part I. H. KAYSER AND H. KONEN. Kayser's classical Handbook reached six volumes before the war checked its growth. Since the appearance of the sixth volume, in 1912, the increase in the known facts of spectroscopy has been so rapid that there has been a great need of an enlargement or revision of this work. Professor Kayser has continued to maintain a bibliography of the subject, and has now at last succeeded with the help of Professor Konen, and in spite of serious difficulties, in producing the first of three parts which will together constitute the seventh volume.

This part does not pretend to be a revision of the entire work, but merely of volumes V and VI, dealing with the emission spectra of the elements and their compounds. The whole of this new seventh volume is now ready for the printer, but the authors explain that it took three years for the printing of the present instalment, and we can only hope that conditions in Germany are now more favorable for rapid publication.

The revision takes account of many changes that have occurred in the interval. X-ray spectra are admitted to the company of their optical relatives. The third decimal place of Ångström units appears unhesitatingly in many of the tables, and there are occasional glimpses of the fourth. All the tables are on the scale of International Ångströms. Valuable items of information, such as King's temperature classifications of certain spectra. the ionization potentials of the elements, etc., are to be found, and will be welcomed. No distinction is yet made between the spectrum lines due to an element in its normal state and those due to the same element in a state of ionization, unless the series identifications are known. It will be a considerable advance when in each table, opposite each line, can be given the form of the atom producing it; but in many cases the necessary information is still lacking.

In so vast a work it is inevitable that there should be a few errors and omissions, but the number of these is surprisingly small, and the proof seems to have been read with gratifying care. One small item in this connection may be worth mentioning. In several places in the text a wave-length appears, for instance, as λ251, when λ2510 is intended. Years ago this would have produced no ambiguity, but now that the very short wave region is being actively explored, one cannot always be quite so certain.

It is pleasant to observe that the new volume contains the same refreshingly vigorous criticisms that have added so much to the interest and value of the older ones. The colossal amount of labor involved in reading all new articles so carefully as to be able to make critical studies of them can well be imagined when we see that in the case of iron alone there are 160 new articles in its bibliography.

The volume is arranged alphabetically by chemical symbols, and covers all the elements down to iron, inclusive. Scientific men all over the world will join in hoping that the authors may find the circumstances now more favorable than they have been, so that the other two parts of this volume may soon appear.—Pp. X+498, S. Hirzel, Leipzig, 1924. F. A. SAUNDERS

Die Grundlagen der Physik. Synthetische Principien der mathematischen Naturphilosophie (Second edition). By HUGO DINGLER.—After a long separation between science and philosophy, the scientists during the time of Helmholtz began to feel new interest in philosophical questions. It was perhaps non-Euclidean geometry due to Bolyai, Lobatschewsky and Riemann, which gave the first impulse to new thoughts regarding the axioms of geometry and the philosophical foundations of all mathematical

and physical sciences. So a new branch, the philosophy of science, grew up, some of whose exponents are Helmholtz, Mach, and Poincare. The discovery of the radioactive phenomena, the quantum theory and the theory of relativity have again increased the philosophical interest in the foundations of the physical sciences. In the wide literature published in this field in the last decades the work of Dingler deserves special attention by its claim to go to the logical foundations of all physical sciences from a very general and fundamental point of view.

In the first part the author deals with the first foundations, considering the principle of the "will" as most fundamental, the problem of validity, the principles of purpose and of logic; in the second part the author studies space, time and causality; in the third part he considers mechanics, and in the last part he gives the philosophical foundations of his system and its relations to other systems of philosophy.

In this brief review I wish only to point out the trend of the ideas of Dingler. Which are the guiding principles which we use in our physical investigations? We have at first to consider the laws of logic, of which the author gives a treatment. Here the conception of "Einfachstheit" or greatest simplicity plays an important role. In a large number of cases, Dingler asserts, we can determine the simplest case by the requirement that it shall be that case in which all determinations in which this is possible at all, are equal among themselves (rule of equality). Applying this rule the author finds that the simplest dependence of two quantities which disappear simultaneously, is the proprotionality $y=ax$. As an example the author mentions Ohm's law. The intensity of the current i depends on the electromotive force e and the conductance d. If the law shall have the simplest form, then the author says we must have $i=aed$ where a is a constant. But as far as simplicity is concerned, we might also say the electromotive force depends on the current and the conductance and write $e=aid$. An interesting but it seems to me not conclusive argument is used in the deduction of Newton's universal law of gravitation and in the definition of force. Yet why is attraction logically simpler than repulsion?

Besides the principles of logic, Dingler assumes a three dimensional Euclidean space and unidimensional absolute time as basis for the explanation of reality. The aim of his synthesis is to explain every process in nature by the principles of Euclidean geometry and Newtonian mechanics. The present theories of relativity and the quantum theory deny the general validity of these principles. We might expect to find a discussion of these modern theories in Dingler's foundations, but except for some hints the author does not enter into these problems.

The general theory of relativity on the contrary gives by means of Hamilton's principle the laws of geometry and physics at once, so that geometry and physics as one science rest on the same basis. The mechanical explanation of all physical phenomena, the great ideal of physics in the time of Helmholtz and Kelvin, is no more recognized. The conception of field of force led gradually to a new theory of the material universe, in which we start not from the material points, but from the time-space continuum.

The unity of nature is badly broken up by our present physical theories, which are in a rather chaotic condition. A protest against such a condition by a philosopher who aims at a clear logical interpretation of the natural phenomena on the basis of a few fundamental principles is surely justified.

In the last part the author gives clearly the relation between his own philosophy and the older systems of thought of Hume, Kant and Mach, the latter being mentioned again and again with the greatest admiration.—Pp. XIV+336, Walter de Gruyter, Berlin and Leipzig, 1923. JAKOB KUNZ

Problems in General Physics for College Courses. By MORTON MASIUS, Worcester Polytechnic Institute.—"The present volume is the outgrowth of a small booklet, first published in 1913, containing 274 problems and intended to serve as a supplement to 'A Textbook of Physics,' edited by A. W. Duff. In subsequent reprints the book

has been considerably enlarged. The present edition contains 1008 problems, a list of the most important equations of general physics, and a large number of examples, completely worked out, with suggestions regarding the best methods of solving problems." These worked-out examples, with the accompanying notes on units, form a valuable feature of the book. Speaking of units, the reviewer is of the opinion that students should be trained to write in their working equations the names of the units which they employ. This has, unfortunately, not been done in the illustrative examples before us. The examples to be solved by the student are largely of the conventional sort, with just the right amount of data for substitution in a certain formula. The danger of this practice—which is well-nigh universal—is that it will train students in a certain cleverness in hitting the right formula rather than in *physics*. Professor Masius has, however, introduced a considerable number of excellent problems that call for real thinking. Modern physics is not forgotten, for numerous problems throughout the book have to do with advances of recent years, and there are a few well-selected problems on electrons. The book deserves a warm welcome from teachers of college physics.—Pp. viii+151. 4-place tables, and 75 fig. Blakiston's, 1924. W. G. CADY

The Properties of Matter. BASEL C. MCEWEN, The Nizam's College, Hyderabad, Deccan, India.—This carefully and judiciously written book is of a grade intermediate between the corresponding part of a physics course for sophomores in American Colleges and a graduate course in the same subject. It begins with a brief sketch of the necessary parts of thermodynamics, and the ten chapters cover: The kinetic theory of matter and its application to the gaseous state; isothermal and adiabatic transformations and the specific heats of gases; the elasticity of gases and the continuity of the liquid and gaseous states; the thermal expansion, diffusion and solubility of gases; equations of state; liquids; capillarity; solids; gravity; with appendices on the Joule-Thomson effect, the theorem of Le Chatelier, and units and dimensions. It is assumed that the reader understands the elements of calculus. Interwoven with the accounts of theory and of classical experiments are ninety exercises with adequate instructions for practice by the student, though it is probably not intended that any student should be expected to do all of them. In the preface the author states that "particular emphasis has been laid upon the experimental treatment of the subject, without which most of the time spent in the study of any branch of physical science is wasted."

To the reviewer this would seem an excellent text-book for use in a course for students who are specializing in chemistry, though for this purpose it would seem desirable to supplement the text by some references to more recent work, with a view to stimulating the interest and self-education of the student. The names of the great authorities are referred to throughout, but references to original sources, classical or modern, are not given. While the treatment throughout is careful and scholarly, there is some danger that it would leave the student with the impression that the subject was exhausted, completed, and embalmed in text-books some years ago. Pp. vi+316, 137 fig., price $3.20. Longmans, 1923. A. WILMER DUFF